GEOLOGICAL SURVEY BRANCH
DEPARTMENT OF MINES AND ENERGY
GOVERNMENT OF NEWFOUNDLAND AND LABRADOR

THE GEOLOGY AND GEOCHEMISTRY OF THE CROSS HILLS PLUTONIC SUITE, FORTUNE BAY, NEWFOUNDLAND (NTS 1M/10)

John Tuach

Report 91

Cover

View looking northeast across the Cross Hills Plutonic Suite toward the Cross Hills.

91-05696/ -

GEOLOGICAL SURVEY BRANCH
DEPARTMENT OF MINES AND ENERGY
GOVERNMENT OF NEWFOUNDLAND AND LABRADOR

THE GEOLOGY AND GEOCHEMISTRY OF THE CROSS HILLS PLUTONIC SUITE, FORTUNE BAY, NEWFOUNDLAND (NTS 1M/10)

An Eocambrian to Cambrian alkaline gabbro–granodiorite–granite–peralkaline granite–syenite suite containing minor Zr–Y–Nb–REE mineralization

John Tuach

Report 91–2

St. John's, Newfoundland
1991

EDITING, LAYOUT AND DRAFTING

Senior Geologist R.F. BLACKWOOD

Editor C.P. G. PEREIRA

Copy Editor D. WALSH

Typesetting B. STRICKLAND

Word Processing J. BANTON
D. DOWNEY
J. MATTHEWS

Supervisor, Cartographic Services K. BYRNE

Cartography D. LEONARD (Photomechanical)
G. DENIEF
T. PALTANAVAGE

Publications of the Geological Survey Branch are available through the Publications and Information Section, Geological Survey Branch, Department of Mines and Energy, P.O. Box 8700, St. John's, Newfoundland, A1B 4J6.
Telephone: (709) 576-3159
Telex: 016-4724
FAX: (709) 576-3493

This project is a contribution to the Canada–Newfoundland Mineral Development Agreement 1984-1989; project carried out by Newfoundland Department of Mines and Energy.

Author's Address: *J. Tuach, P. Geo.*
J. Tuach Geological Consultants, Inc.
P.O. Box 8364, Station 'A'
27 Austin Street
St. John's, Newfoundland
Canada
A1B 3N4

ISBN-0-920769-54-3.

CONTENTS

	Page
ABSTRACT	xiii
INTRODUCTION	1
REGIONAL GEOLOGY	1
PREVIOUS WORK	1
GEOLOGY OF THE CROSS HILLS PLUTONIC SUITE	2
NOMENCLATURE	2
DISTRIBUTION	3
ROCK TYPES	3
Mafic Rocks	3
Granodiorite	3
Biotite Granite	3
Peralkaline Granite	5
Syenite	6
INTRUSIVE RELATIONSHIPS	7
Gabbro and Biotite Granite	7
Biotite Granite and Aplite	7
Aplite–Biotite Granite and Peralkaline Granite	7
Peralkaline Granite and Country Rock	8
PETROGRAPHY AND MINERAL CHEMISTRY	8
Petrography	8
Mafic Rocks	8
Granodiorite	8
Biotite Granite	8
Peralkaline Granite	8
Syenite	8
Mineral Chemistry	9
Plagioclase	9
Pyroxene	9
Amphibole	9
Biotite	9
Chlorite	9
Opaques	9
STRUCTURE	9
ALTERATION	12
MINERAL OCCURRENCES	12
Zr–Y–Nb–REE	15
Base Metals	15
EMPLACEMENT OF THE CROSS HILLS PLUTONIC SUITE	15
GEOCHEMISTRY	17
MAJOR AND TRACE-ELEMENT DATA	17
Introduction	17
Harker Diagrams	17
Major Elements	18
Trace Elements	19
Areal Geochemical Patterns	21
Classification	22
RARE-EARTH-ELEMENT GEOCHEMISTRY	26
Introduction	26
Results	26
Discussion	27

Page

ISOTOPIC SYSTEMS
GEOCHRONOLOGY 28
Introduction 28
Rb–Sr Geochronology 29
Introduction 29
Results 29
Discussion 31
Oxygen 32
Introduction 32
Results 32
Discussion 32

CONTACT RELATIONSHIPS IN AND BETWEEN BIOTITE GRANITE AND PERALKALINE GRANITE: QUENCHING ACROSS AN INTERFACE IN ZONED SILICATE LIQUIDS
CONTACT RELATIONSHIPS
Biotite Granite and Aplite 33
Aplite–Biotite Granite and Peralkaline Granite 33
GEOCHEMISTRY ACROSS THE CONTACTS 33
INTERPRETATION 33

DISCUSSION AND CONCLUSIONS
TECTONOSTRATIGRAPHIC CORRELATIONS 35
TECTONIC SETTING 36
PETROGENESIS 36
METALLOGENESIS 37
MINERAL POTENTIAL 38

ACKNOWLEDGMENTS 38

REFERENCES 38

APPENDIX 1–SAMPLE PREPARATION AND ANALYTICAL TECHNIQUES
A Sample Collection and Preparation 43
B Microprobe Techniques 43
C Major- and Trace-Element Analyses 43
1-C-1 Analytical Techniques 43
1-C-2 Detection Limits, Accuracy and Precision 43
D Rare-Earth-Element Analytical Techniques 43
E Rb–Sr Analyses 44
F Oxygen Isotope Analyses 44

APPENDIX 2–ELECTRON MICROPROBE ANALYSES
A Representative electron microprobe analyses and structural formulae of plagioclase from the Cross Hills Plutonic Suite 45
B Electron microprobe analyses and structural formulae of pyroxene from the Cross Hills Plutonic Suite 46
C Electron microprobe analyses and structural formulae of amphibole from the Cross Hills Plutonic Suite 47
D Electron microprobe analyses and structural formulae of biotite from the Cross Hills Plutonic Suite 48
E Electron microprobe analyses and structural formulae of chlorite from the Cross Hills Plutonic Suite 49

APPENDIX 3–ASSAYS OF SAMPLES FROM THE GRAND LE PIERRE AREA
A Semiquantitative XRF analyses of rock samples (see Map 91-15). Analyses by Metric Lab Ltée., Quebec. Only those values considered to be anomalous are listed 50
B Gold assays of rock-chip samples. Fire assays by Atlantic Analytical Services Limited, Springdale, Newfoundland (February, 1984) 50

Page

APPENDIX 4–FIELD DATA, MAJOR- AND TRACE-ELEMENT ANALYSES 51
A Codes for Granite Field Data 52
B Field Data 55
C Major-Element Data 58
D Trace-Element Data 64
E Summary of geochemical data from the Long Harbour Group, Mooring Cove Formation, and Musgravetown Group in the Grand Le Pierre area 66
F Rare-earth and other elements analyzed by ICP-MS at Memorial University of Newfoundland 68
G Mesonorms and agpaitic indices 68

FIGURES

		Page
Figure 1:	Location map of the Cross Hills Plutonic Suite in Newfoundland. Also shown are the major tectonostratigraphic subdivisions of Newfoundland and location and distribution of Paleozoic (stippled) and Eocambrian to Cambrian plutonic rocks (black). RP–Round Pond, HH–Hare Hill, L–Louil Hills, SC–Swift Current, CR–Cape Roger Mountain, K–Knee Granites, S–Spread Eagle, SM–Saint Marys Diabase, H–Holyrood	1
Figure 2:	Generalized geology and distribution of rocks of the Cross Hills Plutonic Suite, Fortune Bay–Gisborne Lake area, southwestern Newfoundland. Area of detailed mapping shown on Map 91-14 is outlined	2
Figure 3:	Geology of the main outcrop area of the Cross Hills Plutonic Suite	4
Figure 4:	Normative (mesonorms) compositions of analyzed samples from the Cross Hills Plutonic Suite. Fields after Streckeisen and LeMaitre (1979); solid circles–gabbro; half filled circles–hybrid gabbro; open squares–granodiorite; inverted solid triangle–syenite; x–biotite granite; open inverted triangle–aplite; solid upright triangle–peralkaline granite	5
Figure 5:	Geology, mineral occurrences, anomalous radioactivity and sample locations around Bart Pond, English Harbour Road; V–volcanic rocks	7
Figure 6:	Pyroxene compositions (atomic percent) plotted on a CFM diagram. Trends of pyroxene crystalization from Deer *et al.* (1963)	12
Figure 7:	Composition of amphiboles plotted using cation proportions of Al^{IV} + Ca vs. Si + Na + K. Mineral field boundaries after Giret *et al.* (1980), and mineral terminology after Leake (1978). Symbols as for Figure 4. Dashed line enclose igneous amphiboles from the Topsails and St. Lawrence granites; hatched field represents hydrothermal amphiboles from the Topsails and St. Lawrence granites (from Strong and Taylor, 1984)	12
Figure 8:	Chlorite compositions. Solid circles–gabbro; open squares–granodiorite; inverted solid triangle–syenite; x–biotite granite; open inverted triangle–aplite; solid square–peralkaline granite	12
Figure 9:	Geology and mineral occurrences in the Cross Hills Plutonic Suite in the Grand Le Pierre area. Occurrence numbers refer to Table 1. A-A' and B-B' refer to sections shown schematically in Figure 11	13
Figure 10:	Scanning electron microscope spectra of minerals from occurrence # 11 (sample JT-067) and occurrence # 12 (sample JT-124) (see Figure 9): a) fergusonite?- sample JT-124; b,c,d) unidentified minerals–sample JT-124; e) thorite?–sample JT-067; f) thorium oxide–sample JT-067; g,h) unidentified minerals–sample JT-067	16
Figure 11:	Schematic (composite) geological section across the Cross Hills Plutonic Suite in the area to the northwest of Grand Le Pierre. Level of sections shown on Figure 9 and denoted by A-A', B-B'	19
Figure 12:	Harker diagrams showing major-element content of analyzed samples of the Cross Hills Plutonic Suite. Solid circles–gabbro; half-filled circles–hybrid gabbro; open square–granodiorite; inverted solid triangle–syenite; crosses–biotite granite, open upright triangle–aplite; solid upright triangle–peralkaline granite. PGRT–field of peralkaline granite; BGRT–field of biotite granite. Where fields are used for peralkaline granite, solid triangles represent strongly altered and mineralized samples that plot outside the main field	21

Page

Figure 13: Harker diagrams showing Li, Be, F, V, Zn, Ga, Rb, Sr, and Y contents of analyzed samples from the Cross Hills Plutonic Suite. Symbols as in Figure 4 except plus signs are unassigned samples. SiO_2 in percent; all other elements in g/t..... 22

Figure 14: Harker diagrams showing Zr, Nb, Ba, La, Ce, Pb, Th, and U contents of analyzed samples from the Cross Hills Plutonic Suite. Symbols as in Figure 4 except crosses are unassigned samples. SiO_2 in percent; all other elements in g/t..... 23

Figure 15: Areal distribution of trace elements Zr, Nb, Sn, Th and U in rock samples analyzed by Saarberg Interplan Limited. GBBR–gabbro; BGR–biotite granite; PGRT–peralkaline granite; V–volcanic rocks..... 24

Figure 16: Distribution of analyzed samples on the $K_2O + Na_2O$ vs. $K_2O \times 100/(K_2O + Na_2O)$ alteration discriminant diagram of Hughes (1973). The normal field includes data from relatively unaltered volcanic rocks. Solid circles–gabbro; half-filled circles–hybrid gabbro; dashed line around field of biotite granite and aplite; solid lined around field of peralkaline granite; solid triangles–mineralized and altered peralkaline granite..... 24

Figure 17: Distribution of analyzed gabbro, hybrid gabbro-granite and syenite sample on the alkaline–subalkaline–agpaitic syenite discrimination diagram of Currie (1976). Solid circles–gabbro; half-filled circles–hybrid gabbro; inverted triangles–syenite..... 24

Figure 18: Distribution of analyzed gabbro (solid circles) and hybrid gabbro-granite (half-filled circles) on the alkali-silica diagram. Dashed line is alkali basalt–tholeiitic basalt boundary of Irvine and Baragar (1971); solid lines are basalt field boundaries after Kuno (1968). a–alkali basalt; t–tholeiitic basalt; al–alumina basalt; h-a–high-alumina basalt..... 25

Figure 19: Distribution of analyzed samples on the AFM discrimination diagram of Irvine and Baragar (1971). T–tholeiitic; CA–calc alkaline; GBBR–gabbro; GBBH–hybrid gabbro-granite, PGRT–peralkaline granite; BGRT–biotite granite..... 25

Figure 20: Distribution of analyzed gabbro and hybrid gabbro-granite on the TiO_2-K_2O-P_2O_5 oceanic–continental basalt discrimination diagram of Pearce *et al.* (1975)..... 25

Figure 21: Distribution of analyzed felsic rocks on the Al_2O_3-FeO (tot) discriminant diagram of MacDonald (1975). Inverted triangles–aplite; x–biotite granite; open squares–granodiotite; inverted solid triangles–syenite; open triangles–peralkaline granite; solid upright triangles–mineralized and/or altered peralkaline granite..... 26

Figure 22: Fields of I- vs. S- vs. A-type magmas on (a) Na_20 vs. K_20 and (b) Ga vs. Al_20_3 (White and Chappell, 1983) for felsic units of the Cross Hills Plutonic Suite. Symbols explained on diagram..... 26

Figure 23: Distribution of analyzed samples on the SiO_2 vs. $Zr/TiO_1 \times 10^4$ discrimination diagram of Winchester and Floyd (1977)..... 27

Figure 24: Distribution of analyzed samples on the $Zr/TiO_2 \times 10^4$ vs. Nb/Y discrimination diagram of Winchester and Floyd (1977). Symbols as in Figure 23..... 27

Figure 25: Rare-earth-element profiles of a) 4 peralkaline granite and 2 mineralized peralkaline granite samples (JT-067 and JT-124) and b) a gabbro (JT-343), a granodiorite (JT-404) and 2 biotite granite samples (JT-424 and JT-426). Data are normalized to the chondrite values of Evensen *et al.* (1978)..... 28

Figure 26: Rare-earth-element profiles of mineralized peralkaline granite samples from three Saudi Arabian deposits–Ghurayyah, Jabal Tawlah and Jabal Sa'id. Also shown is the range for six unmineralized Saudi Arabian peralkaline granite samples. Data from Drysdall *et al.* (1984)..... 28

Page

Figure 27: Location of Rb–Sr samples and simplified geology, Grand Le Pierre area. Unit symbols as for Figure 3 30

Figure 28: Rb–Sr isochron plots of selected samples from the Cross Hills Plutonic Suite 31

Figure 29: Oxygen isotope data from the Fortune Bay area. Open symbols represent data from Tuach (1987) and Tuach *et al.* (1985). Whole-rock $\delta^{18}O$ values of composite samples of Avalon Zone rocks are shown in the box 32

Figure 30: Distribution of selected major and trace elements in samples from the Bart Pond area. The analyses are interpreted to represent a vertical geochemical section from biotite granite, through aplite, into peralkaline granite towards the peralkaline granite–volcanic contact at the left side of the diagram. Sample locations are shown on Figure 5 34

Map 91-14: Geology and Mineral Occurrences: Grand Le Pierre–Sage Pond area ..... back pocket

Map 91-15: Sample Location and Geology: Grand Le Pierre–Sage Pond area ..... back pocket

PLATES

		Page
Plate 1:	View looking northeast across the Cross Hills Plutonic Suite toward the Cross Hills. The gabbro–biotite granite contact (foreground) is highlighted by a change in vegetation, i.e., more trees over gabbro	3
Plate 2:	Representative samples of the mafic unit in the Cross Hills Plutonic Suite. Clockwise from upper left, samples JT-205, JT-60, JT-262a, and JT-262	5
Plate 3:	Vein networks of biotite granite in gabbro. Outcrop below bridge across the Grand Le Pierre River, approximately 2 km north of Grand Le Pierre	5
Plate 4:	Granodiorite cut by an aplite vein. Sample JT-408a	5
Plate 5:	Quartz veins in biotite granite. South of Triangle Pond (see Map 91-14), looking south	6
Plate 6:	Gas veins and breccias in peralkaline granite. Sample JT-440	6
Plate 7:	Mineralized (Zr–Y–Nb–REE) peralkaline aplite veins cutting medium grained peralkaline granite at occurrence # 12	6
Plate 8:	Contact of biotite granite (right) with aplite (left). Note small pegmatite patches in the biotite granite at the contact. Sample JT-434	7
Plate 9:	Photomicrographs showing the progression of textures in the biotite granite (BGRT), its aplite subunit (APLT) and the peralkaline granite (PGRT): a) sample JT-426, BGRT, equigranular texture; b) sample JT-436, APLT, spherulitic texture; c) sample JT-427, APLT, spherulitic texture; d) sample JT-428, APLT, relict spherulitic texture; e) sample JT-429, APLT, micrographic texture; f) sample JT-431, PGRT, myrmekitic texture; g) sample JT-432, PGRT, graphic texture; h) sample JT-433, PGRT, graphic texture–the cloudy nature of the K-feldspar results from hematite inclusions. All photos except the last are taken under crossed nicols. Scale bar for each photo represents 0.5 mm	10
Plate 10:	Photomicrograph showing tuffisitic texture in mineralized peralkaline granite, sample JT-100, crossed nicols, scale bar represents 0.5 mm	15
Plate 11:	Scanning electron microscope backscatter photograph of euhedral zircon (Z) intergrown with hematite (H). Black is silicate gangue. Scale bar refers to lower half of photo; scale of top (area in box) is 5x scale of bottom. Sample JT-124	15
Plate 12:	Scanning electron microscope backscatter photograph of Nb–Y mineral (fergusonite?). H–hematite. All white is the Nb–Y mineral. Sample JT-124. Spectral scan shown in Figure 10a	15
Plate 13:	Scanning electron microscope backscatter photograph of REE mineral intergrown with zircon (Z). Spectral scan of REE mineral is shown in Figure 10. Scale of top is 2x scale of bottom. Sample JT-124	17
Plate 14:	Photomicrograph of hydrothermal, botryoidal, zoned zircon (Z) from occurrence # 11. Also visible are K-feldspar (F) and quartz (Q). Sample JT-067, plane light	17
Plate 15:	Photomicrograph of botryoidal zircon (Z) surrounding K-feldspar crystals (F). Also visible are quartz (Q) and fine grained hematite (H). Sample JT-067, plane light	18
Plate 16:	Scanning electron microscope backscatter photograph showing botryoidal zircon (Z), thorite (TS) and thorium oxide (T). Sample JT-067. Spectral scans shown in Figures 10e and f	18
Plate 17:	SEM backscatter photograph of Th–Nb silicate (A) and Th–Nb–Fe silicate (B); Z–Zircon. Sample JT-067. Spectral scans shown in Figure 10g and h	18

TABLES

		Page
Table 1:	Mineral occurrences in and adjacent to the Cross Hills Plutonic Suite. The assays presented are of selected grab samples	14
Table 2:	Summary of geochemical data from the Cross Hills Plutonic Suite, Grand Le Pierre–Sage Pond area	20
Table 3:	Radiometric age determinations in the Avalon Zone	29
Table 4:	Rb–Sr analyses. Sample locations shown in Figure 27	31
Table 5:	Oxygen isotope analyses from 3 granite samples and a felsic volcanic sample from the Grand Le Pierre area	32
Table 6:	Major- and trace-element analyses of three samples collected at 5 cm intervals across the colour transition between red and purple aplite. Located approximately 1 km northeast of the section shown in Figure 11	35
Table 7:	Summary of metal content of selected Saudi Arabian Zr–Nb–Y–REE deposits; from Drysdall *et al.* (1984)	37

ABSTRACT

This report describes the geology, geochemistry and associated mineralization of the Cross Hills Plutonic Suite, which outcrops in the Fortune Bay area of the Avalon Zone in Newfoundland. The suite consists of alkaline gabbro, granodiorite and biotite granite and smaller areas of peralkaline granite and minor occurrences of syenite. The plutonic rocks give imprecise Rb–Sr ages of about 560 Ma, and intrude late Hadrynian metavolcanic and metasedimentary rocks of the Long Harbour Group.

*The Suite was intruded at a high crustal level in a northwest-southeast extensional tectonic regime characteristic of the late Hadrynian in the Avalon Zone. Textural data indicate that the granitic magmas solidified, or were quenched, due to loss of vapour pressure. Textural and geochemical data also indicate that the quenching occurred across an internal geochemical boundary in the magma chamber between a liquid of granite composition (*sensu stricto*) and a liquid of peralkaline granite composition. These data provide evidence for the existence of stratification in high-silica magma chambers.*

Minor occurrences of Zr–Nb–Y–Th–REE mineralization occur in aplite veins and fractures in the peralkaline granite. Similarities in the geology and mineralization of the Cross Hills Plutonic Suite to that of major Zr–Nb–Y–REE deposits in Saudi Arabia indicate a potential for comparable major deposits in the Cross Hills Plutonic Suite and by inference throughout the Avalon Zone.

INTRODUCTION

The Cross Hills Plutonic Suite (Bradley, 1962; Tuach, 1984; O'Brien *et al.*, 1984) is a group of spatially and genetically associated gabbro to diabase, granodiorite, biotite granite, peralkaline granite and minor syenite intrusions, which outcrop in the Terrenceville (NTS 1M/10) map area of southeast Newfoundland (Figure 1). The main outcrop area (of about 250 km²) occurs to the north of Grand Le Pierre on Fortune Bay (Figure 2). Smaller areas outcrop at the Southeast Bight Hills (6 km²) and at Anesty Hill (1 km²) and minor, possibly related intrusions, occur immediately west of the main body (Figure 2, Map 91-14) and to the north at Nine Mile Hill.

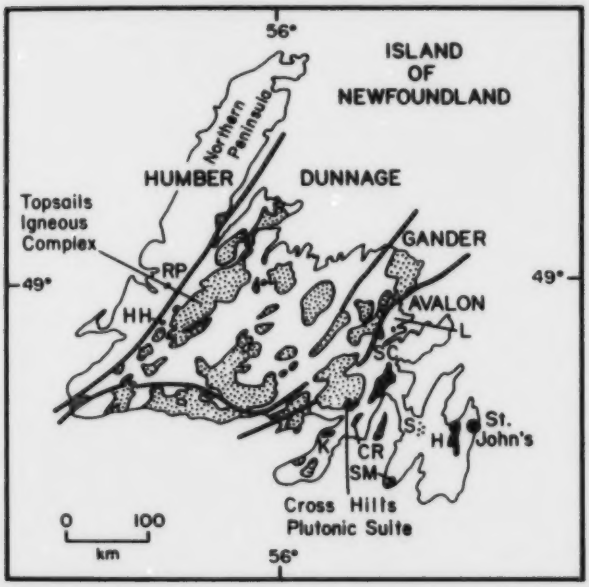

Figure 1. *Location map of the Cross Hills Plutonic Suite in Newfoundland. Also shown are the major tectonostratigraphic subdivisions of Newfoundland and location and distribution of Paleozoic (stippled) and Eocambrian to Cambrian plutonic rocks (black). RP–Round Pond, HH–Hare Hill, L–Louil Hills, SC–Swift Current, CR–Cape Roger Mountain, K–Knee Granites, S–Spread Eagle, SM–Saint Marys Diabase, H–Holyrood.*

This report documents geochemical data and geological interpretations based on field work, undertaken in 1983, which concentrated on an area of approximately 20 km² to the northwest of Grand Le Pierre (Tuach, 1984; Figure 2). The area contains minor Zr–Nb–Y–Th–REE mineralization in association with the peralkaline granite (Hopfengaertner, 1982).

Exposure of the plutonic suite is excellent (Plate 1), and textural and contact relationships are easily observed at most localities. Access is readily available via the Grand Le Pierre–English Harbour road (Map 91-14).

REGIONAL GEOLOGY

The regional geology is illustrated in Figure 2. The high-level, posttectonic, Cross Hills Plutonic Suite intrudes Late Proterozoic, subaerial, lower-greenschist facies, metavolcanic rocks (Belle Bay Formation) and metasedimentary rocks (Anderson's Cove Formation) of the Long Harbour Group (Williams, 1971; O'Brien and Nunn, 1980; O'Brien *et al.*, 1984). The Belle Bay and Anderson's Cove formations are possibly facies equivalent, and are unconformably overlain by peralkaline ash-flows of the Mooring Cove Formation (O'Brien *et al.*, 1984). The Mooring Cove Formation is in turn unconformably overlain by red conglomerates and sandstones of the Rencontre Formation. Rocks of the Rencontre Formation are unconformably overlain by fossiliferous Cambrian rocks to the east of the Grand Le Pierre area.

To the north, the suite is cut by the Ackley Granite Suite, which has provided Late Devonian $^{40}Ar-^{39}Ar$ ages of about 370 Ma (Kontak *et al.*, 1988) and Early Carboniferous Rb–Sr and $^{40}Ar-^{39}Ar$ ages of about 355 Ma (Bell *et al.*, 1977; Tuach, 1987). Imprecise Rb–Sr and U–Pb (zircon) ages reported below indicate that the Cross Hills Plutonic Suite has an Early Cambrian age of about 560 Ma.

These rocks occur in the Avalon Zone (Figure 1) of the Newfoundland Appalachians (Williams and Hatcher, 1983) and are interpreted to represent either a late Precambrian ensialic rift environment (Papezik, 1972; Strong *et al.*, 1978; Strong, 1979) or an island-arc environment (Hughes and Bruckner, 1971). O'Brien *et al.* (1983) have recently reviewed the geology and tectonic setting of the Avalon Zone and suggest that the late Precambrian rocks record the evolution of a Pan-African orogenic belt that was incorporated into the Appalachian Orogen during the Paleozoic.

PREVIOUS WORK

The Terrenceville map area was mapped at a scale of 1 inch to 1 mile by Bradley (1962), and the plutonic rocks, which are the focus of this study, were identified as the Cross Hills Batholith. O'Brien and Nunn (1980) and O'Brien *et al.* (1984) published a revised 1:50,000-scale map and further defined the distribution of these plutonic rocks. Tuach (1984) presented results of 1:15,000 mapping of the intrusive rocks to the northwest of Grand Le Pierre. A summary of previous work was compiled by O'Brien *et al.* (1984).

The peralkaline phase of the Cross Hills Plutonic Suite gave an anomalously high response to an airborne radiometric survey conducted by Saarberg Interplan Limited. Subsequent follow-up ground work led to the discovery of minor Zr–Nb–REE mineral occurrences, which were subsequently mapped and sampled for lithogeochemical analyses (Hopfengaertner, 1982).

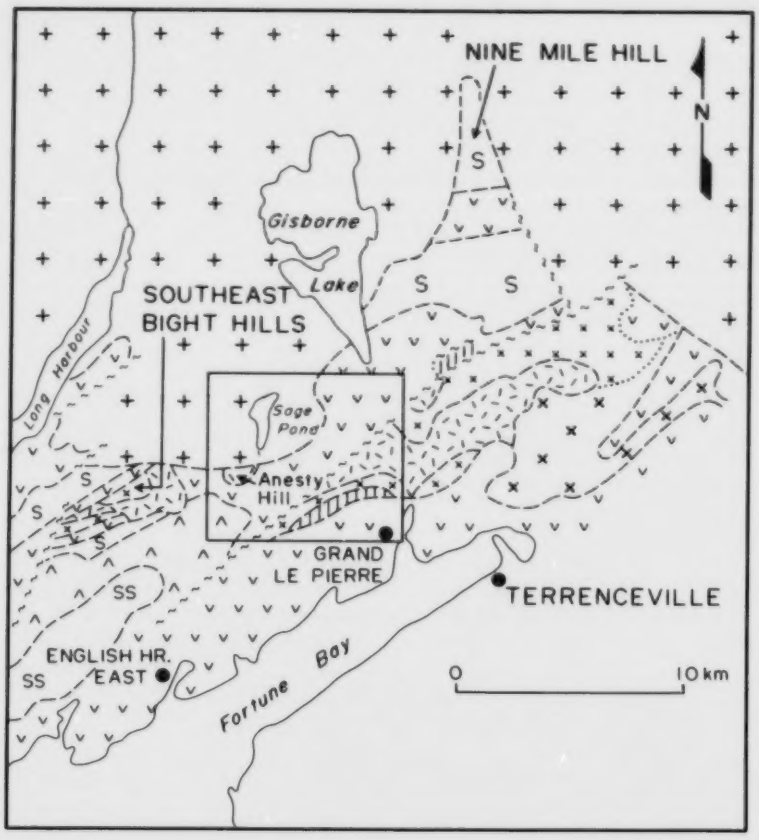

DEVONIAN

ACKLEY GRANITE SUITE

+ *Granite*

CAMBRIAN

CROSS HILLS PLUTONIC SUITE

Gabbro

× *Granodiorite*

× *Biotite Granite*

Peralkaline Granite

LATE PROTEROZOIC

LONG HARBOUR GROUP

SS Recontre Formation: *Red conglomerate*

^ Mooring Cove Formation: *Peralkaline volcanics*

S Anderson's Cove Formation: *Grey sandstone, greywacke*

v Belle Bay Formation: *Felsic volcanics*

Figure 2. *Generalized geology and distribution of rocks of the Cross Hills Plutonic Suite, Fortune Bay–Gisborne Lake area, southwestern Newfoundland. Area of detailed mapping shown on Map 91-14 is outlined.*

GEOLOGY OF THE CROSS HILLS PLUTONIC SUITE

NOMENCLATURE

O'Brien *et al.* (1984) formally proposed the name Cross Hills Plutonic Suite for the rocks assigned by Bradley (1962) to the Cross Hills Batholith. This name was introduced to comply with the recommendations of the North American Commission on Stratigraphic Nomenclature (1983), and also replaces the term Cross Hills Intrusive Suite introduced by Tuach (1984).

The main rock units that constitute the Cross Hills Plutonic Suite are not formally named in this report and are referred to by the dominant rock type of the unit (Figure 3). The subdivisions of the suite are sufficiently distinct such that a new nomenclature would be superfluous, and probably confusing. In addition, suitable geographical names to erect a formal nomenclature are not present in the area underlain by the suite.

The term biotite granite is used to describe the fine- to medium-grained rocks, which plot in the field of granite (sensu stricto) as illustrated in Figure 4. Some, but not all, of the rocks of this unit are alaskite. Significant amounts of albite and minor epidote are present along with up to 5 percent mafic minerals. Chlorite is the dominant mafic mineral and is an alteration product. Biotite was probably the dominant mafic mineral in this granite, and therefore, the name biotite granite is used to distinguish it from the peralkaline granite.

The peralkaline granite plots in the field of alkali-feldspar granite (Figure 4) and is also an alaskite in the strict sense (see Streckeisen, 1973). Some samples contain riebeckite and most have an agpaiitic index value of about 1.0.

DISTRIBUTION

The distributions of the main phases of the Cross Hills Plutonic Suite are shown in Figure 2. The main body, to the north of Grand Le Pierre, consists of a mafic unit (gabbro to diabase), granodiorite, biotite granite, peralkaline granite, and several small areas of syenite; granodiorite is

Plate 1. *View looking northeast across the Cross Hills Plutonic Suite toward the Cross Hills. The gabbro–biotite granite contact (foreground) is highlighted by a change in vegetation, i.e., more trees over gabbro.*

restricted to eastern exposures. A gabbroic body is present at Anesty Hill (Figure 2), and gabbro, diabase and biotite granite occur at Southeast Bight Hills to the west. A small body of diorite, in a roof pendant to the Ackley Granite Suite, occurs in the Gisborne Lake map area, near Nine Mile Hill, and has been assigned to the Cross Hills Plutonic Suite (O'Brien *et al.*, 1984).

ROCK TYPES

The plutonic suite (Figure 3) is subdivided into several units on the basis of field and geochemical evidence (Figure 4). These are a mafic unit (consisting of gabbro and diabase), granodiorite, biotite granite and related aplite, peralkaline granite, and minor syenite.

Mafic Rocks

These consist of a variety of dark-green to grey to black gabbro, diabase and minor diorite intrusive rocks (Plate 2) that are extensively intruded by veins and dykes of biotite granite (Plate 3); minor epidote-rich veins are common. The coarser grained rocks are usually mottled dark-green and white. Small roof pendants and xenoliths of felsic volcanic rocks occur locally and are more common to the east of Grand Le Pierre. The gabbro is medium to coarse grained and has localized patches of pegmatite and the diabase is fine to medium grained and has an ophitic texture. Fine-grained aphyric and plagioclase- and pyroxene-phyric varieties of diabase also occur. Xenoliths of earlier gabbroic and diabase phases are seen in some exposures of the mafic unit (Plate 2). Diorite is the more abundant rock type at the Southeast Bight Hills and at Nine Mile Hill (O'Brien and Nunn, 1980).

Granodiorite

Mottled, purple to orange, massive, equigranular, medium- to coarse-grained hornblende–biotite granodiorite outcrops over a large area to the east of Grand Le Pierre. Abundant felsic and mafic volcanic and diabase xenoliths are common. The granodiorite is locally cut by diabase and aplite dykes, which are up to a metre wide (Plate 4).

Biotite Granite

This is an orange, miarolitic, fine- to medium-grained, equigranular granite containing up to 5 percent mafic minerals. Small orange aplite phases are common, and an important mappable subunit of orange aplite occurs along the southern boundary of the biotite granite, to the northwest of Grand Le Pierre (Figure 3; Map 91-14). Fine- to coarse-grained pegmatite is present locally; the thinner felsic dykes that intrude the mafic rocks locally grade from an aplitic margin to a coarse pegmatite core. Xenoliths of felsic volcanic and mafic intrusive rocks are common in exposures to the northeast of Grand Le Pierre. North and west of Grand Le Pierre, felsic volcanic xenoliths are rare, and xenoliths of mafic intrusive rocks occur only in close proximity to contacts with the main bodies of mafic rocks.

Epidote veins and fracture coatings are ubiquitous, particularly near faults and lineaments. Networks of quartz-filled fractures and veins are locally common. The quartz veins are up to 1 m wide and 100 m long (Plate 5).

Peralkaline Granite

These rocks are purple-brown, miarolitic, fine- to medium- grained granite. Granophyric intergrowths are

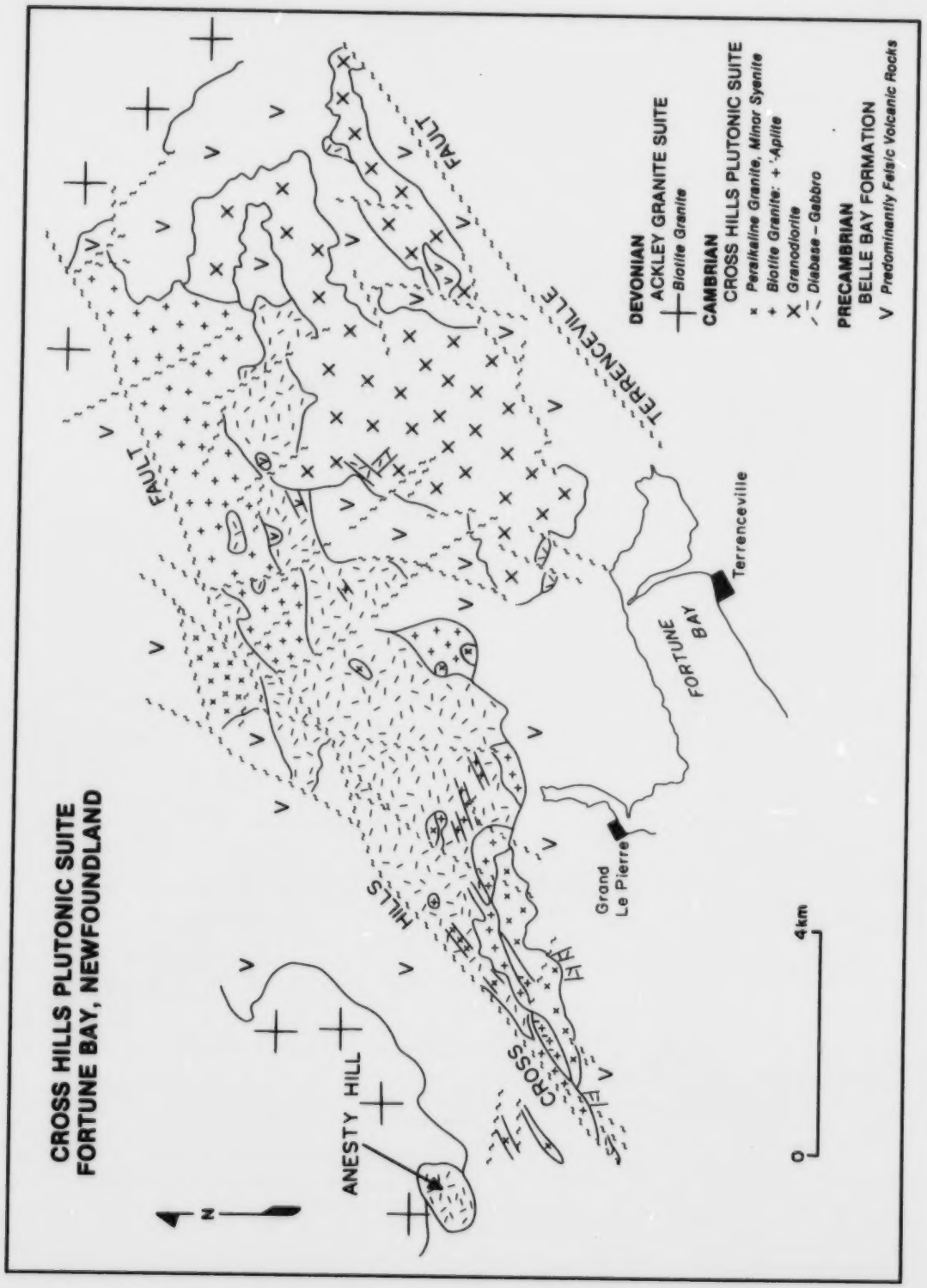

Figure 3. *Geology of the main outcrop area of the Cross Hills Plutonic Suite.*

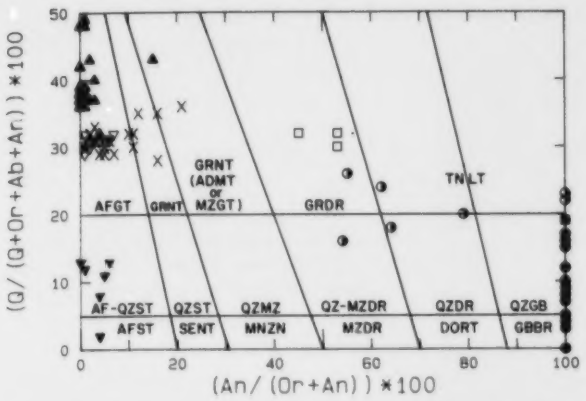

Figure 4. *Normative (mesonorms) compositions of analyzed samples from the Cross Hills Plutonic Suite. Fields after Streckeisen and LeMaitre (1979); solid circles–gabbro; half filled circles–hybrid gabbro; open squares–granodiorite; inverted solid triangle–syenite; x–biotite granite; open inverted triangle–aplite; solid upright triangle–peralkaline granite.*

Plate 2. *Representative samples of the mafic unit in the Cross Hills Plutonic Suite. Clockwise from upper left, samples JT-205, JT-60, JT-262a and JT-262.*

commonly recognized in hand specimen, and sporadic small pegmatite patches occur. Tuffisite (Plate 6), indicative of gas streaming is common. Small purple-brown aplite veins occur throughout the granite and several small (to 5 cm wide), mineralized, sheeted, gently dipping peralkaline aplite veins (Plate 7) cut medium-grained peralkaline granite at occurrence # 12 (see Figure 9).

Hematite staining is common, particularly around fractures and tuffisite. Clay alteration occurs in association with fractures near the southern contact of the granite and the felsic volcanic rocks. Quartz-vein networks and quartz veins, up to 1 m wide, occur in the peralkaline granite and are locally continuous with those in the biotite granite.

Syenite

A 50-m-long outcrop of purple, manganese-stained quartz-syenite is located 5 km northeast of Grand Le Pierre on the Grand Le Pierre road (Figure 3) and a small outcrop

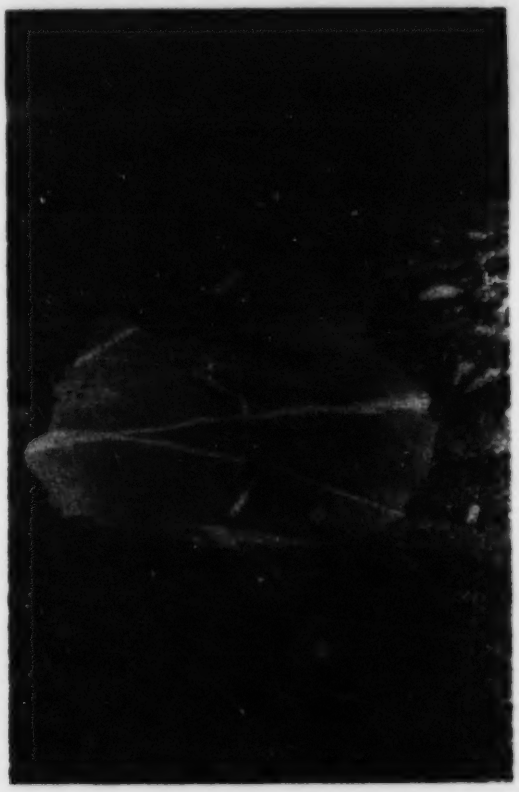

Plate 3. *Vein networks of biotite granite in gabbro. Outcrop below bridge across the Grand Le Pierre River, approximately 2 km north of Grand Le Pierre.*

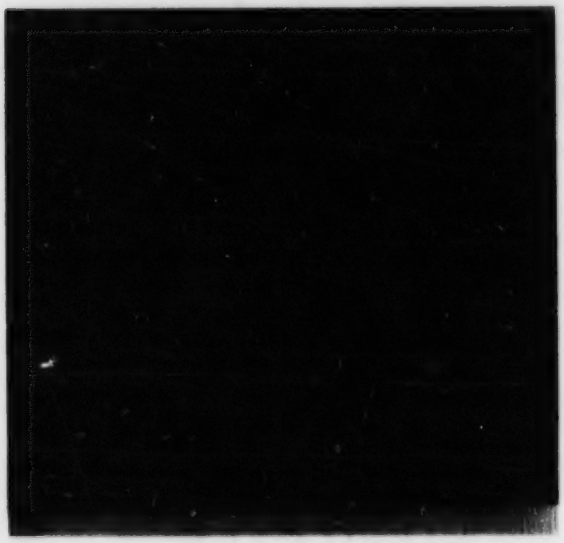

Plate 4. *Granodiorite cut by an aplite vein. Sample JT-408a.*

Plate 5. *Quartz veins in biotite granite. South of Triangle Pond (see Map 91-14), looking south.*

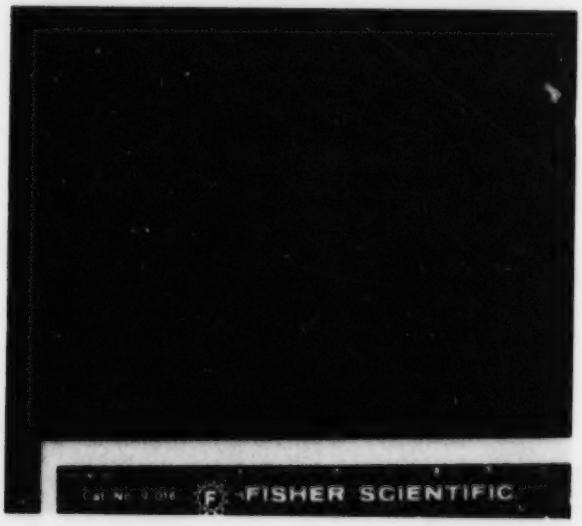

Plate 6. *Gas veins and breccias in peralkaline granite. Sample JT-440.*

Plate 7. *Mineralized (Zr–Y–Nb–REE) peralkaline aplite veins cutting medium-grained peralkaline granite at occurrence #12.*

of orange, alkali feldspar granite was noted 1.5 km to the south. These rocks are medium to coarse grained and equigranular. Two 50-m-wide, east-northeast-trending, subvertical dykes of red-brown, fine-grained, quartz-poor trachyte occur southeast of Anesty Hill (Figure 3) and approximately 1 km to the west of the main exposure of the Cross Hills Plutonic Suite. These dykes exhibit high-background radioactivity and are tentatively correlated with the alkalic and peralkaline phase of the Cross Hills Plutonic Suite.

INTRUSIVE RELATIONSHIPS

All of the main rock types of the Cross Hills Plutonic Suite are intrusive into the Belle Bay or Anderson's Cove formations of the Late Proterozoic Long Harbour Group (O'Brien *et al.* 1984; Figure 2), and roof pendants and xenoliths of country rock are present locally. Mafic rocks and biotite granite of the Cross Hills Plutonic Suite are intruded by the Late Devonian to Early Carboniferous (Kontak *et al.*, 1988) Ackley Granite Suite (Figure 2).

Most contacts are well-exposed and sharp. A narrow chilled margin (usually less than 1 cm wide) is locally present, and recrystallization in the contact aureole occurs over a maximum width of 50 m. However, east of Grand Le Pierre, the intrusion of the mafic unit caused local recrystallization and partial melting of the country rock, roof pendants, and xenoliths, as indicated by diffuse contacts and coarse grain size in felsic volcanic rocks. Granitic veining also occurs in these recrystallized felsic volcanic rocks.

Major contacts and units, in the main outcrop area, show an east-northeast trend (Figure 3; Map 91-14). This trend is emphasized by swarms of biotite granite dykes in the southern part of the mafic unit to the northwest of Grand Le Pierre. These map patterns indicate north-northwest-directed tensional controls on emplacement of the Cross Hills Plutonic Suite.

Biotite granite (Plate 3) and peralkaline granite intrude diabase and gabbro west of Grand Le Pierre. East of Grand Le Pierre, granodiorite and biotite granite intrude these mafic rocks. The granodiorite is locally intruded by small diabase and aplite dykes (Plate 4). However, its relationship to the main body of biotite granite is unknown. Locally, peralkaline granite is intrusive into biotite granite; however, the relationship between these units is commonly gradational as described below. Intrusive contacts occur internally in the mafic unit, and together with the presence of mafic xenoliths in the gabbros (Plate 2), indicate the composite nature of the mafic phase. The relative intrusive relationships between the small syenite bodies and the other phases of the Cross Hills Plutonic Suite were not observed. Most internal contacts in the Cross Hills Plutonic Suite are sharp and narrow (less than 2 cm wide). The more important contact relationships are described below.

Gabbro and Biotite Granite

Hybrid gabbro-granite rocks, containing small granitic patches in a gabbro-diabase host, are common over a distance up to 2 m at the margin of the granite intrusions into mafic rocks. These hybrid rocks are pale orange and become darker toward the orange biotite granite.

Biotite Granite and Aplite

The contact between the biotite granite and related aplitic phase can be traced over a distance of 2 km in the Bart Pond area (Figure 5). The contact is a sharp boundary marked by minor patches of pegmatite within the biotite granite (Plate 8). On a larger scale, the aplite coarsens southward.

Aplite–Biotite Granite and Peralkaline Granite

The contact of the biotite granite and its aplitic phase with the main area of peralkaline granite, to the northwest of Grand Le Pierre, varies from gradational to sharp over a distance of 2 to 20 m. It is described, in more detail, in a later section on contact relationships between biotite granite and peralkaline granite.

Peralkaline Granite and Country Rocks

This contact is well-exposed along the southern boundary of the Cross Hills Plutonic Suite. A chill zone, generally less than 1 cm wide, occurs in the medium-grained granite, and obvious recrystallization of the country rock is restricted to

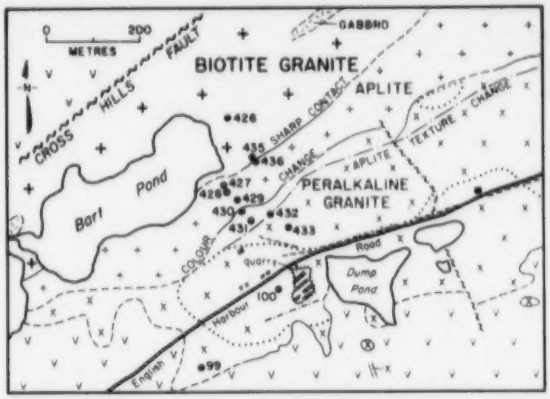

CROSS HILLS PLUTONIC SUITE
Bart Pond Area

Anomalous radioactivity (fractures, spots)
Sericite rich zones
Limit of hematite stains
Lithogeochemical samples • 99
Contact (defined, approximate)

Figure 5. *Geology, mineral occurrences, anomalous radioactivity and sample locations around Bart Pond, English Harbour Road; V–volcanic rocks*

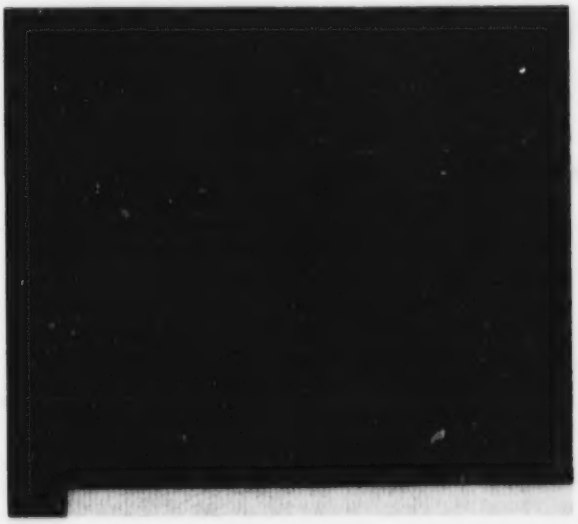

Plate 8. *Contact of biotite granite (right) with aplite (left). Note small pegmatite patches in the biotite granite at the contact. Sample JT-434.*

less than 50 m from the contact. The contact is irregular in detail, and small dykes and sills (< 2m thick) of peralkaline granite occur locally in the Belle Bay Formation for a distance of 50 m to the south (Figure 5).

PETROGRAPHY AND MINERAL CHEMISTRY

Petrography

Mafic Rocks

These rocks are characterized by a grain size of 0.1 mm to 5.0 mm and a primary mineralogy of augite, generally normally zoned plagioclase, brown hornblende, magnetite, ilmenite, and locally biotite, sphene and apatite. The diorite contains up to 5 percent interstitial quartz, and minor interstitial quartz and K-feldspar are common in the hybrid rocks adjacent to granitic dykes. Coarse-grained gabbro from Anesty Hill contains up to 15 percent magnetite. Augite is commonly poikilitic, enclosing euhedral plagioclase and magnetite, and is variably altered to actinolite and/or chlorite (commonly penninite). Plagioclase cores are variably saussuritized and epidotized. Serpentine pseudomorphs after olivine are present in the more mafic rocks. Numerous epidote-bearing fractures are common, and quartz-filled fractures containing accessory fluorite were noted. Optical determinations indicate that the hybrid gabbro contains plagioclase (An_{38}), which is generally unzoned.

Granodiorite

Grain size ranges from 2 to 5 mm. Minerals present are zoned plagioclase, quartz, perthite, hornblende, and biotite, containing accessory sphene and magnetite. Biotite and chlorite occur as interstitial grains, and interstitial graphic intergrowths of quartz and K-feldspar are common. Quartz commonly exhibits weak to moderate undulose extinction. Plagioclase and perthite are variably altered to saussurite, sericite, and epidote, and biotite and hornblende are commonly altered to chlorite.

Biotite Granite

These rocks are characterized by a grain size from 1 to 2 mm (Plate 9a), and a primary mineralogy of quartz, perthite, microcline, plagioclase (albite), biotite and locally minor hornblende. Up to 5 percent mafic minerals are present. Graphic to micrographic intergrowths of quartz and feldspar are ubiquitous and may surround small feldspar crystals. Aplite having a spherulitic texture (Plate 9d) occurs locally and forms a mappable unit up to 200 m wide (Figures 3 and 5). Up to 2 percent opaque minerals are present as euhedral or interstitial crystals along with sphene and allanite. Small miarolitic cavities are commonly filled with quartz. K-feldspar and plagioclase are slightly saussuritized, and biotite and hornblende are usually altered to chlorite. Minor, secondary muscovite occurs locally, and interstitial fluorite grains (up to 0.1 mm diameter) were noted in one sample. Epidote is common in fractures. The rocks to the east of Grand Le Pierre are generally more altered than those to the west.

Peralkaline Granite

These rocks contain quartz, perthitic feldspar, microcline, plagioclase (albite), chlorite, hematite (commonly skeletal), ilmenite, and locally riebeckite and aegirine; allanite, sphene, apatite, and monazite are accessory minerals. The grain size is between 1 and 2 mm, and micrographic to graphic intergrowths of quartz and feldspar, up to 2 mm in diameter, are ubiquitous (Plate 9f-h). Riebeckite and hematite occur as interstitial phases. Feldspars are fresh to weakly sericitized, and chlorite is the most common Fe–Mg mineral and is presumably an alteration mineral after riebeckite. Minor dispersed granular epidote occurs locally, and is commonly found in fractures. Tuffisite veins exhibit a microbreccia texture and may contain finely comminuted granite. Feldspars in these veins do not show additional evidence of secondary alteration; however, the opaque mineral content is commonly greater in the veins than in the host rock. Miarolitic cavities (0.5 cm diameter) are filled with unstrained terminated quartz crystals. Small grains of zircon (up to 0.1 cm diameter) occur in the granite, and up to 2 percent zircon occurs as disseminated grains and in fractures in narrow ($<$ 5 cm wide) aplite veins at occurrence # 12 (see Figure 9).

Syenite

The syenite on the Grand Le Pierre road contains perthite, microcline, plagioclase, quartz, ferrohedenbergite, riebeckite and biotite; the grain size is approximately 3 mm. The syenite dykes to the west of the main intrusive body consist of perthite, microcline, plagioclase, minor quartz, chlorite, and very fine grained, disseminated opaque grains. Sodic amphibole and/or pyroxene occur locally, and accessory fluorite and sphene are present. Grain size is less than 0.5 cm and trachytic flow layering is the dominant texture.

Mineral Chemistry

Microprobe analyses of minerals from several samples were performed to provide some preliminary information on the mineral chemistry of the rocks in the Cross Hills Plutonic Suite. These data are presented here along with some preliminary interpretations. Analytical techniques are outlined in Appendices 1A and 2.

Plagioclase

Plagioclase composition was determined by optical methods and electron microprobe analyses of a few data points from several samples. Analyses of a strongly zoned plagioclase crystal in gabbro (sample JT-311, Appendix 2A) indicate a wide compositional range from An_{67} (core) to An_{43} (rim). Analysis of the core of a crystal in gabbro sample JT-338 gave a result of An_{63}. Determinations by optical methods consistently gave values of An_{68} for plagioclase cores (from various samples), and generally defined values of An_{40} to An_{48} for rims. Analyses of the core and rim of a crystal in gabbro sample JT-262 returned values of An_{24} indicating either non-zoning or a section through the rim of the crystal. Determination of the composition of another crystal in the section, by optical methods (combined Carlsbad–Albite twinning) indicates zonation from An_{32} to An_{54}. Hybrid gabbro contains unzoned plagioclase. Determination of

composition by optical methods gave consistent values of about An_{38} for various samples.

The biotite granite contains unzoned plagioclase, which ranges from An_0 to An_6, as determined by optical methods. The granodiorite contains zoned plagioclase but as albite twinning is rare, the An content could not be determined by optical methods. However, plagioclase cores are more heavily altered than rims, suggesting normal zoning. Electron microprobe analysis of a K-feldspar from granodiorite sample JT-410 returned values of Or_{48}, Ab_{37} and An_{14}.

The composition of plagioclase in the gabbro is representative of crystallization from a silicate magma. The presence of almost pure albite ($> Ab_{99}$) in sample JT-124 (mineralized aplite from mineral occurrence # 13) and also from the peralkaline granite (sample JT-433), indicates subsolidus growth or recrystallization of the plagioclase. The uniform composition of plagioclase in the hybrid gabbro suggests recrystallication and/or re-equilibration during emplacement of the granite.

Pyroxene

The pyroxenes (Appendix 2B) in the gabbro have a relatively low Fe(tot)/Fe(tot) + Mg ratio that is characteristic of augite from a relatively unevolved mafic suite (Figure 6). The pyroxene in the syenite (sample JT-264A) has relatively high values of Fe and Mn, and low values of Al, Na and K, which are characteristic of ferrohedenbergite (cf. Deer *et al.*, 1963).

Amphibole

Amphibole (Appendix 2C) in the gabbro has a mean Fe(tot)/Fe(tot)+Mg ratio (X_{Fe}) of 0.32 and Al^{IV}+Ca:Si+Na+K ratios, which plot in or near the barroisite field (Figure 7). In contrast, amphibole in the peralkaline granite has a high Fe and Na content and a relatively high K content. It also contains significant amounts (up to 8 percent) of MnO. These samples plot in the riebeckite and arfvedsonite fields. As expected, amphibole in the aplite subunit of the biotite granite has an intermediate ratio and alkali content and plots in the barroisite field. The two samples of amphibole from granodiorite have similar X_{Fe} ratios and slightly lower alkali contents and also plot in this field. Amphibole from the syenite sample has a higher Fe content comparable to amphibole from the peralkaline granite, however, amphibole in the syenite has low Na and K content and plots near the barroisite field.

Biotite

The analyses of biotite (Appendix 2D) in the gabbro indicate relatively high Mg, but one result would be classified as phlogopite. Analyses of biotite in the biotite granite show medial Fe(tot)/Fe(tot) + Mg ratios of 0.51 and 0.53, and an analysis of biotite in the syenite has a Fe-rich annite composition. Biotite does not occur in the peralkaline granite.

Chlorite

The composition of chlorites (Appendix 2E; Figure 8) in the biotite granite and the granodiorite are similar with X_{Fe} ratios between 0.44 and 0.57. One analysis of chlorite from the syenite shows a ratio of 0.9.

Opaques

Several of the probed opaque grains in the peralkaline granite contain abundant Ti and Fe and are probably ilmenite. Reliable quantitative analyses were not obtained. Many other opaques contain Fe but no Ti and are probably hematite. These opaque grains commonly contain significant MnO (up to 10 percent).

STRUCTURE

The Cross Hills Plutonic Suite appears to cut the tectonic fabrics, bedding, and major fold structures in the Upper Proterozoic Belle Bay Formation (see map pattern in O'Brien *et al.*, 1984), and a narrow contact aureole (less than 50 m) is developed in which the country rocks display a local hornfels texture. This crosscutting relationship was not directly observed because fabrics in the Upper Proterozoic rocks are commonly poorly developed, and bedding features and small folds are rare. In addition, rocks of the plutonic suite generally do not exhibit a mineral alignment. Therefore, the Cross Hills Plutonic Suite is posttectonic with respect to the deformation that affected the Upper Proterozoic rocks.

The northeast-trending Cross Hills Fault (Bradley, 1962) forms the northwestern boundary of the main body of the Cross Hills Plutonic Suite. This structure is a normal fault, commonly defined by a small topographic depression, with downthrow to the northwest, and is truncated to the northeast by the Ackley Granite Suite (Figure 3; O'Brien *et al.*, 1984). The rocks adjacent to the fault are commonly brecciated, and contain veins and net-veins of quartz and epidote for a distance of 50 m on either side. Isolated quartz veins, up to 2 m wide, occur in, and parallel to, the fault zone.

Numerous northwest-, north-, and north-northeast-trending faults and lineaments occur throughout the area (O'Brien *et al.*, 1984), and effect both the Cross Hills Plutonic Suite and the northwest structures. Brecciation, and quartz and epidote veining are also a common feature associated with these structures.

ALTERATION

The common occurrence of chlorite, epidote and sericite in the plutonic rocks can be attributed to several processes: (1) either reaction with magmatic hydrothermal fluids during devolatilization of the crystallizing magma, or reaction with meteoric fluid systems generated immediately following pluton emplacement and crystallization; (2) fluid migration along later faults and fractures developed in a cooled pluton possibly related to intrusion of the Ackley Granite Suite, or

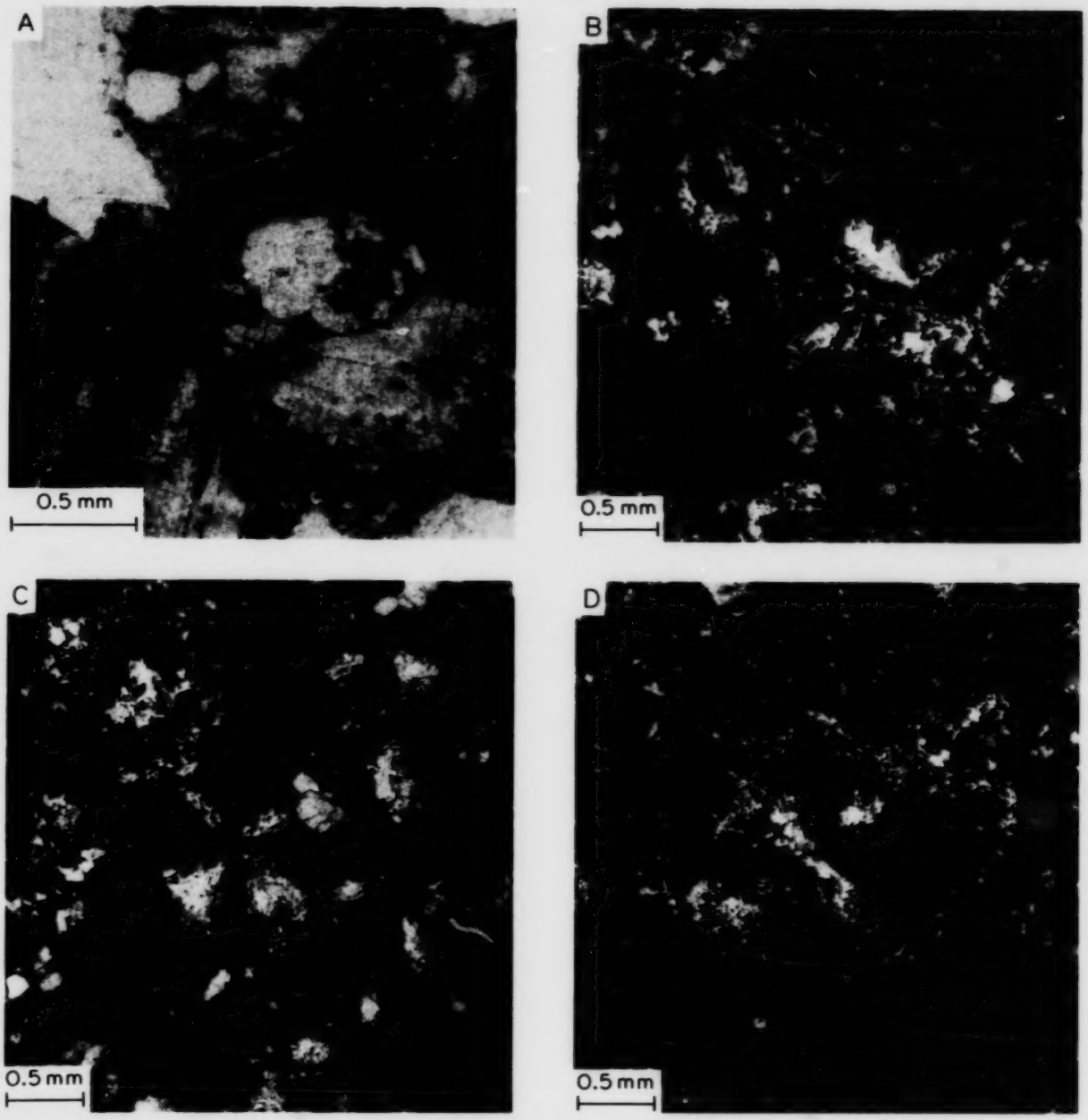

Plate 9. *Photomicrographs showing the progression of textures in the biotite granite (BGRT), its aplite subunit (APLT) and the peralkaline granite (PGRT): a) sample JG-426, BGRT, equigranular texture; b) sample JT-436, APLT, spherulitic texture; c) sample JT-427, APLT, spherulitic texture; d) sample JT-428, APLT, relict spherulitic texture; e) sample JT-429, APLT, micrographic texture; f) sample JT-431, PGRT, myrmekitic texture; g) sample JT-432, PGRT, graphic texture; h) sample JT-433, PGRT, graphic texture—the cloudy nature of the K-feldspar results from hematite inclusions. All photos except the last are taken under crossed nicols. Scale bar for each photo represents 0.5 mm.*

(3) regional metamorphism and devolatilization. Since the Cross Hills Suite is essentially posttectonic, it is unlikely that regional metamorphic effects were significant.

Minor epidote and quartz-filled fractures and veins, and the locally pervasive epidotization of feldspar in the granites adjacent to faults and lineaments, indicate that some alteration occurred during post-consolidation fracturing. Larger quartz veins, up to 3 m wide, having traces of copper mineralization that cut the granites, and one vein located in the Cross Hills Fault, attest to substantial post-consolidation fluid migration.

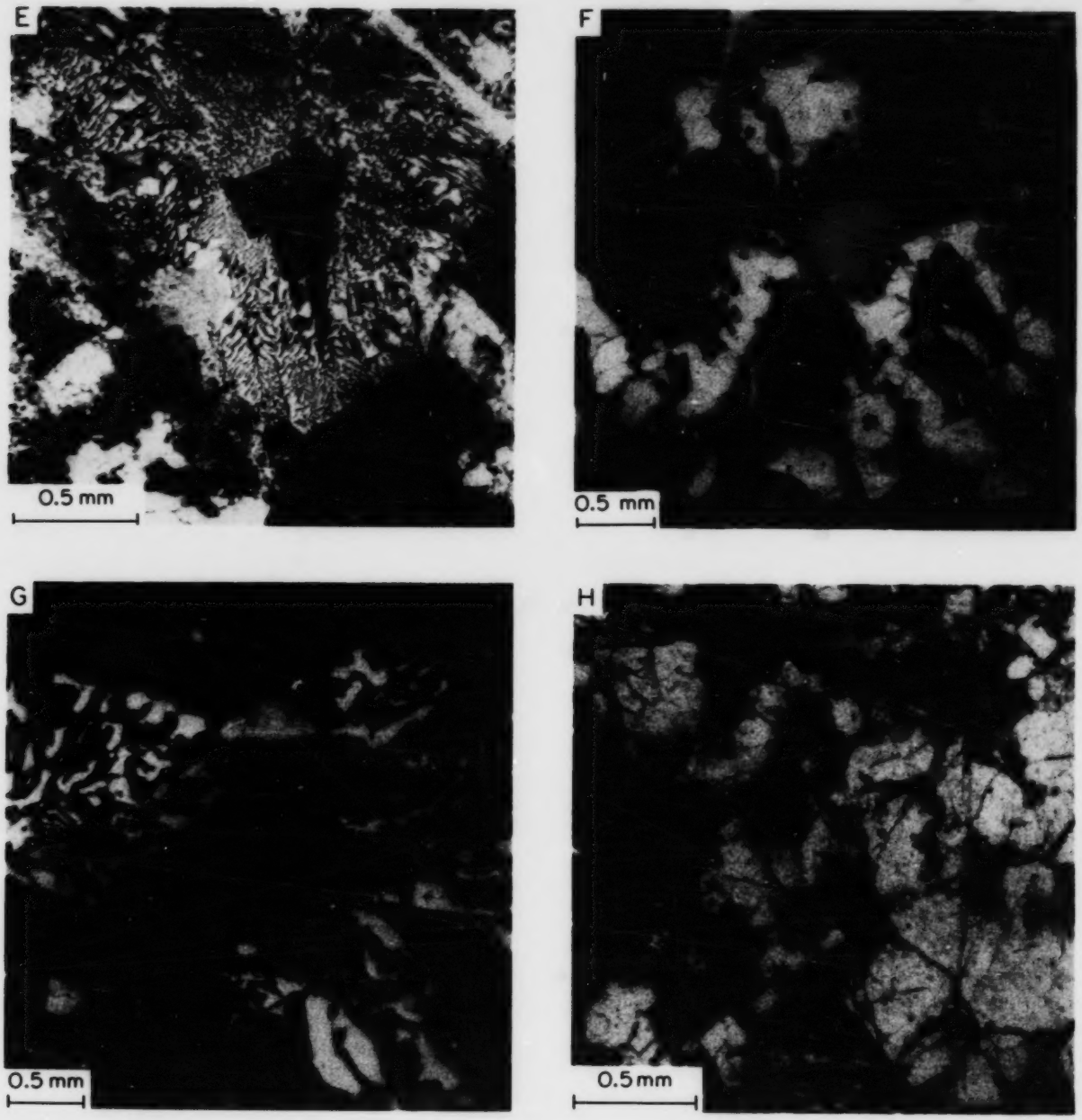

Plate 9. *Continued.*

In the peralkaline granite, an irregular-shaped area of hematite-stained calcite approximately 2 by 5 m is present northeast of Grand Le Pierre (Map 91-14; Figure 9). The calcite crystals are approximately 4 mm in diameter. Its presence suggests that carbonate-rich fluids were formed during the hydrothermal evolution of the Cross Hills Plutonic Suite.

Red-brown hematite- and limonite-stained peralkaline granite having 1 to 5 percent fine-grained, disseminated pyrite is ubiquitous over an area of 200 by 1000 m along the English Harbour road, to the southeast of Bart Pond (Figure 5). Other small areas are present along strike to the east. Hematite grains are common in the granite and are more abundant in tuffisite zones. The tuffisite is interpreted to have developed during crystallization and devolatilization of the magma. This indicates that at least some of the hematite crystallized from an aqueous phase, and suggests that the abundance of hematite and subsequent staining is a feature of magmatic-hydrothermal alteration in the granite. Fine-grained hematite and locally manganese are common on fractures and joints throughout the granitic rocks.

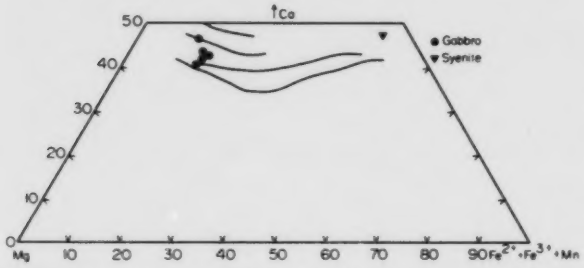

Figure 6. *Pyroxene compositions (atomic percent) plotted on a CFM diagram. Trends of pyroxene crystalization from Deer* et al. *(1963).*

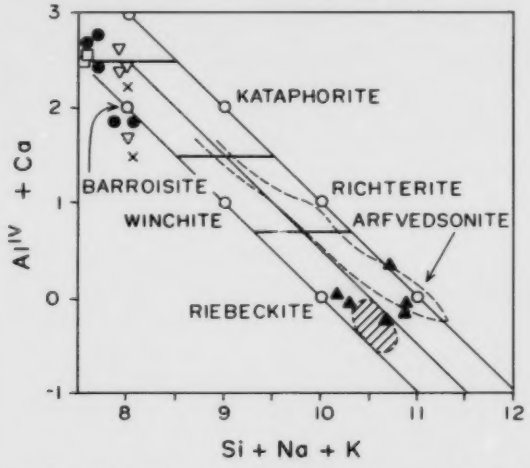

Figure 7. *Composition of amphiboles plotted using cation proportions of Al^{IV} + Ca vs. Si + Na + K. Mineral field boundaries after Giret* et al. *(1980) and mineral terminology after Leake (1978). Symbols as for Figure 4. Dashed line enclosed igneous amphiboles from the Topsails and St. Lawrence granites; hatched field represents hydrothermal amphiboles from the Topsails and St. Lawrence granites (from Strong and Taylor, 1984).*

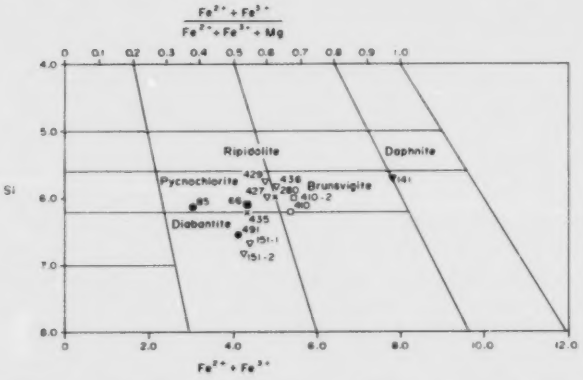

Figure 8. *Chlorite compositions. Solid circles–gabbro; open squares–granodiorite; inverted solid triangle–syenite; x–biotite granite; open inverted triangle–aplite; solid square–peralkaline granite.*

Subvertical veins of pervasive grey-green sericite (confirmed by XRD analyses) alteration up to 3 m wide and 30 m long and trending 070°, occur in a small quarry immediately to the west of Dump Pond (Figure 5). Fine-grained, disseminated and fracture-filling pyrite (up to 3 percent) is present, and traces of galena were noted.

MINERAL OCCURRENCES

Zr–Y–Nb–REE

Radioactive Zr–Y–Nb–REE enrichments in the peralkaline granite are the most significant mineral occurrences (Table 1, Figure 9). Radioactivity is 4 to 5 times the background count at the mineralized locations with high spot values up to 10 times the background count. Anomalous values of Sn, Th, Cu, Ag, Pb and Zn were also recorded (see Appendices 3A, 4D).

The best assay results for Zr–Y–Nb–REE were obtained from chips of thin, peralkaline aplite veins that intrude peralkaline granite in a 3- by 2-m, trenched outcrop at occurrence # 12 (Figure 9; Plate 7). The outcrop contains 5 to 10 percent, gently dipping, up to 5-cm-wide, sheeted aplite veins. A selected sample of vein material (JT-124) assayed 19208 g/t Zr, 2968 g/t Y, 1860 g/t Nb, 1550 g/t Ce, 725 g/t Th and 90 g/t Sn. The host granite has weak anomalous radioactivity but does not have anomalous uranium or thorium values. Previous semi-quantitative analyses also returned anomalously high values of these elements (Appendix 3A). Abundant fine-grained, euhedral zircon (>0.1 mm) is disseminated in the aplite matrix and is concentrated in tuffisites (Plate 10) and fractures in the veins. It is commonly intergrown with hematite (Plate 11). Scanning electron microscope (SEM) analyses reveal a variety of Zr, Y, Nb and REE-rich minerals (Saunders and Tuach, 1989). These include traces of baddelyite (ZrO_2), and possible fergusonite ($YNbO_4$; Plate 12 and Figure 10a). Unidentified Nb and REE-rich minerals were also found (Plate 13 and Figure 10b, c, d).

At occurrence # 11, located approximately 200 m west of Occurrence # 12 (Figure 9), a 10- by 5-m area of anomalous radioactivity (up to 5 times the above background levels) occurs in a south-facing scarp. A selected sample of radioactive chips (JT-067) assayed 6800 g/t Zr, 1619 g/t Y, 809 g/t Nb, 762 g/t Ce, 364 g/t Th and 40 g/t Sn. Botryoidal, zoned zircon (Plate 14) is concentrated in tuffisite and fractures (Plate 10) and fills spaces between feldspar crystals (Plate 15). Zoning may be due to variations in Fe and Mn content (determined by SEM analysis). Some zircons are cored by thorium silicate (Plate 16 and Figure 10e), which may be thorite ($ThSiO_4$). Thorium oxide is also common (Plate 16 and Figure 10f). This is isotropic and may be a metamict product of the thorium silicate. Unidentified Th–Nb minerals were also found (Plate 17 and Figure 10g,h).

The location of radioactive fractures (occurrence # 2, Figure 9) just south of a quarry on the English Harbour Road is shown on Figure 5. A chip sample (JT-131) assayed 620 g/t Th.

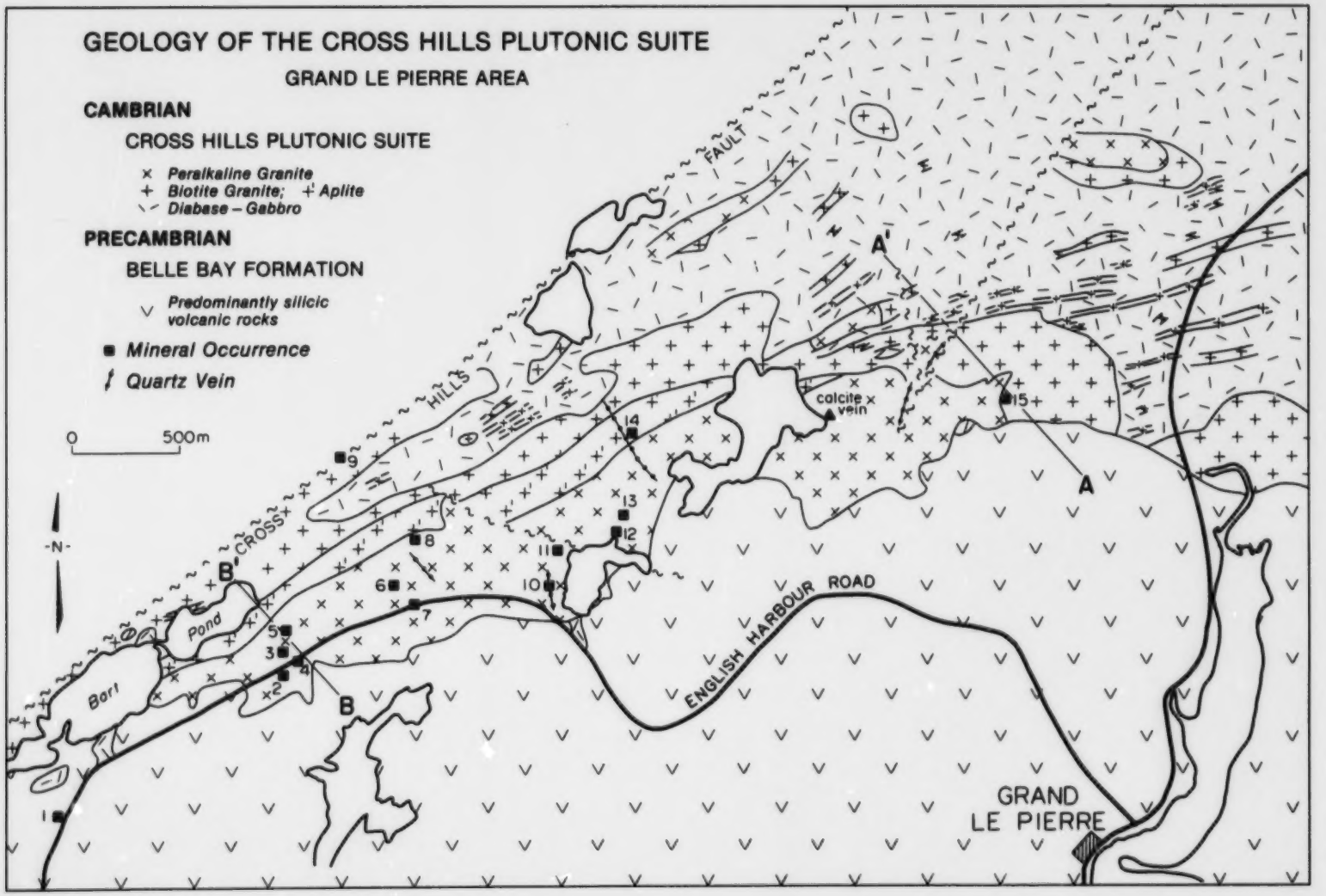

Figure 9. *Geology and mineral occurrences in the Cross Hills Plutonic Suite in the Grand Le Pierre area. Occurrence numbers refer to Table 1. A-A' and B-B' refer to sections shown schematically in Figure 11.*

Table 1. Mineral occurrences in and adjacent to the Cross Hills Plutonic Suite. Assays presented are of selected grab samples*

Occurrence No.	Mineral or Anomaly	Description**		Zr	Nb	Y	Ce	Th	Sn	Sample No.	Comments	Ref.
1	Malachite	Minor stain in sheared rhyolite	Trace over 1 m²								n.a.	T
2	Radioactive, Up to 6 x background	Patchy. In isolated fractures in peralkaline granite	Fractures over 100 x 20 m area	581	Tr	799	Tr	620	Tr	JT-131		T
3	Radioactive	In peralkaline granite	-	11661	806	n.a.	n.a.	268	93	CH-3B-1		H
4	Pyrite, galena	Disseminated in subvertical 2-m-wide sericitized zone in peralkaline granite	2 percent pyrite, trace galena	1190	Tr	139	Tr	Tr	Tr	JT-129	Also 481 g/t Pb and 840 g/t Zn	T
5	Pyrite, galena	In quartz vein cutting peralkaline granite	Trace								n.a.	H
6	Radioactive	In peralkaline granite	-	9518	556	n.a.	n.a.	259	70	19		H
7	Radioactive, pyrite	Fractures, weak anomalous radioactivity in peralkaline granite	Up to 5 percent pyrite							JT-86	All values at background levels	T
8	Radioactive	In peralkaline granite	-	7576	974	n.a.	n.a.	477	47	18		H
9	Chalcocite, malachite	Veinlets in 1-m-wide quartz vein cutting biotite granite in fault zone	Trace over 0.5 m² area							JT-57	n.a.	T
10	Malachite	In 0.5-m-wide quartz vein cutting peralkaline granite	Trace over 0.5 m²								n.a.	T
11	Radioactive	Fracture surfaces in south-facing scarp in peralkaline granite	10 m² area	6800	809	1619	762	364	40	JT-67		T
12	Radioactive, hematite	In aplite veins (to 12 cm, average 3 cm wide) in peralkaline granite. Abundant fine-grained zircon in fractures	1 x 2 m area	20000 19208	2334 1860	n.a. 2968	n.a. 1550	550 725	240 90	11 JT-124	Also 108 g/t Ta and 41 g/t U	H T
13	Radioactive	In peralkaline granite	-	10208	425			187	118	14		H
14	Malachite, chalcocite	In 2-m-wide quartz vein cutting biotite granite	Trace								n.a.	H
15	Radioactive	-	-	6328	316			188	37	22		H

H–Hopfengaertner (1982) T–This report *–All values in g/t. Tr–trace; n.a.–not analyzed **–Unavailable or sketchy for some of the Saarberg Interplan occurrences.

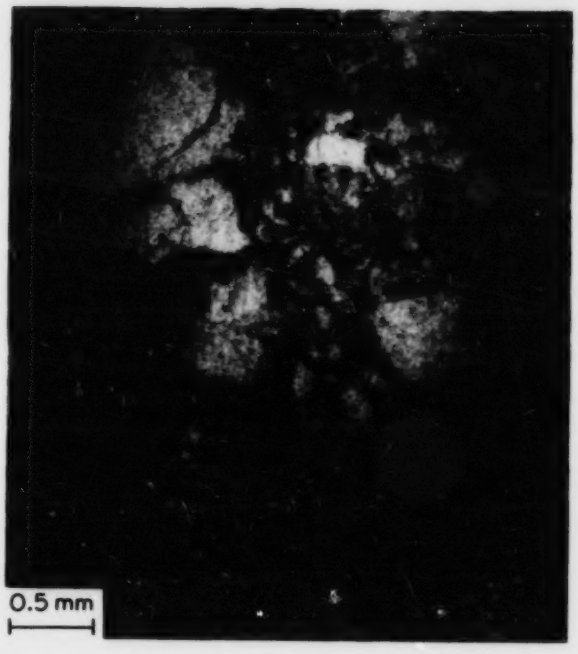

Plate 10. *Photomicrograph showing tuffisitic texture in mineralized peralkaline granite, sample JT-100, crossed nicols, scale bar represents 0.5 mm.*

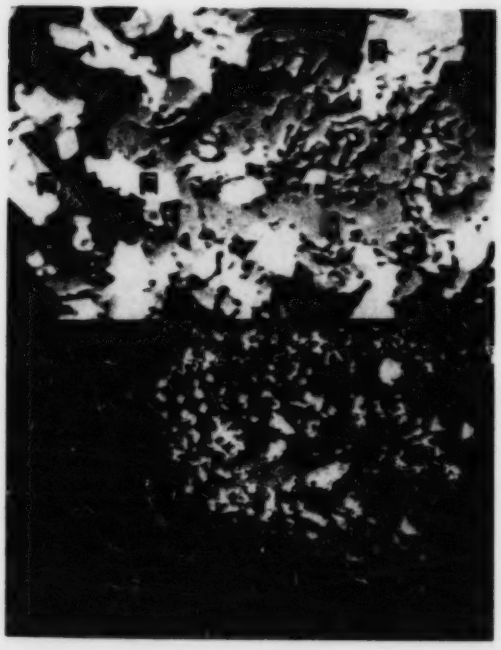

Plate 11. *Scanning electron microscope backscatter photograph of euhedral zircon (Z) intergrown with hematite (H). Black is silicate gangue. Scale bar refers to lower half of photo; scale of top (area in box) is 5x scale of bottom. Sample JT-124.*

Plate 12. *Scanning electron microscope backscatter photograph of Nb–Y mineral (fergusonite?). H–hematite. All white is the Nb–Y mineral. Sample JT-124. Spectral scan shown in Figure 10a.*

Base Metals

Small areas of malachite staining, associated with traces of chalcocite and bornite, occur in quartz veins (Table 1; occurrence #'s 1, 9, 10 and 14 on Figure 9). The quantity of copper present is insignificant; gold and silver values in two assayed samples were below the detection limit (Appendix 3). A small area of malachite staining associated with chalcocite was also noted in rhyolite tuff approximately 5 m west of the west contact of the granodiorite on the Grand Le Pierre–Terrenceville road (see O'Brien *et al.*, 1984).

Traces of disseminated galena were noted in the sericitized zones in and near the quarry on the English Harbour Road (Figure 5). These occurrences are not of economic importance.

EMPLACEMENT OF THE CROSS HILLS PLUTONIC SUITE

The strong east-northeast trend of the units, contacts and dykes in the Cross Hills Plutonic Suite is interpreted to result from north-northwest crustal extension during emplacement of the alkali gabbro, biotite granite and peralkaline granite phases. The field relationships indicate high-level passive stoping and emplacement of the mafic magmas into the Belle Bay Formation, and continued stoping and passive emplacement of the granitic rocks into fractures in the mafic rocks. The relationship of the granodiorite to the rest of the suite is less well known.

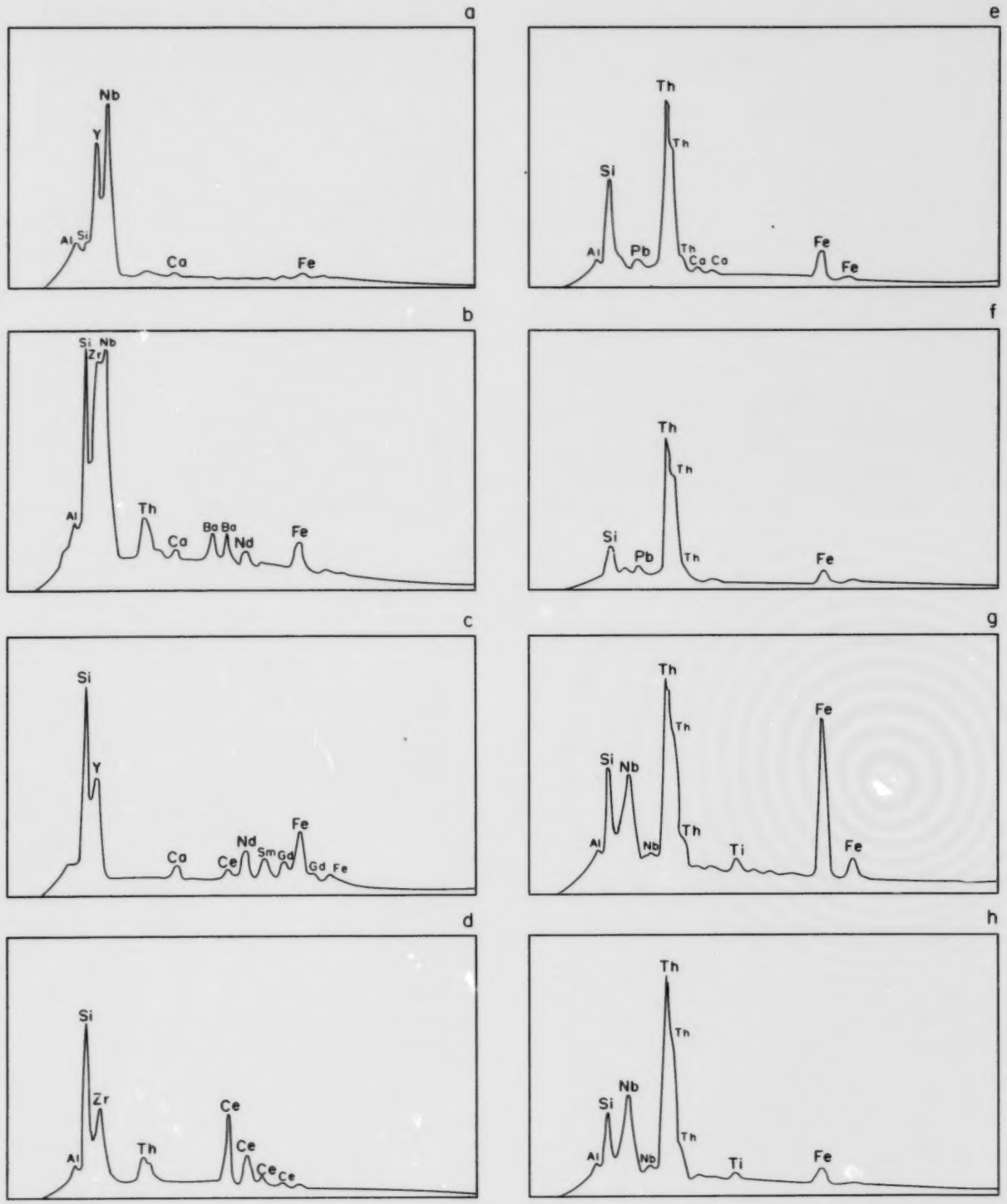

Figure 10. *Scanning electron microscope spectra of minerals from occurrence # 11 (sample JT-067) and occurrence # 12 (sample JT-124) (see Figure 9): a) fergusonite?—sample JT-124; b,c,d) unidentified minerals—sample JT-124; e) thorite?—sample JT-067; f) thorium oxide—sample JT-067; g,h) unidentified minerals—sample JT-067.*

Plate 13. *Scanning electron microscope backscatter photograph of REE mineral intergrown with zircon (Z). Spectral scan of REE mineral is shown in Figure 10. Scale of top is 2x scale of bottom. Sample JT-124.*

The peralkaline granite commonly occurs topographically above the biotite granite, and the biotite granite occurs above the mafic unit. A composite section (Figure 11) summarizes the apparent horizontal and vertical relationships of the various phases of the Cross Hills Plutonic Suite in the detailed study area to the northwest of Grand Le Pierre (Figure 2; Map 91-14). Map patterns and textural and intrusive relationships indicate that toward the west of the suite the roof zone is exposed at progressively higher levels.

GEOCHEMISTRY

MAJOR- AND TRACE-ELEMENT DATA

Introduction

Ninety-nine rock samples were collected and analyzed from the Cross Hills Plutonic Suite. These data are summarized in Table 2 and individual analyses are listed in Appendix 4. Most samples were collected from the detailed study area to the northwest of Grand Le Pierre (Map 91-15); 4 samples were collected from the Southeast Bight Hills, and two samples from the gabbro at Anesty Hill.

Seventeen felsic volcanic samples and 3 mafic volcanic samples from the Belle Bay Formation were analyzed (Appendix 4D), and along with those from the Mooring Cove

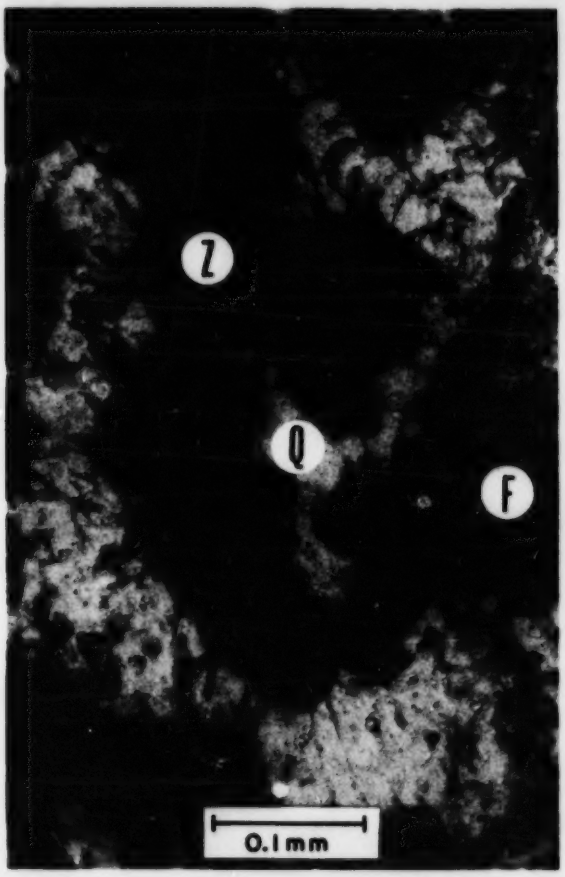

Plate 14. *Photomicrograph of hydrothermal, botryoidal, zoned zircon (Z) from occurrence # 11. Also visible are K-feldspar (F) and quartz (Q). Sample JT-067, plane light.*

Formation (S. O'Brien, personal communications, 1988), provide data for comparative purposes. The analyses from the volcanic rocks are not discussed below, however, they show that the felsic rocks of the Belle Bay Formation have continental affinity and that the Mooring Cove Formation is peralkaline and is possibly equivalent to the peralkaline phase of the Cross Hills Plutonic Suite (O'Brien *et al.*, 1990).

Analyses were performed at the Department of Mines and Energy's laboratory in 1984. Details of analyses, accuracy and precision are given in Appendix 1.

Harker Diagrams

Geochemical data from the Cross Hills Plutonic Suite are summarized on Harker diagrams in Figures 12, 13, 14 and in Table 2. Five main geochemical groups are recognized, which correspond to mapped rock units: these are mafic rocks (gabbro and diabase), granodiorite, biotite granite (includes aplite), peralkaline granite and syenite.

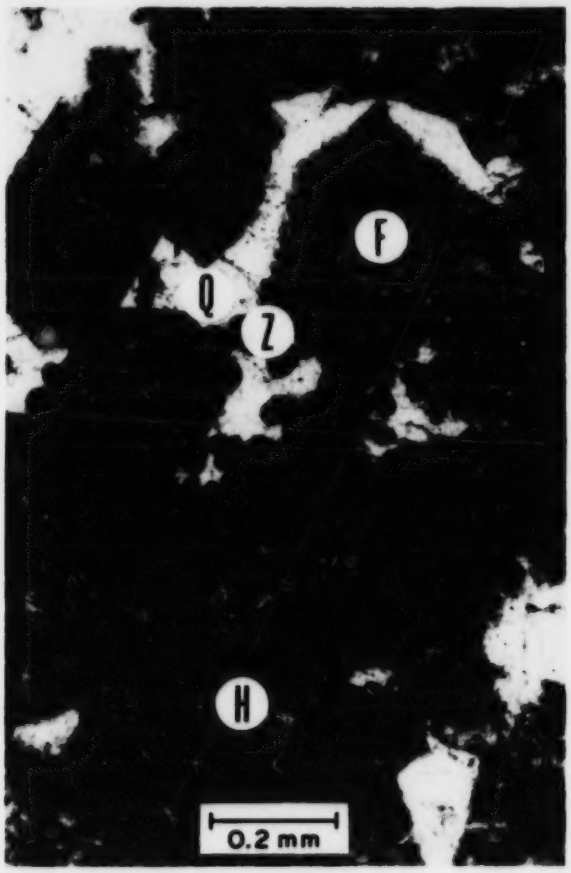

Plate 15. *Photomicrograph of botryoidal zircon (Z) surrounding K-feldspar crystals (F). Also visible are quartz (Q) and fine grained hematite (H). Sample JT-067, plane light.*

Major Elements

The major-element distributions (Figure 12) show the wide compositional range of the Cross Hills Plutonic Suite. Silica varies from a low of 44 percent in gabbro to a high of 78 percent in peralkaline granite. The major rock types have a well-defined silica range with mafic rocks varying from 44.3 to 52 percent, granodiorite from 68.4 to 70.2 percent, biotite granite (including aplite) from 73.5 to 75.8 percent, and peralkaline granite from 75.8 to 77.7 percent. The syenites and the hybrid gabbro-biotite granites have a larger range, which reflects a more varied origin.

The mafic rocks have a large Al_2O_3 range from 13.7 to 18 percent. However, the range of other major-element values is relatively constrained, and a fractionation trend is not evident. Major elements in the hybrid gabbro-biotite granite rocks plot as a trend (mixing line) from the compositional field of gabbro to that of biotite granite. Most major-element compositions of the syenites plot in a separate field and outside of any possible trends evident in the compositions of the other rock types. In addition, CaO and K_2O in the granodiorites plot independently. The aplites do not occupy a separate compositional field and plot with the biotite granites.

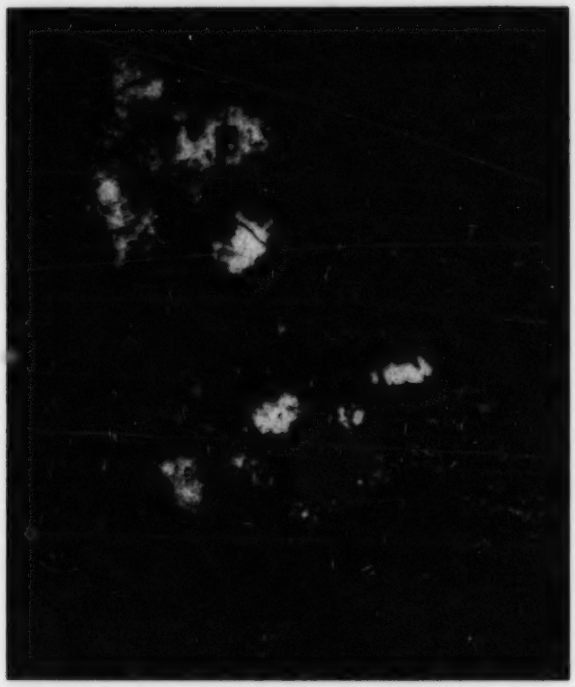

Plate 16. *Scanning electron microscope backscatter photograph showing botryoidal zircon (Z), thorite (TS) and thorium oxide (T). Sample JT-067. Spectral scans shown in Figure 10e and f.*

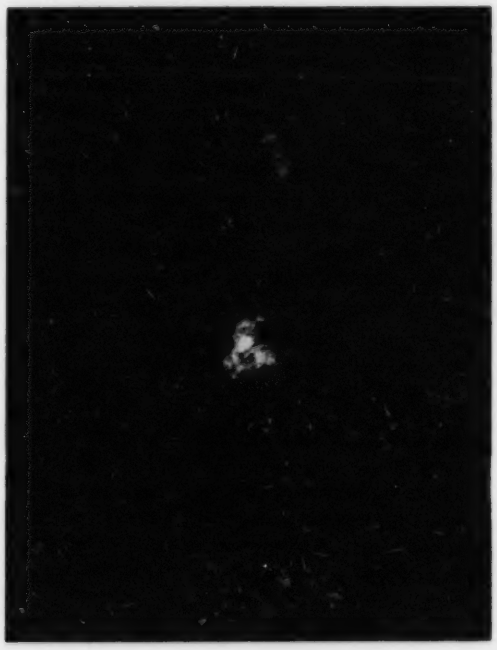

Plate 17. *SEM backscatter photograph of Th–Nb silicate (A) and Th–Nb–Fe silicate (B); Z–Zircon. Sample JT-067. Spectral scans shown in Figure 10g and h.*

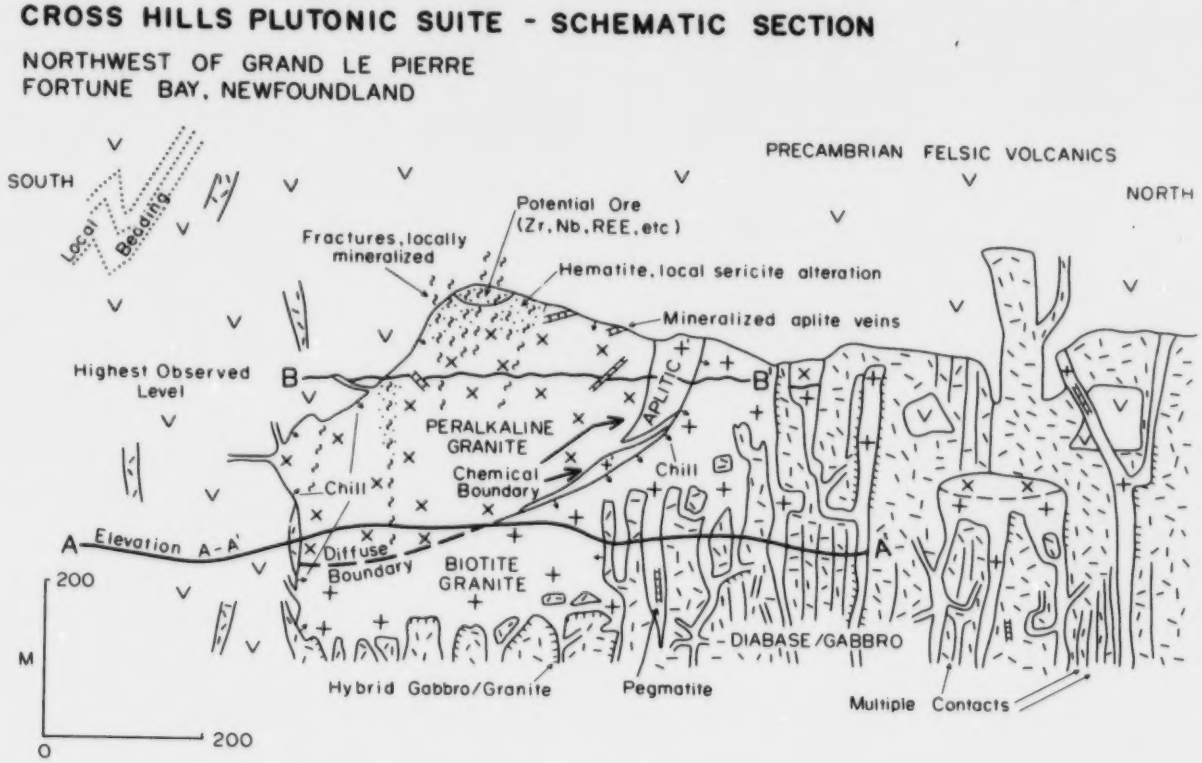

Figure 11. *Schematic (composite) geological section across the Cross Hills Plutonic Suite in the area to the northwest of Grand Le Pierre. Level of sections shown on Figure 9 and denoted by A-A', B-B'.*

In the granitic rocks, MgO, CaO, MnO and P_2O_5 trend to very low values. The peralkaline granites have lower MgO, CaO and TiO_2 than the biotite granites, but have higher total FeO. They have Na_2O contents similar to those of the biotite granites but have distinctly lower K_2O and Al_2O_3; the peralkalinity results from the low Al_2O_3 values (see section on classification below).

Some altered and mineralized samples of peralkaline granite have lower Na_2O and Al_2O_3 than the main field, and 2 samples have higher total FeO.

Trace Elements

The trace elements show some, but not all, of the expected trends and compositional ranges (Figures 13 and 14), which would be expected with the variation in major-element composition. Trace elements in the hybrid gabbro-granite samples plot along a mixing line trend between the gabbro and biotite granite samples (as was observed for the major-element data). The granodiorite samples generally have a distinct trace-element signature. The peralkalinity of the most silicic rocks is emphasized by the relatively high Zr, Y, Nb and Zn values and a tendency for higher Be, U and Th values. In Sr, trends to low values are consistent with the evolved nature of the high-silica rocks and the peralkaline granite composition, however, the Ba content of some samples is relatively high. Relatively higher F, Zn, Zr, Nb, La, and Ce occur in the syenites and are consistent with their alkaline composition (see Figure 17). The aplites again plot with the biotite granite compositions.

Unexpectedly, F values are lowest in the peralkaline granite. The low F in the silicic rocks is complemented by a tendency for lower La and Ce values in the peralkaline granite. In addition, the granitic rocks have lower Li and F values than the mafic rocks. In fact, F values in gabbro in the range of 1000 g/t are exceptionally high for this rock type.

The peralkaline granites were subdivided for mapping purposes into unaltered (PGRT), altered (PGRA), and mineralized (PGRM) units (see Appendix 4) on the basis of alteration and mineralization associated with anomalous radioactivity; some of those samples are indicated by solid triangles, where outside the general field of values, on Figures 11 to 13. Highly mineralized or strongly radioactive samples were not plotted on the Harker diagrams. In general, peralkaline granite having abundant hematite stain and local sericitization (PGRA) has higher high-field-strength (HFS) element contents than unaltered peralkaline granite (PGRT). The highest values for the HFS elements occur in radioactive or mineralized (PGRM) peralkaline granite samples and reflect the processes leading to mineral concentrations of economic interest. Values up to 20000 g/t Zr, 2968 g/t Y,

Table 2: Summary of geochemical data from the Cross Hills Plutonic Suite, Sage Pond - Grand Le Pierre area

	GABBRO <52% SiO_2		HYBRID GBBR-BGRT >52% SiO_2		BIOTITE GRANITE		APLITE		GRANODIORITE*		PERALKALINE GRANITE		SYENITE		ALKALI GRANITE JT-477	MINERALIZED PERALKALINE JT-067	JT-124
	x	s	x	s	x	s	x	s	x	s	x	s	x	s			
SiO_2	47.9	2.78	57.6	3.46	74.4	1.22	75.1	0.56	69.4	0.92	76.6	0.54	65.1	2.55	71.6	74.3	73.8
Al_2O_3	16.3	1.47	14.8	1.31	12.6	0.38	12.4	0.19	14.3	0.23	11.0	0.37	16.1	0.72	12.6	8.8	8.0
Fe_2O_3	3.64	1.74	2.83	0.48	0.73	0.14	0.68	0.15	1.08	0.22	1.88	0.45	2.38	0.93	2.30	6.14	5.80
FeO	6.96	1.70	5.12	1.81	0.76	0.26	0.70	0.18	1.67	0.25	0.45	0.18	2.36	1.08	1.13	0.41	0.11
MgO	7.23	1.26	3.30	1.19	0.26	0.16	0.15	0.04	0.79	0.16	0.05	0.03	0.11	0.08	0.12	0.16	0.08
CaO	9.02	1.08	5.15	1.09	0.62	0.47	0.45	0.06	2.59	0.21	0.09	0.07	0.44	0.27	0.65	0.06	0.13
Na_2O	2.85	0.42	3.86	0.56	3.70	0.22	3.89	0.18	4.06	0.12	3.75	0.21	6.01	0.58	4.20	1.65	1.75
K_2O	1.07	0.65	2.79	0.48	5.16	0.40	5.16	0.26	2.63	0.16	4.57	0.29	5.14	0.79	5.36	5.15	4.62
TiO_2	1.75	1.01	1.50	0.57	0.28	0.05	0.25	0.04	0.36	0.01	0.18	0.03	0.37	0.21	0.41	0.36	0.57
MnO	0.19	0.06	0.16	0.05	0.03	0.01	0.03	0.01	0.09	0.01	0.04	0.03	0.13	0.06	0.08	0.06	0.19
P_2O_5	0.29	0.18	0.26	0.09	0.03	0.01	0.02	0.01	0.06	0.01	0.02	0.01	0.05	0.04	0.03	0.02	0.03
LOI	2.30	0.64	1.57	0.31	0.71	0.13	0.54	0.11	1.28	0.18	0.49	0.11	1.07	0.42	0.33	0.93	0.79
CO_2	0.072	0.042	0.110	0.110	0.072	0.034	0.047	0.027	0.127	0.107	0.075	0.072	0.128	0.133	-	-	
Li	36	9.7	21	6.1	11	2.8	8.1	1.9	13	2.5	8.8	6.5	13	4.8	5	10	8
Be	1.8	0.5	3.7	0.7	5.7	5.5	5.3	0.6	1.9	0.1	8.5	2.2	7.8	7.7	2.2	43.8	51.9
F	449	254	933	286	165	77	394	246	-	-	79	71	1196	1427	189	54	141
V	276	129	210	94	16	6.5	11	2.2	38	7.5	6.0	1.9	6.8	5.9	14	10	15
Cr	136	36	50	34	1.9	2.4	0.6	1.1	2.7	2.1	2.0	2.2	0.3	0.8	0	0	0
Ni	72	39	20	9.3	1.7	0.1	1.2	0.5	1.0	0.0	1.0	0.0	1.0	0.0	1	-	-
Cu	62	23	32	23	3.8	0.1	3.8	0.8	8.7	5.0	12	16	3.0	1.0	3	-	-
Zn	99	27	117	42	50	19	54	23	51	4.6	115	86	147	78	73	149	162
Ga	20	5.0	21	3	20	2.4	22	1.19	16	1.5	27	1.8	35	7.0	26	26	11
Rb	51	30	92	20	175	22	167	8.4	86	4.7	193	21	141	43	81	309	279
Sr	352	108	219	54	47	26	33	5.5	180	8.5	11	5.7	38	27	26	0	4
Y	35	13.7	69	20	83	27.5	97	12	31	4.4	150	59	123	74	88	1619	2968
Zr	136	68	318	172	231	19	259	28	154	3.1	690	234	996	612	994	6800	19208
Nb	9.6	2.9	20	2.7	30	5.3	35	2.7	13	0.6	65	28	244	176	19	809	860
Ag	0.1	0.0	0.1	0	0.1	0	0.1	0.0	0.1	0.0	0.1	0.1	0.1	0.1	0.1	0.1	0.1
Sn	1.0	-	2.0	0	1	0	2.0	1.6	-	-	5.2	3.0	7.0	5.2		40	90
Ba	164	173	225	168	307	84	248	88	647	62	73	64	387	377	416	47	220
La	11.7	6	30	9.5	46	13	62	15	18	2.3	34	22	124	95	115	33	190
Ce	109	51	171	34	194	41	222	29	84	13	200	67	351	224	372	762	1550
Pb	2.7	2.5	9.0	5.3	13	4.4	15	9.1	7.3	2.5	18	13	18	22	7	33	44
Th	2.8	3.4	12	5.4	25	2.9	27	2.9	13	1.0	31	13	32	23	16	364	725
U	0.0	-	4.3	3.2	4.1	1.0	4.8	0.6	-	-	6.2	2.7	6.5	3.7	2.0	64.2	112.5
n**	12		7		20		9		3		22		6		1	1	1

* These samples from Cross Hills Suite - east of Grand Le Pierre.

** Maximum number of samples. For some elements, i.e., F, Ni, Cu, Sn and U, n may be lower.

x – mean; s – standard deviation; major elements and CO_2 in percent, trace elements in g/t; (-) not analyzed.

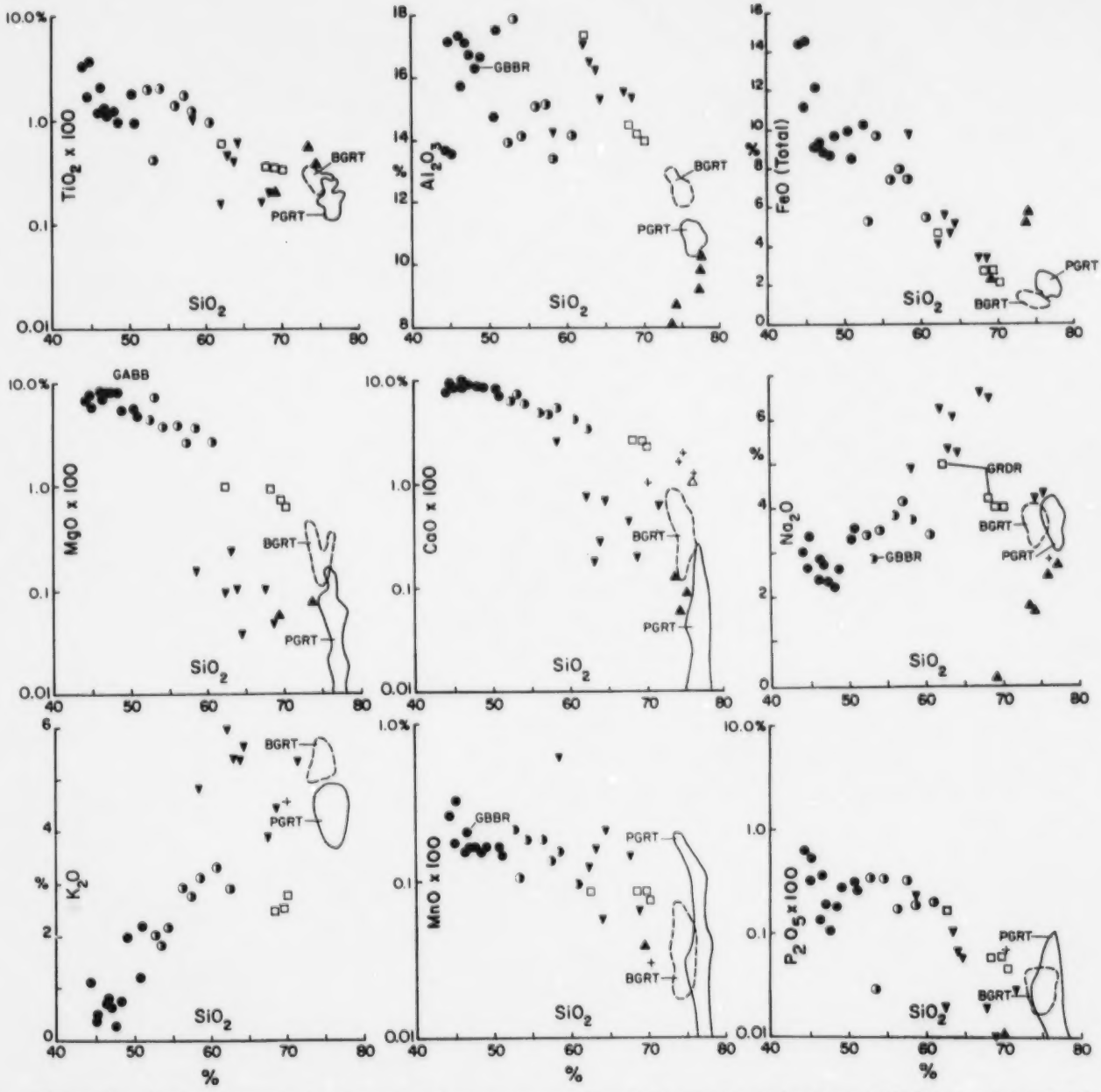

Figure 12. *Harker diagrams showing major-element content of analyzed samples of the Cross Hills Plutonic Suite. Solid circles–gabbro; half-filled circles–hybrid gabbro; open square–granodiorite; inverted solid triangle–syenite; crosses–biotite granite; open upright triangle–aplite; solid upright triangle–peralkaline granite. PGRT–field of peralkaline granite; BGRT–field of biotite granite. Where fields are used for peralkaline granite, solid triangles represent strongly altered and mineralized samples that plot outside the main field.*

2334 g/t Nb and 1550 g/t Ce were recorded along with elevated Sn, La, Th and U.

Areal Geochemical Patterns

The spatial distributions of Zr, Nb, Sn, Th, and U in the granites of the Cross Hills Plutonic Suite were investigated by Saarberg Interplan Limited (Hopfengaertner, 1982) and their results are presented in Figure 15. Analyses were performed on powders of whole-rock samples by X-Ray Laboratories Limited of Mississaugua, and are in general agreement with the analyses of samples collected for this study.

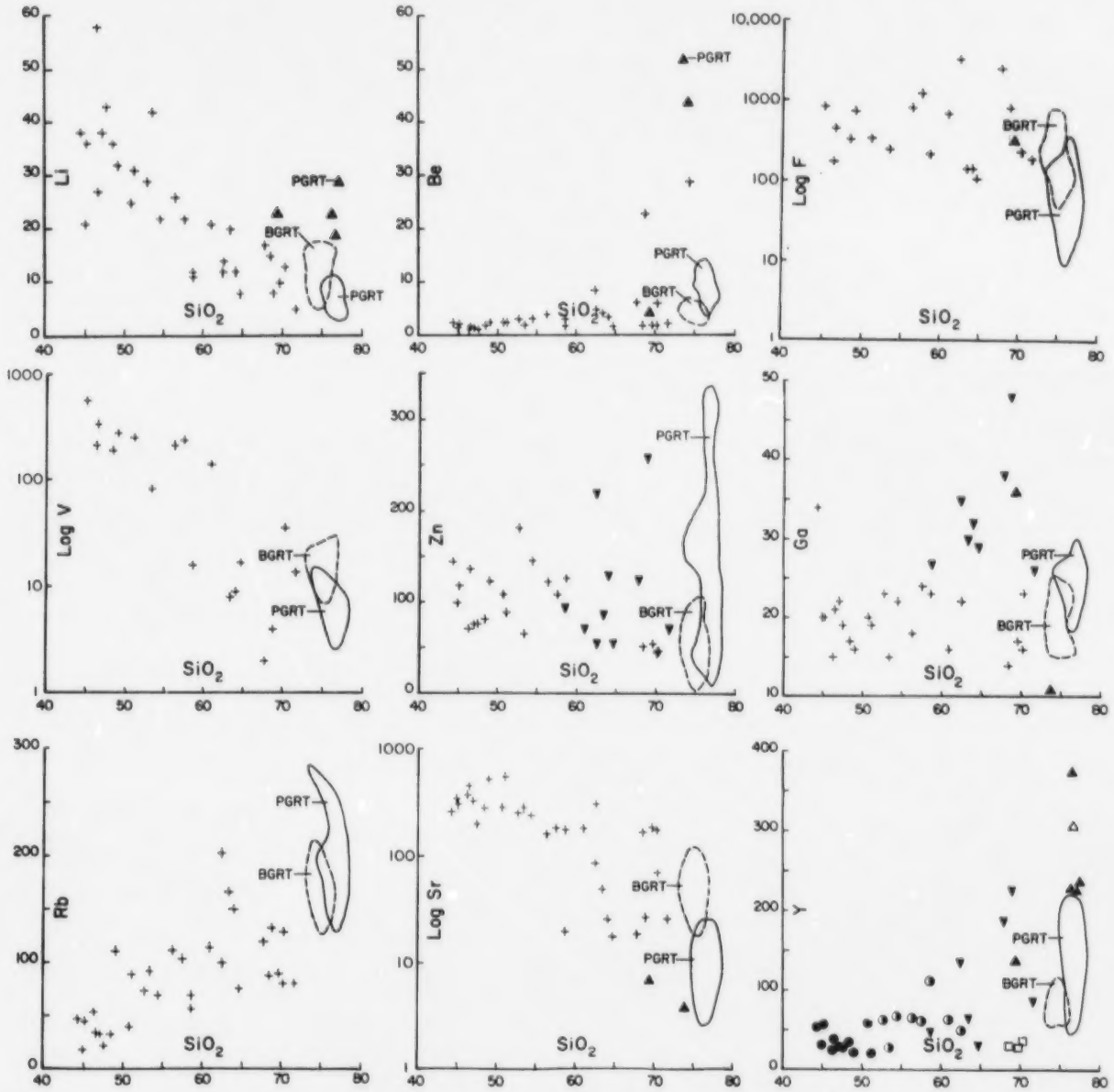

Figure 13. *Harker diagrams showing Li, Be, F, V, Zn, Ga, Rb, Sr, and Y contents of analyzed samples from the Cross Hills Plutonic Suite. Symbols as in Figure 4 except plus signs are unassigned samples. SiO_2 in percent; all other elements in g/t.*

The peralkaline granite has higher Zr, Nb and Sn values than the biotite granite; Zr generally occurs in excess of 600 g/t, Sn in excess of 10 g/t, and Nb in excess of 50 g/t. The Sn values are locally highly anomalous having a maximum value of 90 g/t. Erratic high values of Th and U are recorded, and some areas have Th values in excess of 40 g/t; three samples have Th values of 364, 620 and 725 g/t.

Trends to higher values in these elements focus on the known mineral occurrences in the peralkaline granite. This indicates that the trace-element enrichment processes in the peralkaline granite are directly related to the development of peralkalinity and to mineralization of economic interest.

Classification

Rocks mapped as peralkaline granite, due to the presence of riebeckite and hematite, have agpaitic indices that range

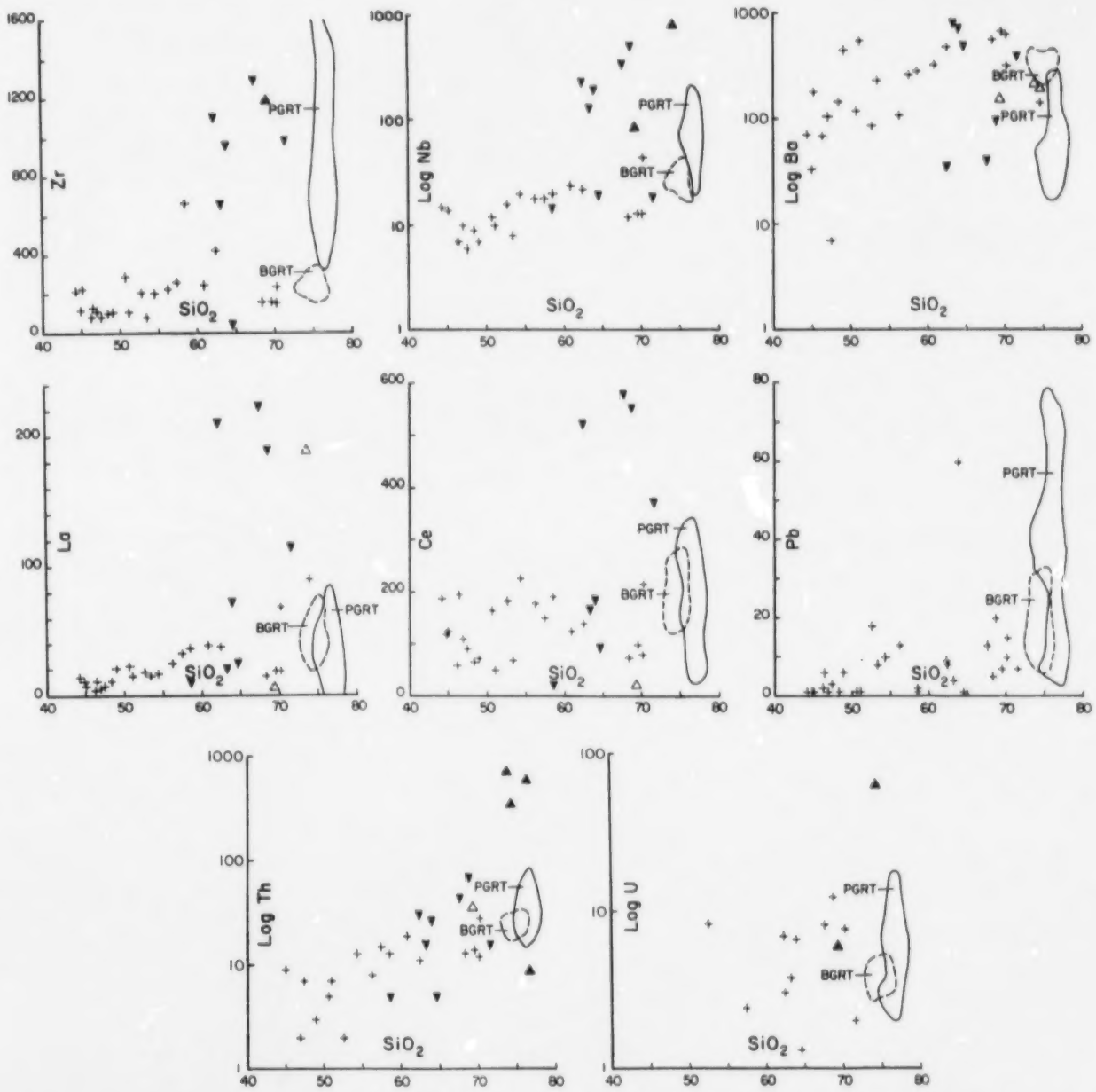

Figure 14. *Harker diagrams showing Zr, Nb, Ba, La, Ce, Pb, Th, and U contents of analyzed samples from the Cross Hills Plutonic Suite. Symbols as in Figure 4 except crosses are unassigned samples. SiO_2 in percent; all other elements in g/t.*

from 0.93 to 1.06, and normative calculations (Barth, 1962a, b; Appendix 4G) indicate that 40 percent of the samples contain normative riebeckite. The biotite granite has agpaitic indices that range from 0.9 to 1.00, and the granodiorite has indices that range from 0.65 to 0.68. The syenite has agpaitic indices that range from 0.88 to 1.01 and only two of the samples have normative riebeckite as a result of the high Al_2O_3 content.

The abundance of graphic and spherulitic textures in the felsic rocks, and the absence of fractionation trends in major elements, indicate that the various granites are quenched, high-level, silicic magmas. In addition, fine-grained mafic and felsic plutonic rocks indicate a high-level subvolcanic environment. Therefore, the data have been plotted on some discriminant diagrams for volcanic rocks to aid interpretation.

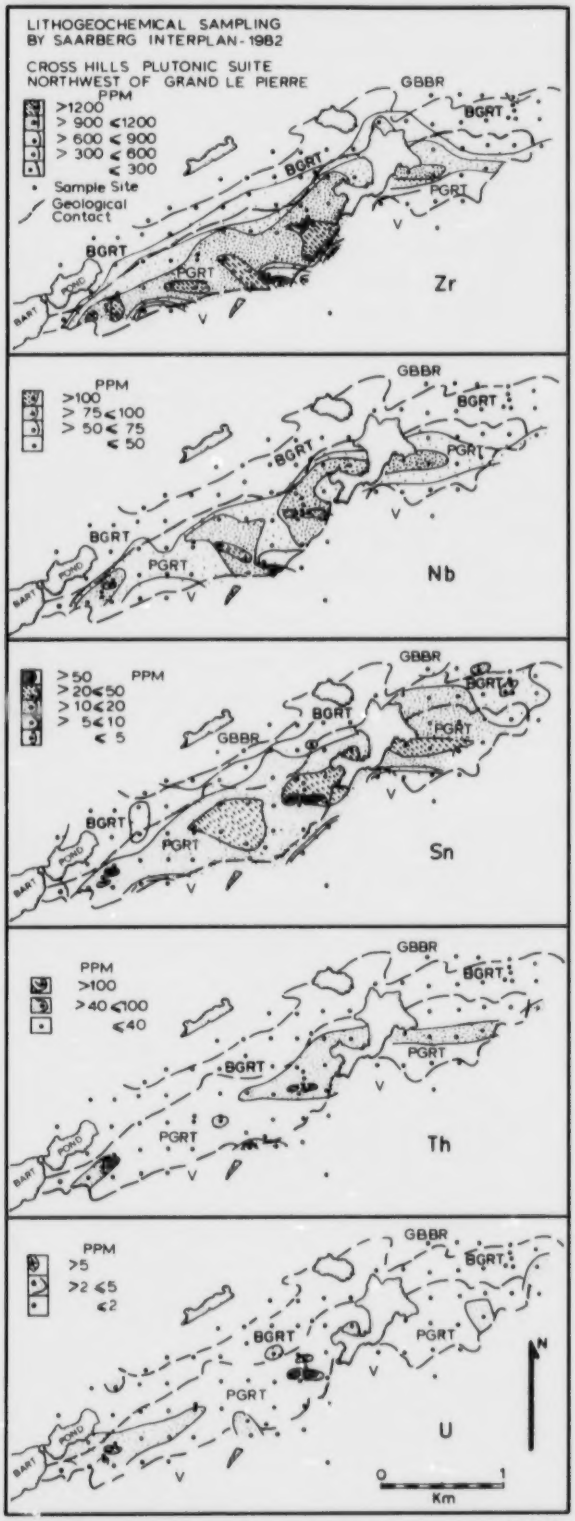

Figure 15. *Areal distribution of trace elements Zr, Nb, Sn, Th and U in rock samples analyzed by Saarberg Interplan Limited. GBBR–gabbro; BGR–biotite granite; PGRT–peralkaline granite; V–volcanic rocks.*

Most of the samples plot in the field of normal igneous volcanic rocks on the alteration diagram of Hughes (1973; Figure 16). A few of the altered peralkaline rocks plot to the right of the normal field due to Na_2O depletion (also shown in the Harker diagrams; Figures 12 to 14).

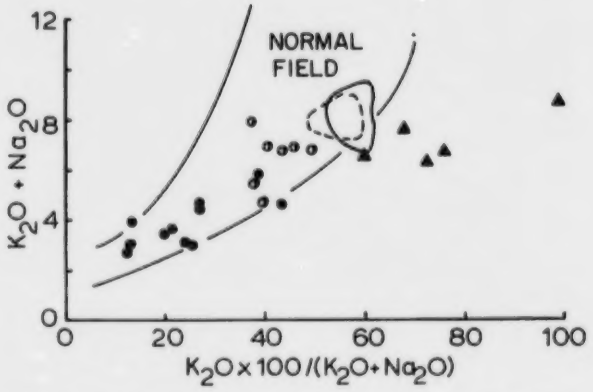

Figure 16. *Distribution of analyzed samples on the K_2O + Na_2O vs. K_2O x 100/(K_2O + Na_2O) alteration discriminant diagram of Hughes (1973). The normal field includes data from relatively unaltered volcanic rocks. Solid circles–gabbro; half-filled circles–hybrid gabbro; dashed line around field of biotite granite and aplite; solid lined around field of peralkaline granite; solid triangles–mineralized and altered peralkaline granite.*

The gabbro and the hybrid gabbro-granite samples plot in the alkaline field on the agpaitic index-SiO_2 discriminant diagram of Currie (1976; Figure 17), and the syenite samples plot in the upper limits of this alkaline field with one sample plotting in the agpaitic syenite field. Most of the mafic samples plot in the alkaline field (Figure 18) according to the classifications of Kuno (1968) and Irvine and Baragar (1971).

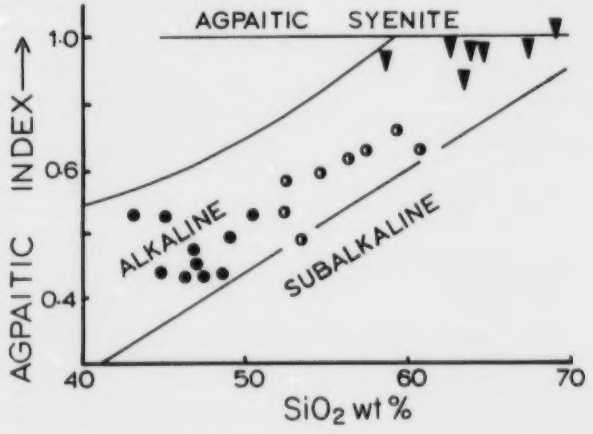

Figure 17. *Distribution of analyzed gabbro, hybrid gabbro-granite and syenite sample on the alkaline–subalkaline–agpaitic syenite discrimination diagram of Currie (1976). Solid circles–gabbro; half-filled circles–hybrid gabbro; inverted triangles–syenite.*

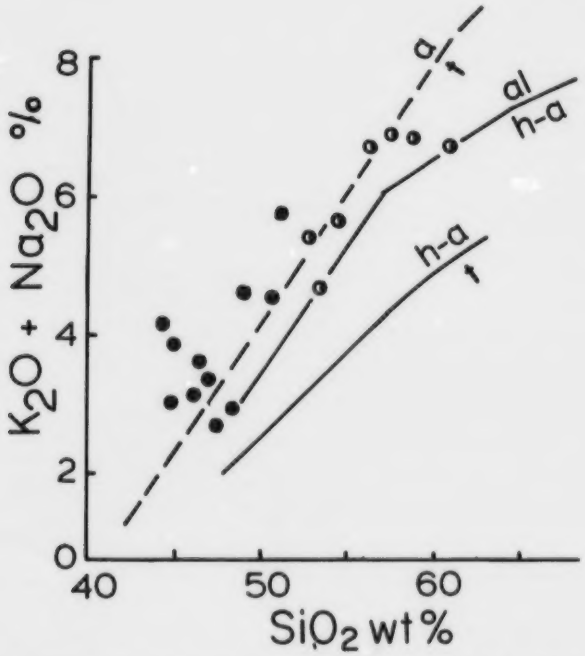

Figure 18. *Distribution of analyzed gabbro (solid circles) and hybrid gabbro-granite (half-filled circles) on the alkali-silica diagram. Dashed line is alkali basalt–tholeiitic basalt boundary of Irvine and Baragar (1971); solid lines are basalt field boundaries after Kuno (1968). a–alkali basalt; t–tholeiitic basalt; al–alumina basalt; h-a–high-alumina basalt.*

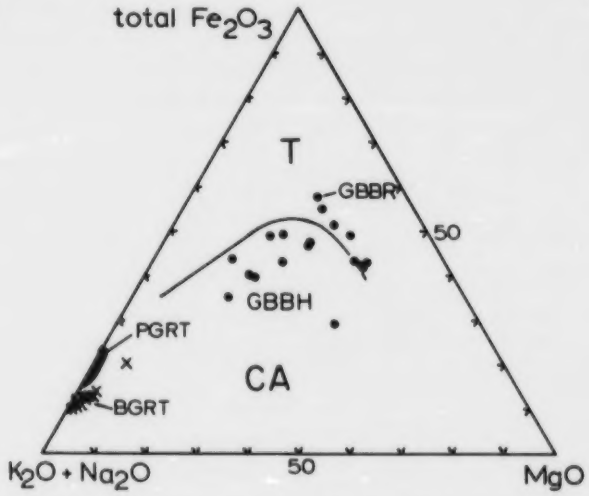

Figure 19. *Distribution of analyzed samples on the AFM discrimination diagram of Irvine and Baragar (1971). T–tholeiitic; CA–calc alkaline; GBBR–gabbro; GBBH–hybrid gabbro-granite, PGRT–peralkaline granite; BGRT–biotite granite.*

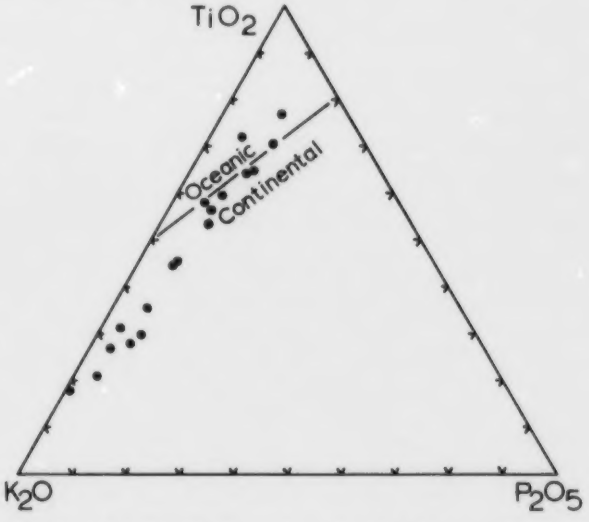

Figure 20. *Distribution of analyzed gabbro and hybrid gabbro-granite on the TiO_2-K_2O-P_2O_5 oceanic–continental basalt discrimination diagram of Pearce* et al., *(1975).*

The data are shown on an AFM diagram (Figure 19, after Irvine and Baragar, 1971). The gabbroic rocks may show a trend to Fe-enrichment. Most of the hybrid rocks plot in a trend that reflects the injection of felsic magma into the gabbro. The biotite granites plot in the calc-alkaline field, and the relative Fe-enrichment of the peralkaline rocks is also well displayed. The alkaline affinity of the mafic rocks indicates that their location in the tholeiitic field on the AFM diagram is fortuitous. However, the position of the data on the TiO_2-K_2O-P_2O_5 discrimination diagram (Figure 20, after Pearce *et al.*, 1975) suggests a continental tectonic environment.

On the Al_2O_3-FeO(tot) classification diagram (Figure 21) of MacDonald (1975) the granodiorites and biotite granites plot in the non-peralkaline fields. Most of the rocks mapped as peralkaline granite plot in the comendite field, in agreement with the field description based on the presence of riebeckite and hematitized riebeckite. Two of the altered and mineralized peralkaline rocks plot in the pantellerite field. The syenite also plots in the peralkaline fields.

On the I-, S-, and A-type granite classification diagrams espoused by White and Chappell (1983) and Whalen *et al.* (1987), the biotite granites plot as A-type granites on an alkali diagram (Figure 22a), whereas the peralkaline rocks straddle the boundary between A- and I-type granites. Due to high Ga contents, the biotite granites plot as I- and A-type granites and the peralkaline granites plot in the A-type field (Figure 22b).

Using the classification diagrams (Figures 23 and 24) of Winchester and Floyd (1977) most of the peralkaline granites plot, as expected, in the comendite–pantellerite field. Some syenite analyses plot in the trachyte field. The biotite granite plots on the boundary of the rhyodacite and rhyolite

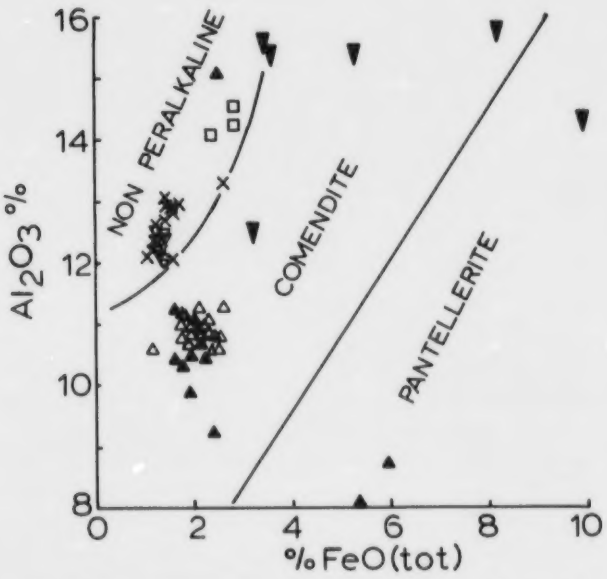

Figure 21. *Distribution of analyzed felsic rocks on the Al_2O_3-FeO (tot) discriminant diagram of MacDonald (1975). Inverted triangles–aplite; x–biotite granite; open squares–granodiorite; inverted solid triangles–syenite; open triangles–peralkaline granite; solid upright triangles–mineralized and/or altered peralkaline granite.*

fields and granodiorite plots in the dacite field. The mafic rocks (gabbro–diabase) tend to plot near the boundary between the subalkaline basalt and alkali basalt field on Figure 23, whereas they plot on the boundary between the basalt and subalkaline basalt fields on Figure 24.

In summary, the mafic and silicic plutonic rocks (excluding granodiorite) have alkaline to peralkaline tendencies. It is possible that the granodiorites are unrelated to the rest of the plutonic suite.

RARE-EARTH-ELEMENT GEOCHEMISTRY

Introduction

Six samples of peralkaline granite, including a mineralized sample from occurrence # 11 and one from the mineralized peralkaline aplite vein at occurrence # 12 (see Figure 9), were analyzed for REE by inductively coupled plasma-mass spectrometry (ICP-MS) (Saunders and Tuach, 1989). A granodiorite sample (JT-404), a gabbro sample (JT-343) and two biotite granite samples (JT-424 and JT-426) were also analyzed. The analytical methods are given in Appendix 1D, data are listed in Appendix 4F and the results are shown in Figure 25.

Results

The four unmineralized peralkaline granite samples have relatively flat REE patterns with negative Eu anomalies.

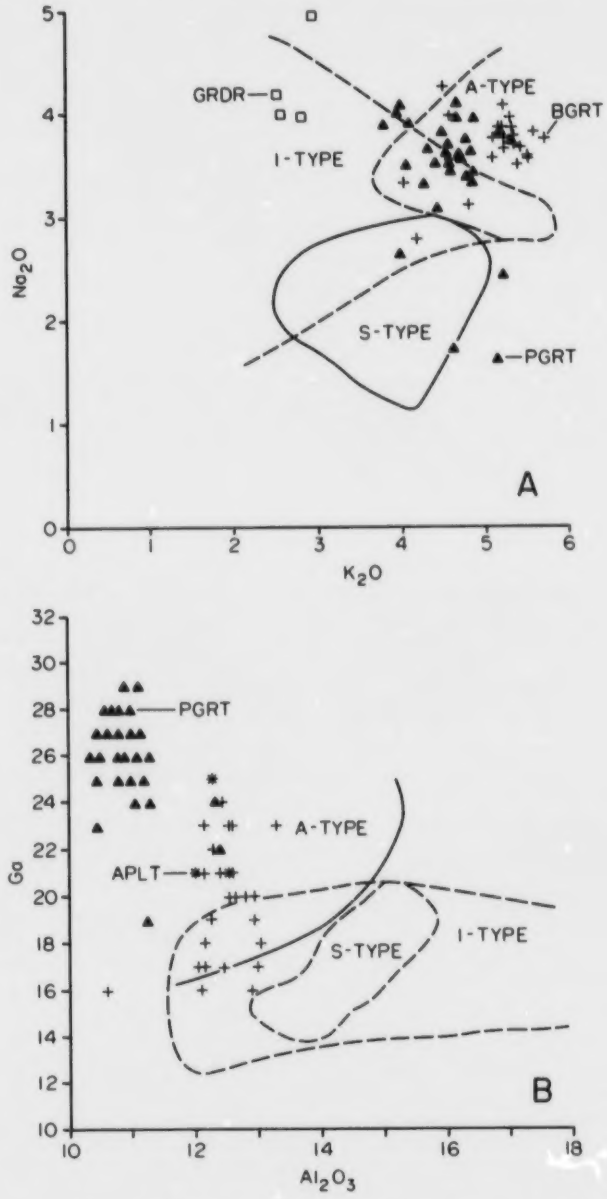

Figure 22. *Fields of I- vs. S- vs. A-type magmas on (a) Na_2O vs K_2O and (b) Ga vs. Al_2O_3 (White and Chappell, 1983) for felsic units of the Cross Hills Plutonic Suite. Symbols explained on diagram.*

However, sample JT-437 is enriched in both light REE (LREE) and heavy REE (HREE). The two mineralized samples JT-067 and JT-124 are enriched in total REE, but have highly enriched, convex-upward HREE patterns. All samples except 155 have HREE maxima at Tm. Four samples (JT-67, JT-124, JT-155, JT-422) also have extremely high Ce values that appear to be somewhat independent of either LREE or HREE concentrations. A Ce-rich mineral has been found in sample JT-124 (Figure 10d). The gabbro sample

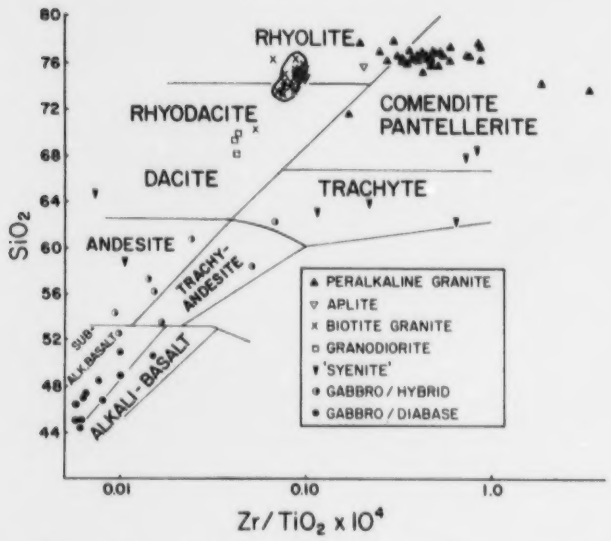

Figure 23. *Distribution of analyzed samples on the SiO_2 vs. Zr/TiO_2 x 10^4 discrimination diagram of Winchester and Floyd (1977).*

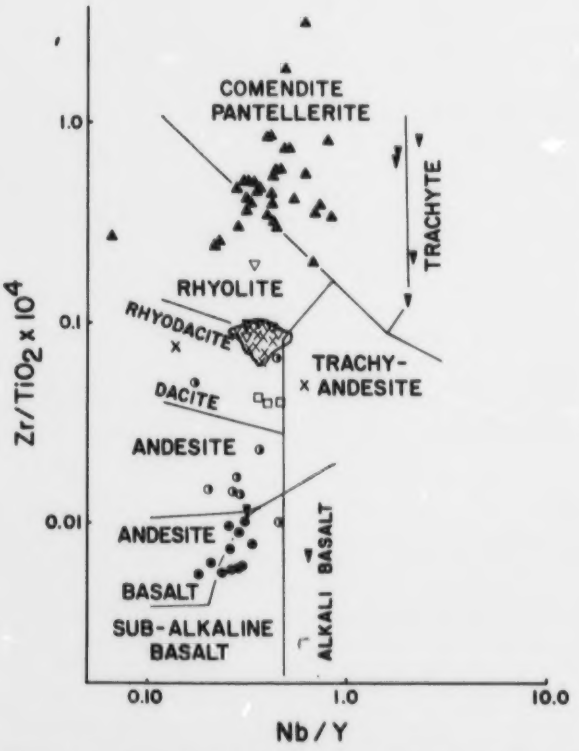

Figure 24. *Distribution of analyzed samples on the Zr/TiO_2x 10^4 vs. Nb/Y discrimination diagram on Winchester and Floyd (1977). Symbols as in Figure 23.*

(JT-343) has a gentle negative-sloping REE pattern with no Eu anomaly. The granodiorite sample (JT-404) has a steep negative-sloping LREE pattern and a very flat HREE pattern accompanied by a slight negative Eu anomaly. The two biotite granite samples have similar patterns but have higher total REE and more pronounced negative Eu anomalies.

Discussion

The REE data indicate a genetic relationship between the various rock types. The biotite granite samples are generally enriched in the lighter REE compared to the non-mineralized peralkaline granite. The earlier fractionation of LREE-rich phases into the biotite granite may contribute to the relative enrichment of HREE over LREE in the peralkaline granite.

Significant enrichment of HREE over LREE is a common feature of peralkaline granite-hosted mineralization. Taylor *et al.* (1981) and Taylor and Fryer (1983) documented a five- to seven-fold HREE enrichment in peralkaline rocks of the Topsails Igneous Complex in Newfoundland (see Figure 1). These rocks contain albite, riebeckite, zircon, fluorite and Fe–Mn carbonate. Miller (1986) reported that the more mineralized 'exotic-rich' peralkaline granite from the Strange Lake Zr–Y–Nb–Be–REE deposit in Labrador, has a high total REE content and is strongly enriched in HREE.

The late Precambrian Cross Hills Plutonic Suite has many geological, geochemical and metallogenic similarities to posttectonic alkali to peralkaline granites from Saudi Arabia, which are of similar late Precambrian age. These granites are typically enriched in Nb, Ta, Sn, REE, Y, Th, U and Zr and, in some cases, contain economically important concentrations of some of these elements (Drysdall *et al.*, 1984; Jackson *et al.*, 1985). In particular, the Ghurayyah and Jabal Tawlah deposits show extreme enrichment in HREE and the Jabal Sa'id deposits are enriched in HREE and sporadically enriched in LREE (Figure 26; Harris and Mariner, 1980; Drysdall *et al.*, 1984).

It has been suggested that under alkaline and oxidizing conditions, HREE are partitioned into F^-- or CO_3^{2-}-bearing fluids (Kosterin, 1959; Flynn and Burnham, 1978; Kerrich and Fryer, 1979; and Taylor *et al.*, 1981). Harris and Mariner (1980) demonstrated that fluorine is enriched in the Ghurayyah Granite and shows a positive correlation with HREE contents. They further suggested that HREE existed as fluoride complexes in the magma until the final stages of crystallization of the granite.

The peralkaline granite phase of the Cross Hills Plutonic Suite is actually depleted in fluorine compared to the biotite granite (Table 2). Although CO_2 contents of the granite are generally low (Table 2), the presence of an irregular 2 by 5 m vein of hematite-stained calcite within the peralkaline granite (centre–Figure 9) suggests that carbonate-rich fluids were formed during the hydrothermal evolution of the Cross Hills Plutonic Suite and that CO_3^{2-} may have contributed to

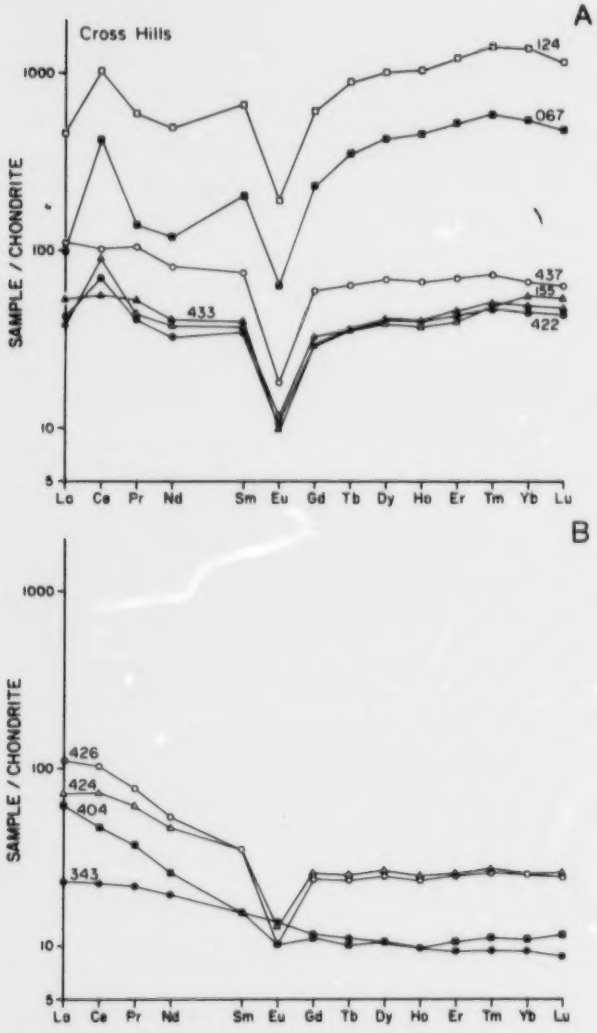

Figure 25. *Rare-earth-element profiles of a) 4 peralkaline granite and 2 mineralized peralkaline granite samples (JT-067 and JT-124) and b) a gabbro (JT-343), a granodiorite (JT-404) and 2 biotite granite samples (JT-424 and JT-426). Data are normalized to the chondrite values of Evensen* et al. *(1978).*

the concentration of elements in the suite (Saunders and Tuach, 1989) as suggested by Taylor *et al.* (1981) for the Topsails Complex.

The inconsistent enrichment of Ce presumably is controlled by its oxidation state. Ronov *et al.* (1967) noted that tetravalent Ce has chemical properties that are more similar to those of the HREE than the other LREE. Its fractionation from the other LREE in some samples suggests that conditions were locally favourable to the maintenance of Ce in the tetravalent state (Saunders and Tuach, 1989). This is supported by the ubiquitous presence of hematite and its abundance in tuffisite, which indicates that oxidizing conditions prevailed during the final stages of granite crystallization.

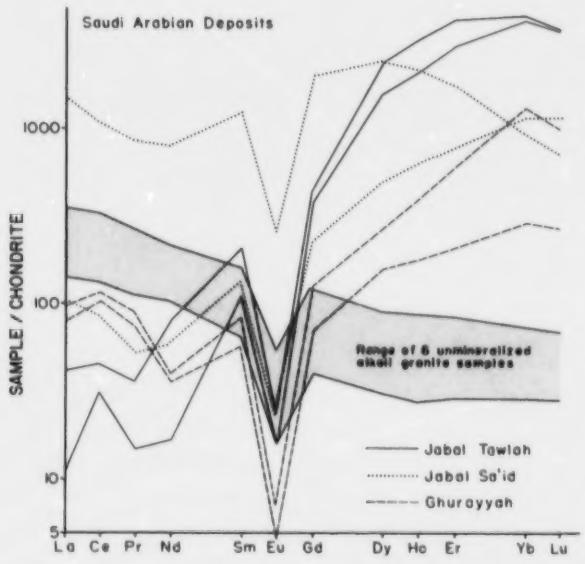

Figure 26. *Rare-earth-element profiles of mineralized peralkaline granite samples from three Saudi Arabian deposits—Ghurayyah, Jabal Tawlah and Jabal Sa'id. Also shown is the range of six unmineralized Saudi Arabian peralkaline granite samples. Data from Drysdall* et al. *(1984).*

ISOTOPIC SYSTEMS

GEOCHRONOLOGY

Introduction

Radiometric age determinations have not been previously reported from the Cross Hills Plutonic Suite, which intrudes the Belle Bay and Andersons Cove formations of the Long Harbour Group. These formations are undated. The southern parts of the Ackley Granite Suite, which cut the Cross Hills Plutonic Suite and the Belle Bay Formation, have been dated at 355 ± 5.9 Ma and at 370 ± 5 Ma by Rb–Sr and $^{40}Ar/^{39}Ar$ techniques respectively (Kontak *et al.*, 1988, see Table 3).

To the west of the Cross Hills Plutonic Suite, the Long Harbour Group is overlain by Late Proterozoic to Cambrian fossiliferous sedimentary rocks (Williams, 1971). The Belle Bay and Andersons Cove formations of the Long Harbour Group have been correlated with the Love Cove, Marystown and possibly Harbour Main groups, to the east, on the basis of rock type and stratigraphy (O'Brien *et al.*, 1984). Rocks of these latter groups have yielded Late Proterozoic, U–Pb zircon ages from 632 to 585 Ma (Table 3).

The Cross Hills Plutonic Suite was previously interpreted to be Devonian in age (Bradley, 1962; O'Brien and Nunn, 1980). Recently, correlation of the peralkaline Mooring Cove Formation (see Appendix 5E) of the Long Harbour Group

Table 3. Radiometric age determinations in the Avalon Zone

UNIT	ROCK TYPE	METHOD	MINERAL	AGE (MA)	REFERENCE
Ackley Granite Suite	Granite	Rb/Sr	W.R.	355 ± 5	1
Ackley Granite Suite	Granite	Rb/Sr	W.R.	355 ± 9	5
Ackley Granite Suite	Granite	$^{40}Ar/^{39}Ar$	Bi, Hbl	355 ± 10	3
Ackley Granite Suite	Granite	$^{40}Ar/^{39}Ar$	Bi, Musc, Hbl	370 ± 5	6
Love Cove Group	Phyllite	$^{40}Ar/^{39}Ar$	Musc	370 - 390	3
Cross Hills Plutonic Suite	Various	Rb/Sr	W.R.	560 ± 30	This Report
Cross Hills Plutonic Suite	Granite	U-Pb	Zircon	547^{+3}_{-6}	7
Swift Current Granite	Granite	Rb/Sr	W.R.	548 ± 11	2
Swift Current Granite	Granite	$^{40}Ar/^{39}Ar$	Hbl	560 - 566	2
Swift Current Granite	Granite	U/Pb	Zircon	580 + 20	2
Harbour Main Group	Rhyolite dyke	U/Pb	Zircon	585.9^{+34}_{-24}	4
Love Cove Group	Felsic volcanic	U/Pb	Zircon	590 ± 30	2
Harbour Main Group	Ash flow	U/Pb	Zircon	606^{+37}_{-29}	4
Marystown Group	Ash flow	U/Pb	Zircon	608^{+20}_{-7}	4
Holyrood Granite	Granite	U/Pb	Zircon	620.5^{+21}_{-18}	4
Harbour Main Group	Flow-banded rhy.	U/Pb	Zircon	622.6^{+23}_{-20}	4
Harbour Main Group	Rhy. clast in cong.	U/Pb	Zircon	623^{+19}_{-17}	4
Harbour Main Group	Rhy. plug	U/Pb	Zircon	632 ± 2	4
Wandsworth Gabbro	Pegmatite	U/Pb	Zircon	763^{+22}_{-18}	4

W.R.–Whole Rock, Bi–Biotite, Hbl–Hornblende, Musc–Muscovite, Rhy.–Rhyolite, Cong.–Conglomerate.

1. Bell *et al.*, 1977
2. Dallmeyer *et al.*, 1981
3. Dallmeyer *et al.*, 1983
4. Krogh *et al.*, 1988
5. Tuach, 1987
6. Kontak, *et al.*, 1988
7. Greg Dunning, (personal communication, 1987)

(which overlies the Belle Bay Formation) with the peralkaline phase of the Cross Hills Plutonic Suite led to the suggestion that the latter could also be Late Proterozoic (Tuach, 1984; O'Brien *et al.*, 1984).

Rb–Sr Geochronology

Introduction

Twelve samples from the Cross Hills Plutonic Suite, (located on Figure 27 and Map 91-15), were analyzed for Rb and Sr content and isotopic composition at Memorial University, and details of the analyses are presented in Appendix 1E. The Rb and Sr concentrations and the Sr-isotope ratios are summarized in Table 4. The Sr content of the peralkaline granite is too low to give meaningful data by the techniques used. Therefore, peralkaline granite samples were not analyzed.

Results of weighted least-squares-regression analyses are shown in Figure 28 for various combinations of the data. Errors are quoted at the 1 sigma level. Most of the regressed lines on the plots have a mean square of weighted deviates (MSWD) greater than 2 and therefore, are errorchrons as defined by Brooks *et al.*, (1972).

Results

Regression of all the data from the Cross Hills Plutonic Suite gives an age of 560.2 ± 22.5 Ma having an initial ratio of 0.7039 and a MSWD of 89.6. The large MSWD implies that the age is meaningless. Similarly, regression of the data from the gabbro and hybrid gabbro-biotite granite gives an indicated age of 602.7 ± 55.8 Ma having an initial ratio of 0.7034 and an MSWD of 91.7, again giving a meaningless age. The distribution of the data from the gabbro samples does not fall on a straight line and therefore, a meaningful regression line cannot be drawn.

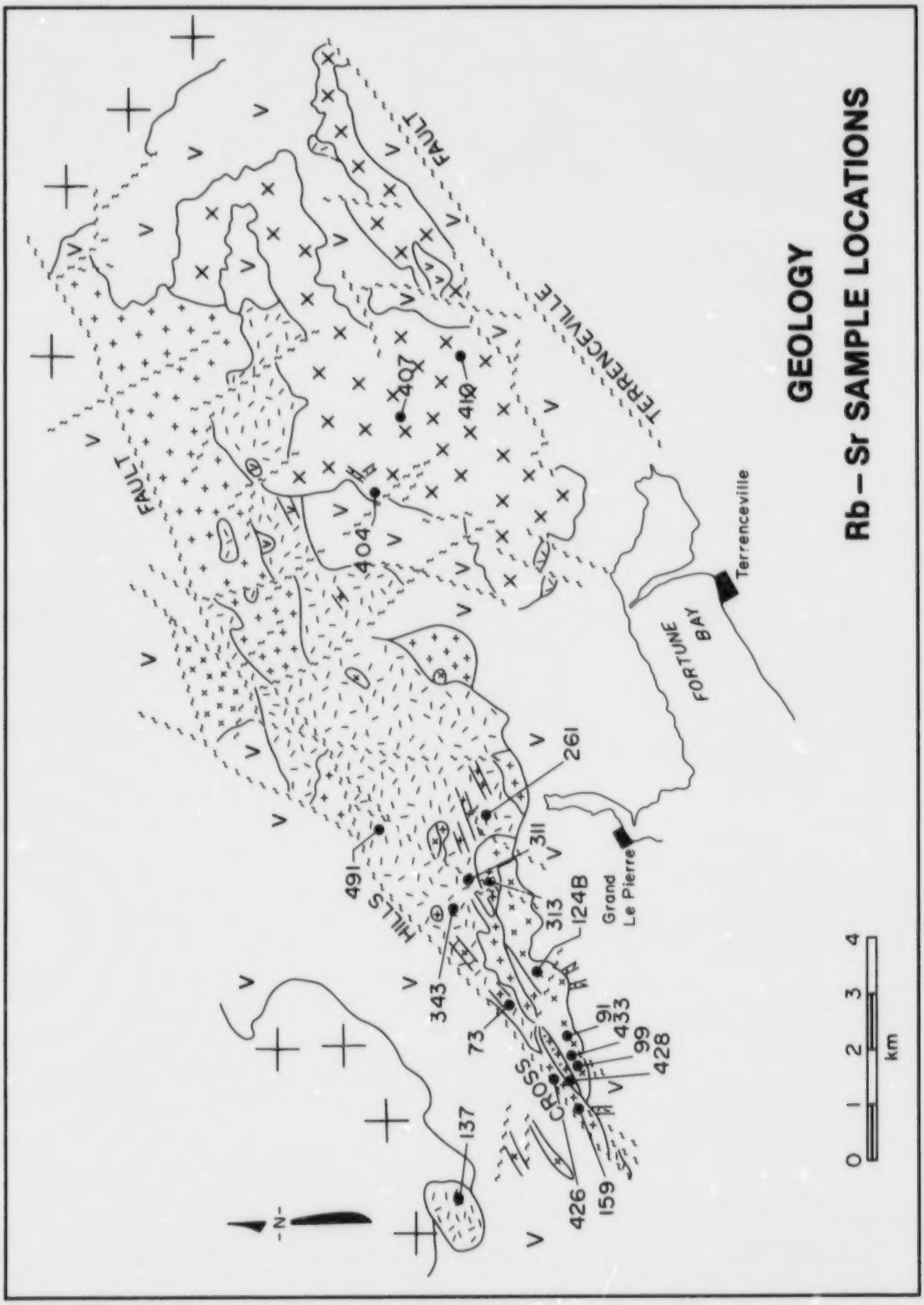

Figure 27. *Location of Rb–Sr samples and simplified geology, Grand Le Pierre area. Unit symbols as for Figure 3.*

Table 4. Rb–Sr analyses. Sample locations shown on Figure 27; see Appendix 4A for rock-type abbreviations

Sample	Rock Type	Rb	Sr	$^{87}Rb/^{86}Sr$	$^{87}Sr/^{86}Sr$
JT-073	GBBR	113.8	192.5	1.713	0.71717±0.00005
JT-137	GBBR	36.5	311.7	0.337	0.70549±0.00003
JT-159	BGRT	196.6	61.7	9.278	0.77184±0.00003
JT-261	GBBH	73.5	266.6	0.799	0.71057±0.00005
JT-311	GBBR	33.3	470.2	0.205	0.70540±0.00004
JT-313	BGRT	182.3	37.6	14.184	0.80594±0.00002
JT-343	GBBR	32.2	337.0	0.277	0.70607±0.00002
JT-404	GRDR	88.9	198.9	12.94	0.71543±0.00004
JT-407	GRDR	82.2	181.1	1.412	0.71639±0.00003
JT-410	GRDR	80.4	185.7	1.254	0.71489±0.00002
JT-426	BGRT	193.7	63.9	8.830	0.77124±0.00005
JT-428	BGRT	128.6	36.1	14.817	0.81741±0.00007
JT-491	GBBH	104.4	323.8	0.933	0.71224±0.00002

The three samples from the granodiorite (Figure 28a) give an indicated age of 647.1 ± 79.1 Ma having an initial ratio of 0.7034 and a MSWD of 0.96. This is the only isochron obtained. However, it is based on only three samples and a very small $^{87}Rb-^{86}Sr$ range and must be considered as tentative at best.

The four samples of biotite granite (Figure 28b) give an age of 515.3 ± 42.9 Ma having an initial ratio of 0.7051 and a large MSWD of 14.3. An errorchron of 515.2 ± 10.6 Ma having an initial ratio of 0.7049 and a MSWD of 14.6 was obtained from the combined data for the biotite granite and the hybrid gabbro-granite (Figure 28c). It is possible that the Rb–Sr system re-equilibrated during intrusion of the biotite granite and this is probably the best age obtainable from the data.

Discussion

The Rb–Sr data do not provide high-precision ages. However, it is clear that the Cross Hills Plutonic Suite is Late Proterozoic to Cambrian in age, as opposed to Devonian.

The data do not permit a significant chronology to be established between the various rock units of the Cross Hills Plutonic Suite. However, the granodiorite may be older than the biotite granite. There are, however, abundant xenoliths in the granodiorite, which may produce the older ages due to incomplete homogenization of the Rb–Sr system.

The biotite granite and hybrid gabbro-granite age has the best MSWD obtained from the dataset. It is possible that the Rb–Sr system equilibrated during mixing and that this age is acceptable. It is similar to the age for biotite granite.

A preliminary Early Cambrian U–Pb zircon age of 547^{+3}_{-6} Ma, obtained from the peralkaline granite (G.

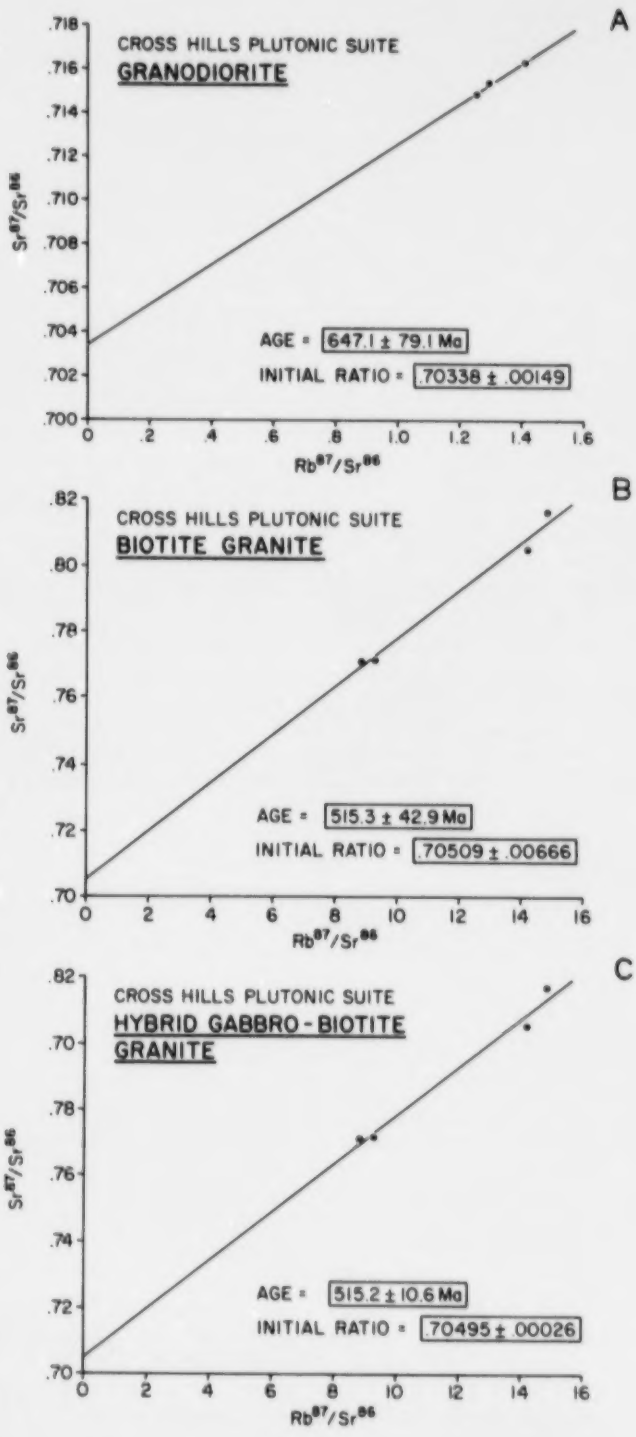

Figure 28. *Rb–Sr isochron plots of selected samples from the Cross Hills Plutonic Suite.*

Dunning, personal communication, 1987) is the best estimate for the age of the Cross Hills Plutonic Suite. This age is comparable to the Rb–Sr age of 560 Ma obtained by regression of all the available Rb–Sr data.

The range of relatively low initial strontium ratios (0.703–0.705) obtained from the data indicates a mantle to lower crustal source for the magmas. An origin for the felsic magmas through widespread crustal melting or contamination is not indicated by the data. Incomplete homogenization and remobilization of the Sr isotopes, however, may have occurred and the Sr data can only be interpreted on a tentative basis.

Oxygen

Introduction

Oxygen isotope analyses were performed on samples of biotite granite and peralkaline granite from the Cross Hills Plutonic Suite and also on a sample of dacite tuff containing epidote-filled veins and vesicles. The sample locations are shown on Map 91-15, and sample numbers, brief descriptions and results are presented in Table 5. Details on sample preparation, analytical method, accuracy and precision are presented in Appendix 1F.

Table 5. Oxygen isotope analyses from 3 granite samples and a felsic volcanic sample from the Grand Le Pierre area. Sample locations on Map 91-15

Sample	Rock Type	WR	q	f	q-f
JT-433	Peralkaline granite	4.20	2.80	4.60	-1.8
JT-435	Biotite granite	4.10	4.00	4.30	-0.3
JT-094	Dacitic volcanic tuff with epidote veins	4.90	1.70	5.60	-3.9

WR = whole rock; q = quartz; f = feldspar

The application of oxygen isotope analyses to the study of granitic rocks and associated hydrothermal systems has been reviewed by Taylor (1978, 1979). Few oxygen isotope data are available from granite systems in Newfoundland with the exception of the Ackley Granite Suite (Tuach *et al.*, 1985, 1988; Tuach, 1987).

Results

The data are listed in Table 5 and illustrated in Figure 29. The $\delta\ ^{18}O$ whole-rock (wr) values are below the primary range of normal granites and extrusive rocks (+6 to +12 per mil). In addition, the quartz–feldspar (q-f) fractionations are disturbed from the projection below normal values of the high temperature 'magmatic' equilibration field given by Δ q-f = +1 + 0.5 per mil (Figure 29), indicating a substantial influence of subsolidus fluids on the oxygen isotope signature. Quartz is resistant to secondary magmatic exchange at temperatures below 300°C (Taylor and Forrester, 1979; Criss and Taylor, 1983; Giletti and Yund, 1984) and can be used to estimate whole-rock composition at this blocking temperature where $\delta\ ^{18}O$ wr = $\delta\ ^{18}O$ quartz–1. Thus, the estimated $\delta\ ^{18}O$ whole-rock values at a temperature of 300°C are also substantially below the range of normal magmatic values and are:

Sample JT-433 (peralkaline granite) −1.8 per mil
Sample JT-435 (biotite granite) −3.0 per mil
Sample JT-094 (dacite tuff) −0.7 per mil

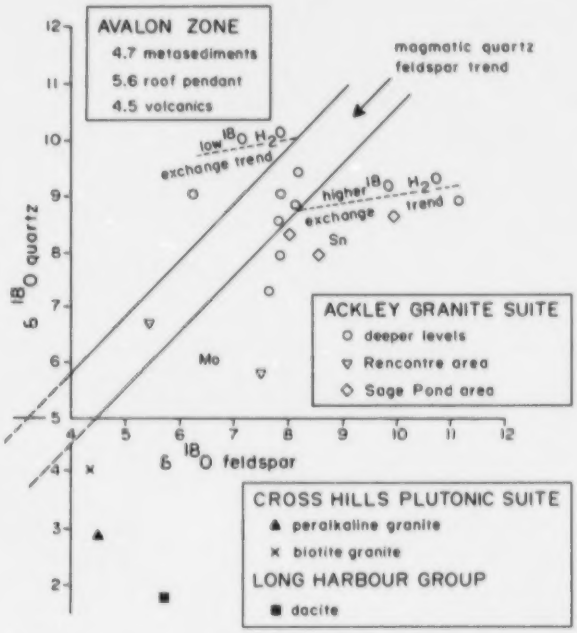

Figure 29. *Oxygen isotope data from the Fortune Bay area. Open symbols represent data from Tuach (1987) and Tuach* et al. *(1985). Whole-rock $\delta\ ^{18}O$ values of composite samples of Avalon Zone rocks are shown in the box.*

Discussion

The low $\delta\ ^{18}O$ signature of the granite of the Cross Hills Plutonic Suite and of the dacitic tuff are similar to $\delta\ ^{18}O$ whole-rock values of composite samples of metasedimentary (4.7), metavolcanic (4.5), and granitic roof pendants (5.6) from rocks of the Avalon Zone (Figure 29). Details of these composites are given in Tuach (1987). These low values can be interpreted as resulting from 1) a source area for all magmas in the Avalon Zone, including the Cross Hills Plutonic Suite, with an inherent low $\delta\ ^{18}O$ signature, or 2), substantial subsolidus to low-temperature equilibration of rocks having a normal magmatic signature with low $\delta\ ^{18}O$ fluids, followed by re-equilibration during regional metamorphism at temperatures above 300°C.

The second interpretation is considered to be the most reasonable explanation for the low $\delta\ ^{18}O$ signature of the

Avalon Zone rocks since various rock types are depleted to a similar degree. After metamorphic re-equilibration to lower values, the trend to negative Δ q-f values could result from interaction with higher $\delta\ ^{18}O$ fluids emanating from the Devonian magmas. The Ackley Granite Suite, representative of this magmatism, has an estimated primary magmatic value of 7.0 + 0.45 per mil (Tuach, 1987; Tuach *et al.*, 1988). The fact that the Cross Hills Plutonic Suite has a low $\delta\ ^{18}O$ signature would indicate that the proposed metamorphic equilibration postdated intrusion of the Cross Hills Plutonic Suite.

The low $\delta\ ^{18}O$ signature means that the values cannot be used to detect a possible metasedimentary component in the source area for Avalon Zone magmas (cf. Taylor, 1978; O'Neil and Chappell, 1977).

CONTACT RELATIONSHIPS IN AND BETWEEN BIOTITE GRANITE AND PERALKALINE GRANITE: QUENCHING ACROSS AN INTERFACE IN ZONED SILICATE LIQUIDS

CONTACT RELATIONSHIPS

Biotite Granite and Aplite

The contact between the biotite granite and chemically related aplitic phase can be traced over a distance of 2 km (Map 91-14; Figure 5) where it is a sharp boundary marked by small patches of pegmatite within the biotite granite (Plate 8). On a larger scale, the aplite coarsens southward. These features indicate a 'quench' in both directions from the contact or boundary.

Aplite–Biotite Granite and Peralkaline Granite

The contact of the biotite granite and its aplitic phase with the main area of peralkaline granite, to the northwest of Grand Le Pierre, is marked by a diffuse zone (2 to 20 m wide) over which, an increase of 30 to 50 percent in total-count radioactivity occurs in a southerly direction (i.e., the peralkaline rocks are more radiogenic). In the western part of the area, which is mapped in detail (Map 91-14), the boundary zone is marked by a relatively rapid colour change from orange (biotite granite) to red-brown (peralkaline granite) over a distance of 0.2 to 5 m. In the central map area, this colour change occurs within a much wider zone (over 100 m) in which the textures change from medium-grained graphic, in the peralkaline rocks, to fine-grained and spherulitic (see Figure 5; Plate 9) at the northern boundary with the aplite. The biotite granite–peralkaline granite boundary, in the east of the study area (Map 91-14), is marked by a gradual colour change from orange to red-brown between granites of similar texture. It is emphasized that chilled contacts were not observed between the aplite–biotite granite and the peralkaline granite even though the boundary zone is well-exposed.

GEOCHEMISTRY ACROSS THE CONTACTS

A detailed geochemical study was undertaken across the contact zone between biotite granite, aplite, and peralkaline granite in the Bart Pond area. Sample locations are shown in Figure 5. This area was selected because 1) the suite of samples from number JT-426, south to number JT-99, provides a geochemical cross-section of the granite bodies; 2) it provides a continuous exposure across a transitional colour change from orange aplite (associated with the biotite granite) to purple aplite (associated with the peralkaline granite) within the aplite unit, which is also accompanied by an increase in background radioactivity; 3) the contact is exposed between medium-grained biotite granite containing pegmatite pods (indicating a quench to the north of the boundary) and the orange aplite, which coarsens southward (indicating a quench to the south of the boundary); and 4) a possible geochemical relationship between the peralkaline granite and the mineralization and alteration zones near Dump Pond could be investigated.

The results of the analyses are summarized in Figure 30, which shows the sample numbers, their relative position on the surface, and the variation in composition toward the southern margin of the peralkaline granite (left of diagram). Only elements and oxides that show significant variation have been plotted.

There is a minor change in composition across the aplite–biotite granite contact, particularly in SiO_2, Al_2O_3, CaO and K_2O and this is accompanied by a minor decrease in the content of F and Rb. More striking is the contrast in composition across the zone of colour change within the aplite, where there is a 2 percent increase in SiO_2 and a 0.5 percent decrease in Al_2O_3 with corresponding changes in most oxides and several trace elements. A comparable compositional break was recorded in three samples collected over a space of 10 cm at the colour transition, approximately one km to the northeast of the detailed section (Table 6).

INTERPRETATION

This arrangement of textures and compositional variation is interpreted to result from pressure-quenching across a compositional boundary in a zoned magma marked by the zone of colour change in the aplite. This quenching occurred near the carapace of the magma chamber. The tuffisites also indicate rapid volatile loss. The peralkaline magma, which contains less than 5 percent small phenocrysts, is thought

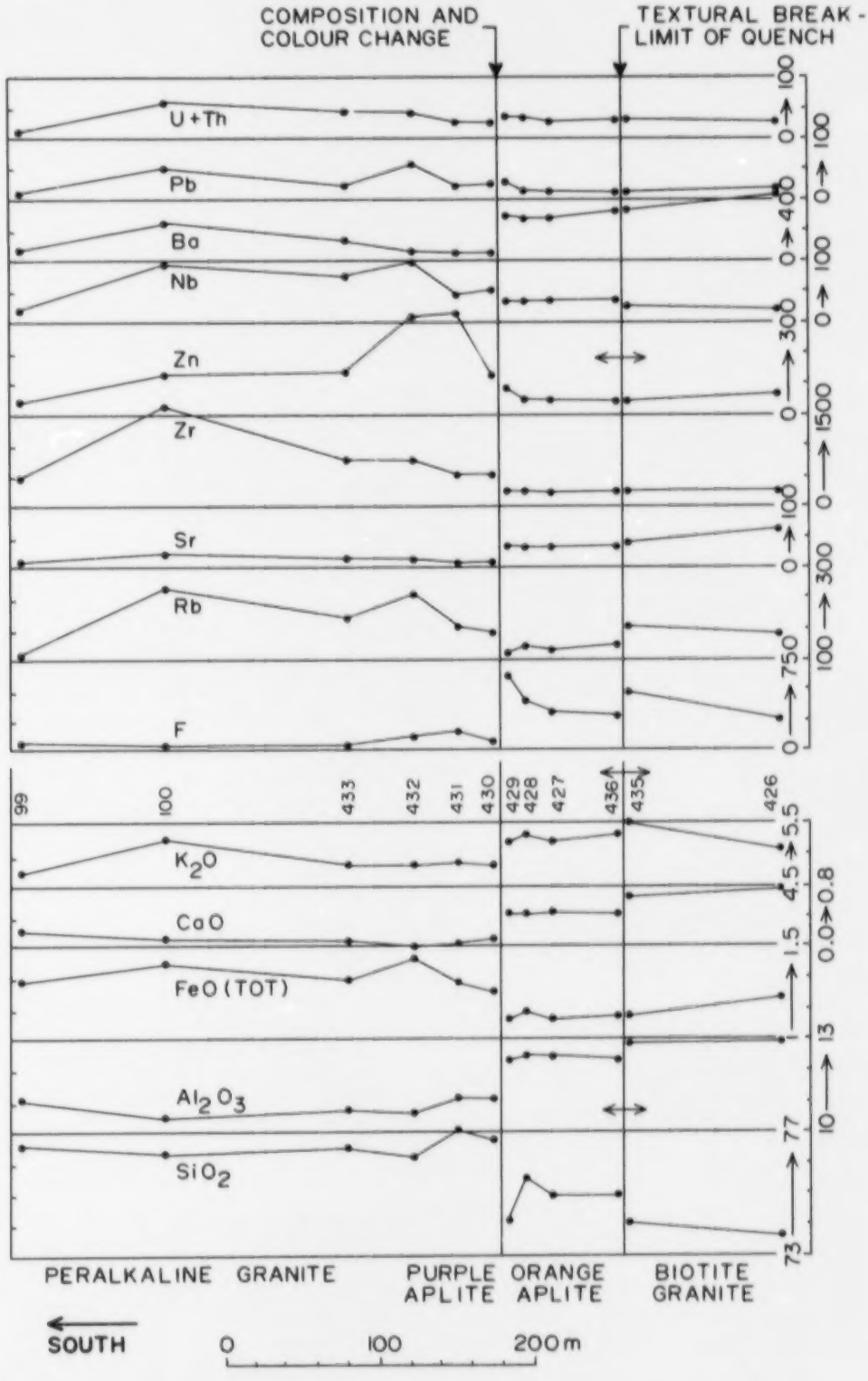

Figure 30. *Distribution of selected major and trace elements in samples from the Bart Pond area. The analyses are interpreted to represent a vertical geochemical section from biotite granite, through aplite, into peralkaline granite towards the peralkaline granite–volcanic contact at the left side of the diagram. Sample locations are shown on Figure 5.*

Table 6. Major- and trace-element analyses of three samples collected at 10 cm intervals across the colour transition between red and purple aplite. Located approximately 1 km northeast of the section shown in Figure 11; see Appendix 4A for rock-type abbreviations

Wt%	JT-84-10	JT-84-11	JT-84-12
SiO_2	75.5	78.0	77.8
TiO_2	0.22	0.16	0.15
Al_2O_3	12.1	11.4	10.9
Fe_2O_3t	1.46	0.96	0.85
MnO	0.02	0.01	0.01
MgO	0.12	0.04	0.02
CaO	0.16	0.08	0.04
Na_2O	3.72	3.41	3.26
K_2O	5.27	5.39	5.29
P_2O_5	0.00	0.00	0.00
LOI	0.24	0.31	0.43
TOTAL	98.81	99.76	98.75
ppm			
V	0	0	0
Cr	5	3	6
Ni	0	0	0
Cu	0	0	0
Zn	24	22	20
Ga	21	21	23
Rb	211	199	199
Sr	37	19	19
Y	73	57	51
Zr	247	207	202
Nb	35	24	23
Ba	226	150	149
La	57	33	37
Ce	87	69	83
Pb	13	11	16
Th	19	11	18
U	5	0	6
Rock type	APLT	PGRT	PGRT

to have overlain a similarly liquid magma of granite composition. The lower contact between aplite and medium grained biotite granite represents the lower limit of the quenched material, which formed a carapace against which the underlying granite magma, to the north, cooled more slowly by conductive heat loss. Minor increase in fluid pressure at this contact is indicated by the localization of the pegmatite pods in the medium-grained granite.

In the eastern exposures, where the contact between the biotite granite and peralkaline granite is marked by colour change in a medium-grained rock, it can be postulated that crystallization occurred across the liquid-liquid boundary predominantly by heat loss.

The change of textures in the aplite–peralkaline granite from glassy spherulitic to the north through progressively coarser graphic intergrowths to equigranular granite, at the carapace, can be ascribed to recrystallization of a quenched glassy rock under a progressively increasing fluid flux. Pegmatite patches in both the peralkaline granite and the biotite granite indicate local areas of relatively higher fluid pressure during cooling, and the abundant tuffisite is indicative of rupturing of quenched granite due to fluid overpressure from vapour-phase exsolution. The chilled contact between the peralkaline granite and the country rock could indicate that recrystallization of glassy material to a graphic texture took place at high sub-solidus temperature or possibly above the solidus following closure of the system and an increase in P_{tot} and/or P_{H_2O}, whereas the material at the chilled contact was relatively cool and did not recrystallize.

DISCUSSION AND CONCLUSIONS

TECTONOSTRATIGRAPHIC CORRELATIONS

In the Avalon Zone of Newfoundland, the Cross Hills Plutonic Suite dated at about 560 Ma, is correlative with a variety of youngest Precambrian to oldest Paleozoic magmatic events (Table 3). Correlative magmatism may also be represented by the peralkaline Louil Hills intrusive suite (Figure 1), in the Eastport map area (O'Brien, 1987), and possibly by the Powder Horn Diorite Complex on the Isthmus of the Avalon Peninsula (C. O'Driscoll, personal communication, 1986).

Stratigraphically dated, Middle Cambrian, basaltic volcanic rocks and correlative feeder pipes of alkaline affinity (Greenough and Papezik, 1985) may be correlative with the later magmatic events in the Cross Hills Plutonic Suite. However, it is probable that the Rb–Sr age of the granitic rocks of the Cross Hills Plutonic Suite are anomalously young and that they are older than the Cambrian mafic plutonism.

In the Humber Zone of Newfoundland (Figure 1), the peralkaline? Round Pond alkali feldspar granite has yielded a latest Precambrian U–Pb zircon age of 602 ± 10 Ma (Williams *et al.*, 1985) similar to a U–Pb zircon age of 617 ± 8 Ma reported by Currie (1987) for the Hare Hill peralkaline granite (Currie, 1987). The Long Range mafic dyke swarm and correlative tholeiitic plateau basalts on the Great Northern Peninsula (Figure 1) have provided $^{40}Ar-^{39}Ar$ ages around 605 Ma (Stukas and Reynolds, 1974). Thus, it is possible that the Cross Hills Plutonic Suite is correlative with these rocks.

Late Precambrian rocks of the Avalon Zone occur along the eastern border of the Paleozoic Appalachian Orogen and have been correlated with similar Pan-African sequences in western Europe and North Africa. (e.g., Rast *et al.*, 1976; Strong *et al.*, 1978). Stratigraphic summaries and correlations between the Canadian Appalachians and North Africa are given in O'Brien *et al.* (1983).

In northern Africa and the Arabian shield, extensive plutonism (ca. 800 to 650 Ma; cf. O'Brien *et al.*, 1983) accompanied and postdated the major episodes of volcanism, and these plutonic events culminated in the emplacement of small gabbro–granite ring complexes of alkaline and peralkaline affinity that have been dated at ca. 700 to 515 Ma (cf. O'Brien *et al.*, 1983). Thus, the stratigraphic correlations between the Avalon Zone and the Pan-African sequences (O'Brien *et al.*, 1983) are further strengthened by the present work.

TECTONIC SETTING

The outcrop pattern of the Cross Hills Plutonic Suite and the sheeted intrusion of the gabbro by biotite granite indicate a northwest-southeast extension during magma emplacement. Smith and Hiscott (1984) have studied the depositional environment of red conglomerates and sandstone of the Rencontre Formation of the Long Harbour Group and have concluded that they were deposited in northeast-elongate, pull-apart basins related to a rifting or transpressional regime in the Avalon Zone. These basins were also developed by northwest-southeast extension. The Rencontre Formation stratigraphically overlies the Mooring Cove Formation, which consists of volcanic rocks interpreted as coeval with the peralkaline phase of the Cross Hills Plutonic Suite (Tuach, 1984; O'Brien *et al.*, 1984). Thus, the late Precambrian settings of magmatism and sediment deposition are comparable.

The presence of Middle Cambrian, alkaline mafic magmatism (Greenough and Papezik, 1985) supports the suggestion of multiphase extension in the Avalon Zone in the late Precambrian to early Paleozoic as suggested by Smith and Hiscott (1984). It is possible that magmatism in the Cross Hills area occurred during a series of discrete periodic extensional events throughout the Avalon Zone.

Alkaline and peralkaline magmatism are generally thought to occur in rift-related continental environments (Bailey, 1974), although extensional environments in overall transpressional, or subduction-related regimes, may also generate similar magmatism. The most recent interpretation of the tectonic setting of the rocks in the Avalon Peninsula invokes a basin and range environment (Strong *et al.*, 1984; Krogh *et al.*, 1988) that involves tensional tectonics in the craton due to crustal thinning above the deeper portions of a subduction zone. The setting of the Cross Hills Plutonic Suite is in accord with this model.

Extensional events in the Avalon Zone that were responsible for most of the late Paleozoic to Cambrian magmatism are generally considered as independent of the development of the Iapetus Ocean (cf. Strong *et al.*, 1978; O'Brien *et al.*, 1983; Greenough, 1984; Krogh *et al.*, 1988). They are considered to be events indigenous to the large-scale development of the Pan-African terranes. However, in the Grenvillian basement of the Humber Zone in Newfoundland, the Hare Hills and Round Pond granites and the Long Range mafic magmatism have been related to rifting that initiated the development of the Paleozoic Iapetus Ocean (cf. Williams *et al.*, 1985). Therefore, it is possible that the late Precambrian to Cambrian magmatic events of alkaline affinity may also be related to continental rifting and development of the Iapetus Ocean (Williams *et al.*, 1989).

PETROGENESIS

The close spatial association between the gabbro–diabase unit, the biotite granite, the peralkaline granite and the minor syenite units implies that these rocks are part of a cogenetic plutonic suite. This cogenetic relationship is further emphasized by the alkaline nature of the suite. The genetic relationship of the granodiorite to the rest of the suite is not so clear. However, it gives a similar Rb–Sr age, within the large errors, and is probably part of the same thermal event.

The sharp discordant contacts of the plutons with the country rocks, together with the fine-grained textures in these plutonic rocks, suggest a high crustal level of emplacement for the mafic rocks and the granites. The miarolitic cavities, variable fine-grained pegmatite, aplite, and tuffisite textures also indicate high-level emplacement together with fluid saturation in the magma during crystallization. The inferred rapid quenching of the magma by loss of excess vapour pressure suggests that the lithostatic pressure was less than 1 kb indicating a maximum depth of emplacement of 3 km.

The aplite, which contains less than 5 percent small phenocrysts, together with the interpretation of an origin by quenching, indicates that the magma was almost completely liquid prior to crystallization. This, in turn, implies a magma temperature, immediately prior to quenching, in excess of 830°C (Clemens *et al.*, 1986).

Petrogenetic models for similar granitic rocks in Arabia have been presented by Harris and Mariner (1980), Drysdall *et al.* (1984) and Jackson *et al.* (1985). The granites of the Cross Hills Plutonic Suite and the Arabian Shield granites

Table 7. Summary of metal content of selected Saudi Arabian Zr–Nb–Y–REE deposits from Drysdall *et al.* (1984)

Location	Million tonnes	Depth (metres)	Grade (g/t)								
			Nb	Ta	Sn	La	Ce	Y	Th	U	Zr
Ghurayyah	440	250	2256	212	290	61	144	1326	399	117	8578
Jabal Tawlah	6.4	85	3405	175	381	19	137	5216	693	8	37300
Umm al Birak	6.6	150	1663	121	84	371	800	311	46	28	5129
Jabal Sa'id	23	100	1290	82	199	587	1301	4151	834	134	>17000
Jabal Hamra	18	100	1731	146	194	2593	3432	1592	263	75	13267

(Drysdall *et al.*, 1984) can be classified as A-type granites (Loiselle and Wones, 1979; Collins *et al.*, 1982). A-type (or anorogenic) granites are generally considered to be derived from partial melting, under high-temperature and vapour-absent conditions, of a crust from which a granitic melt has previously been derived (Loiselle and Wones, 1979; Collins *et al.*, 1982). In this model, hydrous minerals thought to be residual with respect to the first phase of melting (amphibole, biotite, and accessory minerals including zircon) are broken down by the second episode of higher temperature melting to incorporate water, halogens and the highly charged cations into the magma (characteristic of A-type melts).

Alternatively, the abundance of highly charged cations and halogens may result from a process of metasomatism in the mantle and lower crust, which may in turn relate to extensional tectonics affecting the mantle. Halogens and highly charged cations permeating the lower crust may depress the solidus and promote high-volume melting (cf. Bailey, 1980; Thompson *et al.*, 1984; Jackson *et al.*, 1985).

Fluorine, which is commonly abundant in A-type granite, is depleted in the peralkaline granites of the Cross Hills Plutonic Suite, perhaps due to its loss from the magmatic system in a volatile phase.

The low initial Sr ratios, from 0.7033 to 0.705, indicate a source area in the mantle or possibly the lower crust and are similar to those for the Saudi Arabian granites (Jackson *et al.*, 1985). These values, similar to values of A-type granites in general, imply a rapid magma ascent and little crustal contamination. Unfortunately, the oxygen isotope data cannot be used as a source indicator due to re-equilibration.

METALLOGENESIS

Fine-grained peralkaline aplite veins (occurrence # 12, Figure 9; Table 1) with significant enrichment of Zr, Nb, Y and REE attest to the magmatic origin of at least some of the mineralization in the peralkaline phase of the Cross Hills Plutonic Suite. The similarity in geochemical signature of the peralkaline granite and the mineralized rocks corroborates this association. Thus, the petrogenesis discussed above is an integral part of the metallogenic process.

The mineralization in the Cross Hills Plutonic Suite shows remarkable similarities in enrichment patterns and host rocks to major deposits of Zr, Nb and REE mineralization in the Arabian Shield (Drysdall *et al.*, 1984; Jackson *et al.*, 1985). These deposits are hosted by small, peralkaline A-type granites that represent the youngest plutonic events in the Arabian Shield. Harris and Mariner (1980), and Drysdall *et al.* (1984), suggested that the mineralization, particularly with respect to the high Nb, Zr, Y, REE, F and Sn contents, is derived from parental, REE-enriched granites.

In Saudi Arabia (Table 7), mineralization is hosted by stocks and dykes of microgranite porphyry, aplite–pegmatite sheets, pegmatitic and siliceous pods, veins and apophyses, and by matrix to intrusion breccias (Jackson *et al.*, 1985). Gradations between the mineralization styles indicate that the mineralization varies in origin from magmatic-hydrothermal to lower temperature hydrothermal. Similar variations in style are evident from the occurrences in the peralkaline phase of the Cross Hills Plutonic Suite.

Drysdall *et al.* (1984) suggested that the granophile elements were retained in the melt, as high-coordination complexes with alkali ions, especially in the presence of fluorine, until the final stages of crystallization and/or separation of a vapour phase. In particular, they note that zircon is soluble in peralkaline melts (Watson, 1979). In the Cross Hills Plutonic Suite, the tight grouping of Na_2O and K_2O, on the geochemical plots, argues against metasomatic processes and indicates that these alkali oxides were not active agents in transporting trace elements in a fluid medium. In addition, Drysdall *et al.* (1984) suggested that differences in fluid composition influenced the relative fractionation of the REE and high-field-strength elements during the mineralization process.

The presence of a compositional boundary in the silicic magma chamber of the Cross Hills Plutonic Suite and the lack of phenocrysts in the aplite suggest that liquid-state fractionation processes operated in the magma chamber to create much of the observed chemical variation. Alternatively, crystal fractionation (as suggested by Jackson *et al.*, 1985) operated in a deeper magma chamber and immiscibility between the granitic magmas was maintained in the chamber represented by the current exposure of the Cross Hills Plutonic Suite.

It is probable that convection cells operated in the different compositional units to promote internal homogenization. Crystallization of the magma resulted in fluid overpressure and transport of some of the elements of economic interest to new depositional sites in the peralkaline granite.

MINERAL POTENTIAL

Zircon, Nb, Y and REE minerals are an integral part of the new technological age and a growing demand is forecast for these commodities. Present reserves, which are adequate for current industrial requirements, are obtained from placer deposits, from small specialized lode mines, or as by products from other mines and metallurgical processes. Major reserves are known in the more inaccessible parts of the world; for example the Be–Nb–Ta–Y deposits at Thor Lake in the North West Territories (Davidson, 1978; Trueman *et al.*, 1985), the Zr–Y–F–Nb deposits at Strange Lake in Labrador (Currie, 1985; Miller, 1986), and the deposits in Saudi Arabia (Drysdall *et al.*, 1984; Jackson *et al.*, 1985). However, these deposits have yet to be developed, and their remote location requires larger markets and large mines to provide the economics of scale.

The similarities in geochemical-enrichment trends, styles of mineralization and age and composition of host rocks between the Zr–Nb–Y mineralization in the Cross Hills Plutonic Suite and the major deposits in the Arabian Shield are remarkable. These similarities indicate a potential for similar deposits in association with the Cross Hills Plutonic Suite. This potential can be extended to other late Precambrian–Early Cambrian peralkaline plutons (e.g., the Louil Hills; O'Brien, 1987) in the Avalon Zone of Newfoundland and throughout the Avalon Zone in eastern North America. Some potential for similar mineralization also exists in the late Precambrian plutons in the Humber Zone.

The known occurrences in the Cross Hills Plutonic Suite are too small to be of economic significance. Furthermore, the abundance of outcrop makes it unlikely that a major deposit is present at any of the known showings. The main potential is with buried deposits or with, as yet, undiscovered showings or peralkaline granite associated with the Cross Hills Plutonic Suite or with another intrusive body.

High-grade Zr–Nb–Y–REE deposits in an accessible location, adjacent to a well-developed industrial infrastructure, may provide a significant competitive advantage in the future supply of these minerals. Therefore, potential deposits in the Avalon Zone may provide an attractive exploration target.

ACKNOWLEDGMENTS

Cindy Saunders performed much of the scanning electron microscope and microprobe work and assisted with the preparation of this manuscript. D'Arcy Taylor assisted with field work in 1983. Lawson Dickson is thanked for his assistance and interest. S. O'Brien and D. Wilton provided thoughtful reviews.

REFERENCES

Bailey, D.K.
1974: Continental rifting and alkaline magmatism. *In* The Alkaline Rocks. *Edited by* H. Sorenson. John Wiley and Sons, New York, pages 148-159.

1980: Volcanism earth degassing and replenished lithosphere mantle. Philosophical Transactions of the Royal Society of London, Series A297, pages 309-322.

Barth, T.F.W.
1962a: Theoretical Petrology, Second Edition. John Wiley and Sons, New York, 416 pages.

1962b: A final proposal for calculating the mesonorm of metamorphic rocks. Journal of Geology, Volume 70, pages 497-498.

Bell, K., Blenkinsop, J. and Strong, D.F.
1977: The geochronology of some granitic bodies from eastern Newfoundland and its bearing on Appalachian evolution. Canadian Journal of Earth Sciences, Volume 14, pages 456-476.

Bradley, D.A.
1962: Gisborne Lake and Terrenceville map areas, Newfoundland (1M/15 and 10). Geological Survey of Canada, Memoir 321, 56 pages.

Brooks, C., Hart, S.R. and Wendt, I.
1972: Realistic use of two-error regression treatments as applied to rubidium-strontium data. Reviews of Geophysics and Space Physics, Volume 10, pages 551-577.

Cawthorn, R.G. and Collerson, K.D.
1974: The recalculation of pyroxene end-member parameters and the estimation of ferrous and ferric iron content from electron microprobe analyses. Mineralogist, Volume 59, pages 1203-1208.

Clayton, R.N. and Mayeda, T.K.
1963: The use of bromine pentafluoride in the extraction of oxygen from oxides and silicates for isotopic analysis. Geochimica et Cosmochimica Acta, Volume 27, pages 43-52.

Clemens, J.D., Holloway, J.R. and White, A.J.R.
1986: Origin of an A-type granite: experimental constraints. American Mineralogist, Volume 71, pages 317-324.

Collins, W.J., Beams, S.D., White, A.J.R. and Chappell, B.W.
1982: Nature and origin of A-type granites with particular reference to southeastern Australia. Contributions to Mineralogy and Petrology, Volume 80, pages 1189-1200.

Criss, R.E. and Taylor, H.P.
1983: An $^{18}O/^{16}O$ and D/H study of Tertiary hydrothermal systems in the southern half of the Idaho batholith. Geological Society of America Bulletin, Volume 94, Number 5, pages 640-663.

Currie, K.L.
1976: The alkaline rocks of Canada. Geological Survey of Canada, Bulletin 239, 228 pages.

1985: An unusual peralkaline granite near Lac Brisson, Quebec-Labrador. *In* Current Research, Part A. Geological Survey of Canada, Paper 85-1A, pages 73-80.

1987: A preliminary account of the geology of the Harrys River map area, southern Long Range of Newfoundland. *In* Current Research, Part A. Geological Survey of Canada, Paper 87-1A, pages 653-662.

Dallmeyer, R.D., Odom, A.L., O'Driscoll, C.F. and Hussey, E.M.
1981: Geochronology of the Swift Current granite and host volcanic rocks of the Love Cove Group, southwestern Avalon Zone, Newfoundland: evidence of a late Proterozoic volcanic–subvolcanic association. Canadian Journal of Earth Sciences, Volume 18, pages 699-707.

Dallmeyer, R.D., Hussey, E.M., O'Brien, S.J. and O'Driscoll, C.F.
1983: Chronology of tectonothermal activity in the western Avalon Zone of the Newfoundland Appalachians. Canadian Journal of Earth Sciences, Volume 20, pages 355-363.

Davidson, A.
1978: The Blackford Lake Intrusive Suite: An Aphebian alkaline plutonic complex in the Slave Province, Northwest Territories. *In* Current Research. Geological Survey of Canada, Paper 78-1A, pages 119-127.

Deer, W.A., Howie, R.A. and Zussman, J.
1963: Rock Forming Minerals, Volume 1. Lowe and Brydone, Norfolk, England, 333 pages.

Dickson, W.L.
1983: Geology, geochemistry and mineral potential of the Ackley Granite and parts of the North West Brook and Eastern Meelpaeg Complexes, southeast Newfoundland (Parts of map areas 1M/10, 11, 14, 15, 16; 2D/1, 2, 3 and 7). Newfoundland Department of Mines and Energy, Mineral Development Division, Report 83-6, 129 pages.

Drysdall, N., Jackson, J., Ramsay, C.R., Douch, C.J. and Hackett, D.
1984: Rare element mineralization related to Precambrian alkali granites in the Arabian Shield. Economic Geology, Volume 79, pages 1366-1377.

Evensen, N.M., Hamilton, P.J. and O'Nions, R.K.
1978: Rare-earth abundances in chondritic meteorites. Geochimica et Cosmochimica Acta, Volume 42, # 6A, pages 1199-1212.

Flynn, R.T. and Burnham, C.W.
1978: An experimental determination of rare earth partition coefficients between a chloride-containing vapor phase and silicate melts. Geochimica et Cosmochimica Acta, Volume 42, # 6A, pages 679-684.

Giletti, B.J. and Yund, R.A.
1984: Oxygen diffusion in quartz. Journal of Geophysical Research, Volume 89, pages 4039-4046.

Giret, A., Borin, B. and Leger, J.M.
1980: Amphibole compositional trends in oversaturated and undersaturated alkaline plutonic ring–complexes. Canadian Mineralogist, Volume 18, pages 481-495.

Greenough, J.D.
1984: Petrology and geochemistry of Cambrian volcanic rocks from the Avalon Zone in Newfoundland and New Brunswick. Ph.D. Thesis, Memorial University of Newfoundland, St. John's, 487 pages.

Greenough, J.D. and Papezik, V.S.
1985: Petrology and geochemistry of Cambrian volcanic rocks from the Avalon Peninsula, Newfoundland. Canadian Journal of Earth Sciences, Volume 22, pages 1594-1601.

Harris, N.B.W. and Mariner, G.F.
1980: Geochemistry and petrogenesis of a peralkaline granite complex from the Midian Mountains, Saudi Arabia. Lithos, Volume 13, pages 325-337.

Hopfengaertner, D.F.
1982: Geology, geophysics and geochemistry of Licence 1989, Claim Block 2455, Grand Le Pierre area. Assessment report Saarberg Interplan Limited. Newfoundland Department of Mines and Energy. Assessment File # [1M/10(205)].

Hughes, C.J.
1973: Spilites, keratophyres, and the igneous spectrum. Geological Magazine, Volume 109, pages 513-527.

Hughes, C.J. and Bruckner, W.D.
1971: Late Precambrian rocks of the eastern Avalon Peninsula, Newfoundland—a volcanic island complex. Canadian Journal of Earth Sciences, Volume 8, pages 899-915.

Irvine, T.N. and Baragar, W.R.A.
1971: A guide to the chemical classification of the common volcanic rocks. Canadian Journal of Earth Sciences, Volume 8, pages 523-548.

Jackson, N.J., Drysdall, A.R. and Stoeser, D.B.
1985: Alkali granite-related Nb-Zr-REE-U-Th mineralization in the Arabian Shield. *In* High Heat Production (HHP) Granites, Hydrothermal Circulation and Ore Genesis. *Edited by* C. Halls. The Institution of Mining and Metallurgy, London, pages 459-478.

Kerrich, H.R. and Fryer, B.J.
1979: Archaean precious-metal hydrothermal systems, Dome Mine, Abitibi Greenstone Belt. II. REE and oxygen isotope relations. Canadian Journal of Earth Sciences, Volume 16, pages 440-458.

Kontak, D.J., Tuach, J., Strong, D.F., Archibald, D.A. and Farrar, E.
1988: Plutonic and hydrothermal events in the Ackley Granite, southeast Newfoundland, as indicated by total fusion $^{40}Ar/^{39}Ar$ geochronology. Canadian Journal of Earth Sciences, Volume 25, pages 1151-1160.

Kosterin, A.W.
1959: The possible modes of transport of the rare earths by hydrothermal solutions. Geochemistry, Volume 4, pages 381-387.

Krogh, T.E., Strong, D.F., O'Brien, S.J. and Papezik, V.S.
1988: Precise U-Pb zircon dates from the Avalon Terrane in Newfoundland. Canadian Journal of Earth Sciences, Volume 25, pages 442-453.

Kuno, H.
1968: Differentiation of basaltic magmas. *In* Basalts, Volume 2. *Edited by* H.H. Hess and A. Poldervaart. John Wiley and Sons, New York, pages 623-688.

Leake, B.E.
1978: Nomenclature of amphiboles. Canadian Mineralogist, Volume 16, pages 501-520.

Loiselle, M.C. and Wones, D.R.
1979: Characteristics and origin of anorogenic granites. Geological Society of America, Program with Abstracts, Volume 11, page 468.

MacDonald, R.
1975: Nomenclature and petrochemistry of the peralkaline oversaturated extrusive rocks. Bulletin Volcanologique, Volume 38, pages 498-547.

Miller, R.R.
1986: Geology of the Strange Lake alkalic complex and the associated Zr-Y-Nb-Be-REE mineralization. *In* Current Research. Newfoundland Department of Mines and Energy, Mineral Development Division, Report 86-1, pages 11-19.

North American Commission on Stratigraphic Nomenclature
1983: North American stratigraphic code. American Association of Petroleum Geologists, Bulletin, Volume 67, Number 5, pages 841-875.

O'Brien, S.J.
1987: Geology of the Eastport (west half) map area. Bonavista Bay, Newfoundland. *In* Current Research, Newfoundland Department of Mines and Energy, Mineral Development Division, Report 87-1, pages 257-270.

O'Brien, S.J. and Nunn, G.A.G.
1980: Terrenceville (1M/10) and Gisborne Lake (1M/15) map areas, Newfoundland. *In* Current Research. Newfoundland Department of Mines and Energy, Mineral Development Division, Report 80-1, pages 120-133.

O'Brien, S.J., Wardle, R.J. and King, A.F.
1983: The Avalon Zone: a Pan-African terrane in the Appalachian Orogen of Canada. Geological Journal, Volume 18, pages 195-222.

O'Brien, S.J., Nunn, G.A.G., Dickson, W.L. and Tuach, J.
1984: Geology of the Terrenceville (1M/10) and Gisborne Lake (1M/15) map areas, southeast Newfoundland. Newfoundland Department of Mines and Energy, Mineral Development Division, Report 84-4, 54 pages.

O'Brien, S.J., Strong, D.F. and King, A.F.
1990: The Avalon Zone type area: southeastern Newfoundland Appalachians. *In* Avalonian and Cadomian Geology of the North Atlantic. *Edited by* R.A. Strachan and G.K. Taylor. Blackie, Glasgow and London, pages 166-194.

O'Neil, J.R. and Chappell, B.W.
1977: Oxygen and hydrogen isotope relations in the Berridale batholith. Journal of the Geological Society of London, Volume 133, pages 559-571.

Papezik, V.S.
1972: Late Precambrian ignimbrites in eastern Newfoundland and their tectonic significance. Proceedings, 24th International Geological Congress, Section 1, pages 147-152.

Pearce, T.H., Gorman, B.E. and Birkett, T.C.
1975: The TiO_2-K_2O-P_2O_5 diagram: a method of discriminating between oceanic and non-oceanic basalts. Earth and Planetary Science Letters, Volume 24, pages 419-426.

Rast, N., O'Brien, B.H. and Wardle, R.J.
1976: Relationships between Precambrian and lower Paleozoic rocks of the 'Avalon Platform' in New Brunswick, the Northeast Appalachians and the British Isles. Tectonophysics, Volume 30, pages 315-338.

Ronov, A.B., Balashov, Yu.A. and Migdisov, A.A.
1967: Geochemistry of the rare earths in the sedimentary cycle. Geochemistry International, Volume 4, pages 1-17.

Saunders, C.M. and Tuach, J.
1989: Zr-Nb-Y-REE mineralization in the Cross Hills Plutonic Suite. *In* Current Research. Newfoundland Department of Mines, Geological Survey of Newfoundland, Report 89-1, pages 181-192.

Smith, S.A. and Hiscott, R.N.
1984: Latest Precambrian to Early Cambrian basin evolution, Fortune Bay, Newfoundland: fault bounded basin to platform. Canadian Journal of Earth Sciences, Volume 21, pages 1379-1392.

Steiger, R.H. and Jager, E.
1977: Subcommission on Geochronology: Convention on the use of decay constants in geo- and cosmochronology. Earth and Planetary Science Letters, Volume 36, pages 359-362.

Streckeisen, A.L.
1973: Plutonic rocks. Classification and nomenclature recommended by the IUGS Subcommission on the Systematics of Igneous Rocks. Geotimes, Volume 18, # 10, pages 26-30.

Streckeisen, A. and LeMaitre, R.W.
1979: A chemical approximation to the modal QAPF classification of the igneous rocks. Neues Jahrbuchouer Mineralogic Abhandlungen, Volume 136, pages 169-206.

Strong, D.F.
1979: Proterozoic tectonics of northwestern Gondwanaland: new evidence from Eastern Newfoundland. Tectonophysics, Volume 54, pages 81-101.

Strong, D.F., O'Brien, S.J., Taylor, S.W., Strong, P.G. and Wilton, D.H.
1978: Geology of the Marystown and St. Lawrence map areas of Newfoundland. Newfoundland Department of Mines and Energy, Mineral Development Division, Report 77-8, 81 pages.

Strong, D.F., O'Brien, S.J. and Dostal, J.
1984: Petrochemical evolution of Late Proterozoic rocks in the Avalon Zone type-area in Newfoundland. Geological Society of America, Program with Abstracts, Northeastern Meeting, Rhode Island, U.S.A., March, 1984.

Strong, D.F. and Taylor, R.P.
1984: Magmatic-subsolidus and oxidation trends in composition of amphiboles from silica-saturated peralkaline igneous rocks. Tschermaks Mineralogische und Petrographische Mitteilungen, Volume 32, pages 211-222.

Stukas, V. and Reynolds, P.H.
1974: $^{40}Ar/^{39}Ar$ dating of the Long Range dikes, Newfoundland. Earth and Planetary Science Letters, Volume 22, pages 256-266.

Taylor, H.P., Jr.
1978: Oxygen and hydrogen isotope studies of plutonic granitic rocks. Earth and Planetary Science Letters, Volume 38, pages 177-210.

1979: Oxygen and hydrogen isotope relationships in hydrothermal mineral deposits. *In* Geochemistry of Hydrothermal Ore Deposits. *Edited by* H.L. Barnes. John Wiley and Sons, New York, pages 236-277.

Taylor, H.P. and Forrester, R.W.
1979: An oxygen and hydrogen isotope study of the Skaergaard intrusion and its country rocks: a description of a 55 m.y.-old fossil hydrothermal system. Journal of Petrology, Volume 20, pages 355-419.

Taylor, R.P. and Fryer, B.J.
1983: Rare earth lithogeochemistry of granitoid mineral deposits. Canadian Institute of Mining and Metallurgy Bulletin, Volume 76, pages 74-80.

Taylor, R.P., Strong, D.F., and Fryer, B.J.
1981: Volatile control of contrasting trace element distributions in peralkaline granitic and volcanic rocks. Contributions to Mineralogy and Petrology, Volume 77, pages 267-271.

Thompson, R.N., Harrison, M.A., Hendry, G.L. and Parry, S.J.
1984: An assessment of the relative roles of crust and mantle in magma genesis: an elemental approach. Philisophical Transactions of the Royal Society of London, Volume A310, pages 549-590.

Trueman, D.L., Peterson, J.C., de St. Jorre, L. and Smith, D.G.W.
1985: The Thor Lake, N.W.T. base-metal deposit. *In* Granite-Related Mineral Deposits: Geology, Petrogenesis and Tectonic Setting. *Edited by* R.P. Taylor and D.F. Strong. Canadian Institute of Mining and Metallurgy, extended abstracts, Halifax, 1985, pages 279-284.

Tuach, J.
1984: Metallogenic studies of granite-associated mineralization in the Ackley Granite and Cross Hills Plutonic Complex, Fortune Bay area, Newfoundland. *In* Current Research, Part A. Geological Survey of Canada, Paper 84-1A, pages 499-504.

1987: The Ackley high-silica magmatic/metallogenic system and associated post-tectonic granites, southeast Newfoundland. Unpublished Ph.D. thesis, Memorial University of Newfoundland, St. John's, 455 pages.

Tuach, J., Kerrich, R., Strong, D.F. and Willmore, L.M.
1985: Variations in oxygen isotope ratios related to source terranes and to hydrothermal regimes in the Ackley Granite, Newfoundland. *In* Granite-Related Mineral Deposits: Geology, Petrogenesis and Tectonic Setting. *Edited by* R.P Taylor and D.F. Strong. Canadian Institute of Mining and Metallurgy, extended abstracts, Halifax, 1985, pages 285-289.

Tuach, J., Kerrich, R., Willmore, L.M. and Strong, D.F.
1988: Source terranes, magmatic evolution, and hydrothermal regimes in the Mo-, Sn- mineralized Ackley Granite, Newfoundland: evidence from combined geochemical and oxygen isotope data. *In* Recent Advances in the Geology of Granite-Relatead Mineral Deposits. *Edited by* R.P. Taylor and D.F. Strong. Canadian Institute of Mining and Metallurgy, Special Volume 39, pages 342-350.

Watson, E.B.
1979: Zircon saturation in felsic liquids: experimental results and applications to trace element geochemistry. Contribution to Mineralogy and Petrology, Volume 70, pages 407-419.

Whalen, J.B.
1976: Geology and geochemistry of molybdenite showings of the Ackley Granite, Fortune Bay, Newfoundland. Unpublished M.Sc. thesis, Memorial University of Newfoundland, St. John's, 267 pages.

Whalen, J.B., Currie, K.L. and Chappell, B.W.
1987: A-type granites: geochemical characteristics, discrimination and petrogenesis. Contributions to Mineralogy and Petrology, Volume 95, pages 407-419.

White, A.J.R. and Chappell, B.W.
1983: Granitoid types and their distribution in the Lachlan fold Belt, southeastern Australia. Geological Society of America, Memoir 159, pages 21-34.

Williams, H.
1971: Geology of Belleoram map area (1M/11), Newfoundland. Geological Survey of Canada, Paper 70-65, 39 pages.

Williams, H. and Hatcher, R.D. Jr.
1983: Appalachian suspect terranes. Geological Society of America, Memoir 158, pages 33-53.

Williams, H., Gillespie, R.T. and Van Breeman, O.
1985: A Late Precambrian rift-related igneous suite in western Newfoundland. Canadian Journal of Earth Sciences, Volume 22, pages 1727-1735.

Williams, H., Dickson, W.L., Currie, K.L., Hayes, J.P. and Tuach, J.
1989: Preliminary report on a classification of Newfoundland granite rocks and their relationships to tectonostratigraphic zones and lower crustal blocks. *In* Current Research, Part B. Geological Survey of Canada, Paper 89-1B, pages 47-53.

Winchester, J.A., and Floyd, P.A.
1977: Geochemical discrimination of different magma series and their differentiation products using immobile elements. Chemical Geology, Volume 20, pages 325-343.

York, D.
1969: Least-squares, fitting of a straight line with correlated errors. Earth and Planetary Science Letters, Volume 39, pages 84-93.

Note: Geological Survey Branch file numbers are included in square brackets.

APPENDIX 1

SAMPLE PREPARATIONS AND ANALYTICAL TECHNIQUES

1A. Sample Collection and Preparation

Approximately 2 kg of sample were collected as fresh chips from outcrop using a sledgehammer, and a fresh, fist-sized sample was collected from each sample site. The chips were reduced in size to less than 5 mm in a jaw crusher, and approximately 100 g were powdered to -300 mesh using a ceramic disk pulverizer in preparation for analysis. Each hand sample was slabbed, a thin section was prepared, and half was assigned to a reference collection maintained by the Department of Mines and Energy in St. John's.

1B. Microprobe Techniques

Quantitative electron microprobe analyses of minerals in polished thin sections were performed at the Department of Earth Sciences, Memorial University of Newfoundland. A three-spectrometer JEOL JXA-50A automated electron microprobe microanalyzer with Krisel control through a PDP-11 mini-computer was used for the analyses. Operating conditions were an accelerating voltage of 15 Kv, a beam current around 0.022 microamps, a beam diameter of 1 to 2 micrometers, and a counting rate of up to 60,000 with a default time of 30 seconds. The alpha correction program was used for the analyses.

Acceptable analyses totalled between 98 and 102 percent for non-hydrous silicate phases, although three feldspar analyses having low totals are included as they give an approximate idea of the An contents. The analyses of the hydrous silicates were monitored by frequent re-analyses of the standards, and were used if the values for the standard were acceptable. Precision is estimated to be within 5 percent and accuracy to be within 10 percent. The similarity of values obtained from biotite from repeat analyses within grains, and between grains in the same sample (Appendix 2), testify to the validity of the data presented. In addition, there is good agreement between microprobe analyses and AA-whole-rock analyses of biotite separates (see Table 6 of Tuach, 1987).

A Hitachi S-570 scanning electron microscope with a solid-state backscatter detector, and a Trachor Northern 5500 energy-dispersive X-ray analyzer were used to assist in mineral identification. Accelerating voltage was 15 kv or 20 kv.

1C. Major- and Trace-Element Analyses

1C1. Analytical Techniques

Most major elements, Li, Be, Ni, Cu, Zn, Ag, Pb, total Fe as Fe_2O_3, and Sn were determined by atomic absorption spectrometry; FeO was analyzed by titration; P_2O_5 was analyzed colourimetrically; S, CO_2, and H_2O+ were analyzed using infrared detection apparatus; F was determined by the ion-selective electrode technique; U by neutron-activation analyses, and other trace elements by X-ray fluorescence. Loss on ignition was determined by heating samples in a muffle furnace to 1100°C for 2 hours and measuring weight loss.

The X-ray fluorescence analyses were performed on pressed pellets at the Department of Earth Sciences, Memorial University of Newfoundland, using a Phillips 1450 X-ray fluorescence spectrometer with a rhodium tube. Uranium concentration was determined by Atomic Energy of Canada Limited and all other analyses were performed at the Department of Mines and Energy laboratory in St. John's. The atomic-absorption analyses were performed on a Varian Model 875 atomic-absorption spectrometer with digital readout.

1C2. *Detection Limits, Accuracy and Precision*

Estimates of analytical detection limits, accuracy and precision with reference to international standards were presented by Dickson (1983). The accuracy and precision of the major elements is estimated to be within 2 percent. Only those trace elements having an estimated accuracy and precision of $\pm$ 5 percent were used in this study.

1D. Rare-Earth-Element Analytical Techniques

Rare-earth-element analyses were carried out by ICP-MS at the Department of Earth Sciences, Memorial University of Newfoundland. This was achieved by sodium peroxide sintering of a 0.1 g sample aliquot, followed by dissolution of the sinter cake, and separation and dissolution of the resulting REE hydroxide-bearing precipitate. The sample was then analyzed

by inductively coupled plasma-mass spectrometry using the method of internal standardization to correct for matrix and drift effects. The sodium peroxide sintering technique ensures complete digestion of accessory phases such as zircon or fluorite, which may be resistant to acid digestion.

Detection limits (3 standard deviations of the background) are generally about 10 percent of chondrite values.

1E. Rb–Sr Analyses

Rb–Sr analyses were carried out on 12 samples at the Department of Earth Sciences, Memorial University of Newfoundland. Replicate Rb–Sr analyses, sufficient to provide a precision of approximately 0.3 percent on the Rb/Sr ratio, were obtained using a standard whole-rock pressed pellet and X-ray fluorescence techniques (computer controlled Phillips PW1450). The estimated 2 standard deviation error for Rb and Sr concentration is $\pm$ 1 percent.

Aliquots of each sample were dissolved in HF-$HClO_4$ mixtures in teflon beakers, and Sr was separated by standard ion-exchange methods. The separated Sr was loaded as the phosphate on single Ta filaments, and analyzed for its isotopic composition on a Micromass 30B thermal ionization mass spectrometer. Data acquisition and filament current was computer controlled. The intensity of the ^{88}Sr beam was maintained between 1 and 2 volts (Gain 1), and collected in a Faraday 'cup' detector.

Data were fitted to isochrons using the regression method of York (1969), with modifications from Brooks *et al.* (1972). The decay constant recommended by Steiger and Jager (1977), $^{87}Rb = 1.42 * 10^{-11}$ yr^{-1}, was used for computation.

1F. Oxygen Isotope Analyses

The preparation, and oxygen isotope analysis, of samples from the study area were performed at the University of Western Ontario by Dr. R. Kerrich. Oxygen was extracted from minerals with bromine pentafluoride and quantitatively converted to CO_2 prior to mass spectrometric analysis (Clayton and Mayeda, 1963). Isotope data are reported as $\delta\ ^{18}O$ in per mil relative to SMOW (Standard Mean Ocean Water). The overall reproducibility of $\delta\ ^{18}O$ whole-rock values has averaged -0.16 per mil (1 standard deviation). Analysis of NBS-28 gives 9.8 per mil.

APPENDIX 2 – ELECTRON MICROPROBE ANALYSES

2A. Representative electron microprobe analyses and structural formulae of plagioclase from the Cross Hills Plutonic Suite.

Sample No.	JT-124	JT-262	JT-262	JT-311	JT-311	JT-338	JT-410	JT-433
An.	1	1-Core	1-Rim	1-Core	1-Rim	1	1	1
Major oxides (weight percent).								
SiO_2	69.83	64.45	64.51	52.09	57.16	54.52	71.36	72.39
TiO_2	0.02	0.00	0.01	0.05	0.07	0.05	0.03	0.05
Al_2O_3	18.89	22.86	22.22	28.84	24.94	28.82	13.77	19.02
FeO	0.74	0.18	0.26	0.00	0.28	0.65	1.00	0.21
CaO	0.02	4.56	4.89	13.33	8.53	12.90	1.88	0.03
Na_2O	11.95	6.12	7.92	3.56	6.06	4.21	2.68	9.71
K_2O	0.02	2.79	0.45	0.09	0.10	0.07	5.29	0.12
TOTAL	101.65	100.95	100.27	97.90	97.15	101.25	96.02	101.54
No. of cations on the basis of 32 oxygens.								
Si	12.057	11.327	11.358	9.631	10.521	9.765	12.978	12.309
Ti	0.003	0.000	0.001	0.007	0.10	0.007	0.004	0.006
Al	3.846	4.737	4.613	6.287	5.413	6.087	2.953	3.813
Fe	0.107	0.026	0.038	0.000	0.043	0.097	0.152	0.030
Ca	0.004	0.859	0.923	2.641	1.683	2.476	0.366	0.005
Na	4.001	2.086	2.704	1.276	2.163	1.462	0.945	3.202
K	0.004	0.626	0.101	0.021	0.023	0.016	1.228	0.026
Mole proportions								
Ab	99.80	58.42	72.54	32.41	55.91	36.98	37.22	99.03
Or	0.11	17.52	2.71	0.54	0.61	0.40	48.35	0.81
An	0.09	24.06	24.75	67.06	43.49	62.62	14.43	0.17
Rock type*	PGRM	GBBR	GBBR	GBBR	GBBR	GBBR	GRDR	PGRT

* See Appendix 4A for rock-type abbreviations

2B. Electron microprobe analyses and structural formulae of pyroxene from the Cross Hills Plutonic Suite.

Sample No.	JT-073		JT-137	JT-262	JT-264A	JT-311		JT-343
An.	3		1	1	1	3		3
Major oxides (weight percent).								
	$\bar{x}$	$\bar{s}$				$\bar{x}$	$\bar{s}$	
SiO_2	51.08	0.12	52.00	53.08	49.12	52.30	0.90	52.21
TiO_2	1.21	0.06	1.27	1.19	0.02	1.80	0.81	1.01
Al_2O_3	3.23	0.31	1.93	3.36	0.04	0.59	0.40	2.25
FeO	8.69	0.65	8.92	10.05	25.54	7.45	0.53	9.00
MnO	0.23	0.06	0.19	0.29	2.05	0.27	0.11	0.29
MgO	15.63	0.29	14.75	13.69	1.46	15.18	0.31	15.00
CaO	20.32	1.03	21.04	19.24	21.64	22.65	0.42	20.66
Na_2O	0.32	0.03	0.25	0.54	0.30	0.31	0.18	0.34
K_2O	0.00	0.01	0.00	0.04	0.02	0.01	0.02	0.00
TOTAL	100.71	0.44	100.35	101.47	100.19	100.58	0.69	100.27
No. of cations on the basis of 6 oxygens[1].								
Si	1.875		1.928	1.913	2.003	1.931		1.924
Al^{iv}	0.125		0.072	0.087	0.003	0.026		0.076
Al^{vi}	0.015		0.013	0.056	0.005	-		0.022
Ti	0.033		0.035	0.027	0.001	0.050		0.028
Fe (3)	0.065		0.006	-	-	0.034		0.023
Fe (2)	0.201		0.270	0.281	0.871	0.196		0.254
Mn	0.007		0.006	0.005	0.071	0.008		0.009
Mg	0.855		0.815	0.781	0.089	0.836		0.824
Ca	0.799		0.836	0.823	0.946	0.896		0.816
Na	0.023		0.018	0.031	0.024	0.022		0.024
K	-		-	-	0.001	-		-
X_{Fe}[2]	0.24		0.25	0.27	0.91	0.22		0.26
Rock type*	GBBR		GBBR	GBBR	SENT	GBBR		GBBR

[1] Recalculated to give 4 cations per unit formula (Cawthorn & Collerson, 1974)

[2] $X_{Fe} = Fe(t)/Fe(t) + Mg$

x – mean; s – standard deviation

* See Appendix 4A for rock-type abbreviations

2C. Election microprobe analyses and structural formulae of amphibole from the Cross Hills Plutonic Suite.

Sample No.	JT-073-1	JT-073-2	JT-137	JT-151		JT-259		JT-262	JT-264A	JT-311	JT-404	
An.	1	1	1	3		3		1	2	1	3	
Major oxides (weight percent)				$\bar{x}$	$\bar{s}$	$\bar{x}$	$\bar{s}$				$\bar{x}$	$\bar{s}$
SiO_2	55.27	53.92	47.91	50.31	0.47	51.56	0.22	49.56	48.13	51.17	47.73	0.58
TiO_2	0.02	0.12	0.28	0.27	0.08	1.56	0.19	1.91	0.20	1.53	1.30	0.05
Al_2O_3	1.16	2.08	6.44	3.19	0.29	0.92	0.12	6.52	1.73	5.34	6.49	0.19
FeO	12.79	15.43	14.29	20.29	1.31	32.39	1.01	11.75	34.13	12.64	16.55	0.41
MnO	0.15	0.39	0.34	0.94	0.19	1.02	0.13	0.16	2.12	0.30	0.50	0.02
MgO	16.16	15.59	13.42	10.85	0.79	0.01	0.01	15.04	0.89	14.91	13.01	0.50
CaO	12.09	9.68	11.48	10.97	0.05	0.33	0.25	11.93	9.51	11.70	10.62	0.56
Na_2O	0.15	0.57	0.99	1.36	0.02	7.04	0.27	1.80	0.27	1.18	1.34	0.16
K_2O	0.04	0.05	0.37	0.53	0.06	1.02	0.06	0.27	0.67	0.35	0.35	0.05
TOTAL	97.82	97.82	95.91	98.73	0.82	95.85	0.47	98.95	96.97	99.13	97.90	0.95
No. of cations on the basis of 23 oxygens												
Si	7.912	7.908	7.185	7.513		8.299		7.097	7.786	7.308	7.062	
Al^{iv}	0.088	0.092	0.815	0.487		0.299		0.903	0.214	0.692	0.938	
Al^{vi}	0.108	0.267	0.323	0.074		0.474		0.198	0.116	0.207	0.194	
Ti	0.002	0.013	0.032	0.030		0.189		0.206	0.024	0.164	0.145	
Fe	1.532	1.703	1.792	2.534		4.361		1.407	4.618	1.510	2.048	
Mn	0.018	0.048	0.043	0.119		0.139		0.019	0.291	0.036	0.063	
Mg	3.448	3.408	3.000	2.415		0.002		3.210	0.215	3.174	2.869	
Ca	1.855	1.521	1.845	1.756		0.057		1.831	1.649	1.791	1.684	
Na	0.042	0.162	0.288	0.394		2.197		0.500	0.085	0.327	0.384	
K	0.007	0.009	0.071	0.101		0.209		0.049	0.138	0.064	0.066	
X_{Fe}	0.31	0.33	0.37	0.51		0.99		0.30	0.96	0.32	0.42	
Rock type*	GBBR	GBBR	GBBR	APLT		PGRT		GBBR	SENT	GBBR	GRDR	

Sample No.	JT-407	JT-427	JT-428	JT-429		JT-431	JT-432-1	JT-432-2	JT-437	JT-441	JT-477	
An.	1	1	2	3		2	2	2	2	2	3	
Major oxides (weight percent)				$\bar{x}$	$\bar{s}$						$\bar{x}$	$\bar{s}$
SiO_2	47.49	45.60	47.70	46.78	1.46	50.86	51.99	51.40	52.01	48.43	45.55	1.12
TiO_2	0.73	0.44	0.35	0.34	0.06	0.78	0.72	0.70	0.68	1.39	0.91	0.05
Al_2O_3	5.63	5.95	4.27	3.86	0.52	1.24	1.21	1.37	1.21	0.77	4.61	0.81
FeO	19.33	17.79	18.64	17.74	0.66	30.16	24.01	24.26	23.99	31.94	26.64	1.15
MnO	0.85	1.03	1.20	1.01	0.14	3.18	4.98	5.17	4.77	2.47	1.74	0.10
MgO	11.27	11.05	11.05	10.83	0.38	0.98	2.28	1.83	2.24	0.44	5.16	0.72
CaO	10.50	10.30	10.83	10.61	0.09	1.74	1.06	1.06	0.90	0.60	9.87	0.59
Na_2O	1.48	2.27	1.84	1.66	0.59	5.64	7.52	7.91	6.70	5.98	2.22	0.38
K_2O	0.48	0.83	0.76	0.64	0.13	0.83	1.02	1.00	1.01	0.88	0.88	0.08
TOTAL	97.76	95.26	96.64	93.47	1.33	95.41	94.77	94.70	93.50	92.90	97.52	0.78
No. of cations on the basis of 23 oxygens												
Si	7.152	7.067	7.290	7.360		8.214	8.305	8.259	8.381	8.143	7.207	
Al^{iv}	0.848	0.933	0.710	0.640		-0.214	-0.305	-0.259	-0.381	-0.143	0.793	
Al^{vi}	0.152	0.154	0.060	0.077		0.458	0.533	0.518	0.611	0.296	0.067	
Ti	0.083	0.051	0.040	0.040		0.095	0.087	0.085	0.082	0.176	0.108	
Fe	2.435	2.306	2.383	2.335		4.075	3.208	3.260	3.233	4.492	3.526	
Mn	0.108	0.135	0.155	0.135		0.435	0.674	0.704	0.651	0.352	0.233	
Mg	2.530	2.552	2.517	2.540		0.236	0.543	0.438	0.538	0.110	1.217	
Ca	1.695	1.711	1.774	1.789		0.301	0.181	0.183	0.155	0.108	1.674	
Na	0.432	0.682	0.545	0.506		1.767	2.330	2.465	2.094	1.950	0.681	
K	0.092	0.164	0.148	0.128		0.170	0.208	0.205	0.208	0.189	0.178	
X_{Fe}	0.49	0.47	0.49	0.48		0.95	0.85	0.88	0.86	0.98	0.74	
Rock type*	GRDR	APLT	APLT	APLT		PGRT	PGRT	PGRT	PGRT	PGRT	AGRN	

* See Appendix 4A for rock-type abbreviations

2D. Electron microprobe analyses and structural formulae of biotite from the Cross Hills Plutonic Suite.

Sample No.	JT-073	JT-264A	JT-343[1]	JT-491-1	JT-491-2
An.	1	1	1	1	1
Major oxides (weight percent)					
SiO_2	37.45	35.75	35.86	38.00	38.26
TiO_2	3.46	0.94	3.16	4.45	4.79
Al_2O_3	15.54	10.89	15.20	12.99	13.03
FeO	13.66	37.04	13.01	21.00	20.46
MnO	0.09	0.95	0.07	0.40	0.43
MgO	20.15	0.60	19.58	10.44	10.94
CaO	0.00	0.02	0.25	0.02	0.09
Na_2O	0.21	0.02	0.50	0.12	0.08
K_2O	9.77	7.24	4.23	8.83	8.49
TOTAL	93.46	93.44	91.81	96.25	96.55
No. of cations on the basis of 22 oxygens					
Si	5.696	6.073	5.369	5.769	5.759
Al^{iv}	2.304	1.927	2.631	2.231	2.241
Al^{vi}	0.081	0.254	0.053	0.095	0.072
Ti	0.531	0.120	0.356	0.508	0.542
Fe	2.097	5.263	1.629	2.667	2.576
Mn	0.014	0.137	0.009	0.051	0.055
Mg	3.092	0.152	4.370	2.363	2.455
Ca	0.000	0.004	0.040	0.003	0.015
Na	0.032	0.007	0.145	0.035	0.023
K	1.500	1.569	0.808	1.711	1.631
X_{Fe}	0.40	0.97	0.27	0.53	0.51
Rock type*	GBBR	SENT	GBBR	GBBH	GBBH

[1] Partly chloritized

* See Appendix 4A for rock-type abbreviations

2E. Election microprobe analyses and structural formulae of chlorite from the Cross Hills Plutonic Suite.

Sample No.	JT-066	JT-085		JT-141	JT-151-1	JT-151-2	JT-200
An.	1	3		1	1	1	1
Major oxides (weight percent)							
		$\bar{x}$	$\bar{s}$				
SiO_2	29.14	29.58	1.18	24.68	31.38	33.40	28.35
TiO_2	0.03	0.03	0.02	0.03	0.16	0.20	0.00
Al_2O_3	17.64	16.60	0.62	18.74	16.85	18.30	18.72
FeO	24.57	17.85	0.14	40.73	25.03	24.84	28.84
MnO	5.59	0.42	0.02	1.32	0.62	0.67	1.18
MgO	12.53	20.55	0.96	2.61	11.48	10.54	12.63
CaO	0.12	0.09	0.01	0.05	0.18	0.16	0.05
Na_2O	0.04	0.02	0.02	0.07	0.05	0.05	0.06
K_2O	0.11	0.01	0.01	0.07	0.72	0.99	0.14
TOTAL	89.77	85.15	2.58	88.30	86.47	89.15	89.97
No. of cations on the basis of 28 oxygens							
Si	6.101	6.151		5.673	6.652	6.808	5.925
Al^{iv}	4.080	4.033		4.507	3.529	3.372	4.255
Al^{vi}	0.274	0.037		0.571	0.682	1.024	0.357
Ti	0.005	0.005		0.005	0.025	0.030	-
Fe	4.302	3.105		7.832	4.437	4.234	5.042
Mn	0.991	0.074		0.257	0.110	0.115	0.208
Mg	3.911	6.370		0.894	3.627	3.202	3.935
Ca	0.026	0.020		0.012	0.040	0.036	0.011
Na	0.016	0.008		0.031	0.020	0.020	0.024
K	0.029	0.002		0.020	0.194	0.257	0.036
X_{Fe} [1]	0.52	0.33		0.90	0.55	0.57	0.56
Rock type*	PGRT	GBBR		SENT	APLT	APLT	BGRT

Sample No.	JT-410-1	JT-410-2	JT-427	JT-429	JT-435	JT-436	JT-491
An.	1	1	1	2	1	1	1
Major oxides (weight percent)							
SiO_2	28.13	27.65	27.79	26.22	29.33	26.25	31.97
TiO_2	0.10	0.02	0.10	0.05	0.38	0.13	1.51
Al_2O_3	14.67	15.30	19.52	18.00	15.67	17.52	16.10
FeO	29.21	30.48	26.04	26.21	24.43	28.12	24.39
MnO	0.84	0.85	0.66	1.11	0.59	0.90	0.58
MgO	13.17	13.25	11.29	13.81	17.13	12.37	13.86
CaO	0.04	0.02	0.29	0.07	0.09	0.08	0.15
Na_2O	0.00	0.00	0.04	0.14	0.01	0.01	0.00
K_2O	0.02	0.01	0.33	0.05	0.07	0.03	1.38
TOTAL	86.18	87.58	86.06	85.66	87.70	85.41	89.94
No. of cations on the basis of 28 oxygens							
Si	6.192	6.030	5.986	5.733	6.148	5.809	6.520
Al^{iv}	3.807	3.933	4.194	4.450	3.872	4.371	3.661
Al^{vi}	-	-	0.762	0.190	-	-	0.211
Ti	0.039	0.004	0.016	0.008	0.059	0.021	0.231
Fe	5.378	5.560	4.691	4.794	4.283	6.624	4.160
Mn	0.156	0.156	0.120	0.206	0.104	0.169	0.100
Mg	4.322	4.306	3.624	4.501	5.352	4.080	4.213
Ca	0.008	0.005	0.067	0.016	0.020	0.019	0.033
Na	-	-	0.016	0.060	0.004	0.004	-
K	0.005	0.002	0.090	0.014	0.019	0.008	0.358
X_{Fe} [1]	0.55	0.56	0.56	0.52	0.44	0.56	0.50
Rock type*	GRDR	GRDR	APLT	APLT	BGRT	APLT	GBBH

[1] $X_{Fe} = Fe(t)/Fe(t) + Mg$

* See Appendix 4A for rock-type abbreviations

APPENDIX 3

ASSAYS OF SAMPLES FROM THE GRAND LE PIERRE AREA

3A. Semiquantitative XRF analyses of rock samples (see Map 91-15). Analyses by Metric Lab Ltée., Quebec. Only values considered to be anomalous are listed.

Sample	Ce (g/t)	Te (g/t)	Ag (g/t)	Sn (g/t)	Nb_2O_5 (g/t)	Zr (%)	Pb (g/t)	Y (g/t)	Zn (g/t)	Mn (g/t)	Showing Number
JT-067	200	-	-	244	375	1.23	-	1100	30	250	11
JT-124	1000	-	-	511	1500	2.7	-	1600	40	800	12
JT-129	-	-	15	-	-	0.07	100	150	200	100	4
JT-131	-	-	-	-	-	0.06	-	-	-	-	2

3B. Gold assays of rock-chip samples. Fire assays by Atlantic Analytical Services Limited, Springdale, Newfoundland (February, 1984).

Sample	Au (g/t)	Comments
JT-050	<0.34	* Rhy. tuff with chalcocite-bearing quartz veins (also FRX-37)
JT-052	<0.34	* Silicified tuff/chert with 5% pyrite
JT-053	0.34	* As above
JT-111	<0.34	* Sericite schist with 1 to 2% pyrite
JT-124	0.68	* Aplite vein in peralkaline granite–radioactive
JT-161	<0.34	* Flow-banded rhyolite with pyritic fractures
JT-170	<0.34	* Tin-bearing quartz topaz greisen (Ackley Granite)
JT-203	<0.34	* Biotite granite with 5 to 10% pyrite (Float.)
JT-240	0.34	* Sericitized volcanic rocks
JT-281	<0.34	* Ackley Granite with 2 to 5% pyrite
JT-468	<0.34	* Pyrite rich zones in tuff
JT-469	<0.34	* Pyrite rich zones in tuff
JT-472	<0.34	* Pyrite rich zones in tuff
JT-473	<0.34	* Pyrite rich zones in tuff–heavy sericitization
JT-480	<0.34	* Pyrite rich zones in altered tuff
JT-490	<0.34	* Pyrite rich zones in tuff and ash flow
JT-497A	<0.34	* Greisen? on margin of Cross Hills biotite granite
JT-502	<0.34	* Pyrite rich zones in tuff

APPENDIX 4

FIELD DATA, MAJOR- AND TRACE-ELEMENT ANALYSIS

4A. Codes for Granite Field Data

ROCK TYPE
APLT–aplite
BGRT–biotite granite
DORT–diorite
GBBH–gabbro-granite hybrid
GBBR–gabbro
GRDR–granodiorite
PGRA–altered peralkaline granite
PGRM–mineralized peralkaline granite
PGRT–peralkaline granite
SENT–syenite

SAMPLE TYPE
1 –single grab sample
3 –composite sample

COLOUR (% refers to amount of mafics)
0 –white <20%
1 –white & black 20-50%
2 –black & white 50-80%
3 –black >80%
4 –grey
5 –green
6 –buff
7 –orange or yellow
8 –red or purple
9 –pink

GRAIN SIZE (mm)
0 < 0.004, glassy
1 0.004–0.025, aphanitic
2 0.025–0.062, aphanitic
3 0.062–0.250, v.f. grained
4 0.25–0.50, v.f. grained
5 0.50–1.00, fine grained
6 1.00–2.00, med. grained
7 2.00–5.00, med.-coarse grained
8 5.00–10.0, coarse grained
9 >10.0, very coarse grained

TEXTURE
0 uniform
1 porphyritic
2 miarolitic
5 tuffisitic
6 granophyric
8 veined

MAFIC MINERALS (%)
0 absent
1 10
2 20

METALLIC MINERALS (%)
01 to 15 % (two columns)

FELDSPAR ALTERATION
0 unaltered
1 cloudy
3 epidote
5 hematite

FABRIC
0 no fabric
1 cataclastic
3 igneous flow

FLUORITE
0 absent
1 present

MUSCOVITE (PRIMARY)
0 absent
1 present

ALTERATION
0 fresh
2 gossanous
3 hydrothermal, white
4 hydrothermal, rusty
5 chloritized mafics
6 pyritic
8 epidotized

PHENOCRYSTS (%)
0 absent
1 1
2 2-5
3 6-10
4 11-15
5 16-20
6 21-25
7 26-30
8 31-40
9 41-50

PHENOCRYSTS (type)
0 absent
1 feldspar megacrysts
8 quartz phenocrysts
9 feldspar phenocrysts

PRIMARY FEATURES
0 massive
7 mafic xenoliths

METALLIC MINERALS
0 absent
1 pyrite
4 galena
8 Fe oxides
(**MAINMETAL** = main phase
MINMETAL = subordinate phase)

4B. Field Data; see Appendix 4A for rock-type abbreviations and numerical codes.

ROCK TYPE	FIELD NUMBER	UTM EAST	UTM NORTH	SAMPTYPE	COLOUR	GRAINSIZE	TEXTURE	PRIMARY	ALTER	FELDALTER	FABRIC	FLUORITE	MUSCOVITE	PHENOCR%	PHENTYPE	MAFIC%	MAINMETAL	MINMETAL	METAL%	LAB NUMBER
APLT	JT83068	663100	5284260	1	9	0	1	0	0	0	0	1	0	1	9	2	8		5	7040013
	JT83093	662260	5284090	1	8	0	2	0	0	0	0	0	0	4	9	1	8		3	7040034
	JT83096	660900	5282920	1	8	1	1	0	0	0	0	0	0	2	9	0	8		5	7040037
	JT83151	661950	5283920	1	7	0	0	0	0	0	0	0	0	0	0	0	8	0	1	7040072
	JT83423	664300	5284850	1	7	6	2	0	0	0	0	0	0	0	0	1	8		4	7040134
	JT83427	661600	5283700	1	7	6	6	0	0	0	0	0	0	0	0	1	8		2	7040138
	JT83428	661600	5283680	1	7	5	6	0	0	0	0	0	0	0	0	1	8		5	7040139
	JT83429	661630	5283640	1	8	4	6	0	0	0	0	0	0	0	0	1	8		4	7040141
	JT83436	661750	5283799	1	7	2	0	0	0	0	0	0	0	0	0	1	8		2	7040147
BGRT	JT83069	663040	5284400	1	7	6	8	0	0	0	0	0	0	0	0	1	8		2	7040014
	JT83070	663120	5284580	1	7	6	2	0	0	0	0	0	0	2	9	1	8		3	7040015
	JT83072	663120	5284680	1	7	5	0	0	0	0	0	0	0	0	0	1	8		1	7040017
	JT83074	663070	5284940	1	7	5	8	0	8	0	1	0	0	0	0	1	8	0	2	7040021
	JT83079	663400	5284700	1	7	6	8	0	0	0	1	0	0	0	0	1	8		1	7040024
	JT83158	660750	5283060	1	7	6	0	0	0	0	0	0	0	0	0	1	8		2	7040066
	JT83159	661190	5283500	1	7	6	0	0	0	0	0	0	0	0	0	0	8		2	7040076
	JT83200	666320	5285145	1	7	6	0	0	0	0	0	0	0	0	0	1	8		2	7040086
	JT83305	664800	5284860	1	8	6	0	0	0	0	0	0	0	0	0	1	8		2	7040113
	JT83306	664970	5285040	1	7	5	0	0	0	0	0	0	0	0	0	0	8		2	7040114
	JT83310	665800	5284980	1	7	6	0	0	0	0	0	0	0	0	0	1	8		2	7040117
	JT83313	665100	5285030	1	7	6	2	0	0	0	0	0	0	0	0	1	8		2	7040121
	JT83314	665370	5284730	1	8	6	0	0	0	0	0	0	0	0	0	1	8		2	7040122
	JT83315	665320	5284850	1	7	6	2	0	0	0	0	0	0	0	0	1	8		2	7040123
	JT83424	663920	5284780	1	7	6	6	0	0	0	0	0	0	0	0	1	8		4	7040135
	JT83426	661600	5283900	1	7	6	6	0	0	0	0	0	0	0	0	1	8		3	7040137
	JT83435	661750	5283800	1	7	6	0	0	0	0	0	0	0	0	0	1	8		2	7040146
	JT83479	669300	5286900	1	7	5	0	7	0	0	0	0	0	0	0	1	8		2	7040155
	JT83484	652450	5283300	1	7	6	2	0	5	0	0	0	0	0	0	1	8		2	7040156
	JT83486	652500	5283600	1	7	6	2	0	5	0	0	0	0	0	0	1	8		2	7040157
DORT	JT83406	672500	5287600	1	4	5	1	0	0	0	0	0	0	1	9	5	8		2	7040128
GBBH	JT83071	663120	5284630	1	1	6	1	0	0	0	0	0	0	0	0	4	8		2	7040016
	JT83073B	663150	5284760	1	1	4	0	0	0	0	0	0	0	0	0	3	8		5	7040019
	JT83199	666320	5285150	1	2	6	0	0	0	0	0	0	0	0	0	4	8		2	7040085
	JT83261	666220	5285150	1	2	7	0	0	0	0	0	0	0	0	0	5	8		5	7040101
	JT83262A	667600	5286500	1	2	7	0	0	0	0	0	0	0	0	0	4	8		5	7040103
	JT83312	664980	5285130	1	3	6	0	0	0	0	0	0	0	0	0	4	8		5	7040119
	JT83491	666200	5286900	1	1	6	0	0	0	0	0	0	0	0	0	3	8		3	7040159
GBBR	JT83059	661980	5284220	1	2	7	0	0	0	0	0	0	0	0	0	6	8		5	7040004
	JT83060	662010	5284200	1	1	7	0	0	0	0	0	0	0	0	0	4	8		5	7040005
	JT83060	662010	5284200	1	1	7	0	0	0	0	0	0	0	0	0	4	8		5	7040005
	JT83073	663150	5284760	1	2	5	0	0	0	0	0	0	0	0	0	5	8		2	7040018
	JT83085	664450	5283860	1	5	8	0	0	0	0	0	0	0	0	0	3	8		5	7040028
	JT83095	660930	5282940	1	5	8	1	0	0	0	0	0	0	8	1	4	8		5	7040036
	JT83137	659750	5285570	1	5	7	0	0	0	0	0	0	0	0	0	5	8		15	7040062

4B. Continued.

ROCK TYPE	FIELD NUMBER	UTM EAST	UTM NORTH	SAMPTYPE	COLOUR	GRAINSIZE	TEXTURE	PRIMARY	ALTER	FELDALTER	FABRIC	FLUORITE	MUSCOVITE	PHENOCR%	PHENTYPE	MAFIC%	MAINMETAL	MINMETAL	METAL%	LAB NUMBER
	JT83262	667600	5286500	1	2	6	0	0	0	0	0	0	0	0	0	5	8		5	7040102
	JT83311	665090	5285420	1	4	6	0	0	0	0	0	0	0	0	0	4	8		5	7040118
	JT83338	664400	5286250	1	3	4	0	0	0	0	0	0	0	0	0	5	8		5	7040124
	JT83343	664420	5285600	1	2	6	0	0	0	0	0	0	0	0	0	5	8		5	7040125
	JT83487	652000	5283600	1	5	4	0	0	0	0	0	0	0	0	0	4	8		10	7040158
	JT83492	666220	5286895	1	2	6	0	0	0	0	0	0	0	0	0	5	8		2	7040161
GRDR	JT83404	672000	5287600	1	1	7	2	7	0	0	0	0	0	0	0	2	8		2	7040127
	JT83407	673600	5287000	1	1	7	0	0	0	0	0	0	0	0	0	2	8		2	7040129
	JT83410	674500	5286100	1	1	7	0	7	0	0	0	0	0	0	0	2	8		2	7040131
PGRA	JT83056	661920	5284350	1	7	6	2	0	0	3	1	0	0	0	0	1	8	0	2	7040003
	JT83086	662300	5283700	1	8	6	0	0	0	0	0	0	0	0	0	1	1	8	6	7040029
	JT83087	662390	5283650	1	8	6	2	0	2	0	0	0	0	0	0	0	8		5	7040031
	JT83091	662190	5283430	1	6	7	2	0	4	1	0	0	0	0	0	0	8		5	7040032
	JT83126	661800	5283450	1	9	6	5	0	0	0	1	0	0	0	0	0	8	1	10	7040055
	JT83127	661800	5283450	1	8	6	8	0	6	5	1	0	0	0	0	0	1	8	3	7040056
	JT83129	661800	5283450	1	0	6	0	0	3	1	0	0	2	0	0	0	1	4	5	7040057
	JT83134	661815	5283435	1	8	6	2	0	5	0	1	0	0	0	0	0	1	8	15	7040061
PGRM	JT83067	663130	5284000	1	8	5	2	0	2	0	1	0	0	0	0	2	8		10	7040012
	JT83081	663570	5284570	1	8	6	0	0	0	0	0	0	0	0	0	1	8		5	7040025
	JT83100	661700	5283360	1	8	6	5	0	6	0	1	0	0	0	0	0	1		5	7040042
	JT83124	663400	5284100	1	8	3	0	0	0	0	0	0	0	0	0	0	8		15	7040052
	JT83124B	663400	5284100	1	8	6	0	0	0	0	0	1	0	0	0	0	8		2	7040053
	JT83131	661810	5283440	3	7	4	2	0	0	0	0	0	0	2	8	0	1	8	3	7040058
PGRT	JT83064	662940	5283750	1	8	6	2	0	0	0	0	0	0	0	0	2	8		5	7040008
	JT83065A	663100	5283850	1	8	4	2	0	0	0	0	0	0	2	9	2	8		10	7040009
	JT83066	663090	5284080	1	8	5	2	0	0	0	0	0	0	5	9	2	8		5	7040011
	JT83083	663650	5284320	1	8	6	0	0	0	0	0	0	0	0	0	1	8		4	7040026
	JT83091A	662190	5283440	1	8	6	2	0	0	0	0	0	0	2	9	0	8		8	7040033
	JT83099	661640	5283200	1	8	5	0	0	0	0	0	0	0	0	0	0	8		5	7040041
	JT83125	663390	5284110	1	8	6	2	0	0	0	0	0	0	0	0	0	8		10	7040054
	JT83152	662060	5283840	1	8	7	2	0	0	0	0	1	0	0	0	0	8	0	5	7040073
	JT83155	663420	5283780	1	8	7	2	0	0	0	0	0	0	0	0	0	8		5	7040075
	JT83259	665910	5285900	1	8	6	2	0	0	0	0	0	0	0	0	1	8		3	7040099
	JT83307	665020	5284600	1	8	6	2	0	0	0	0	0	0	0	0	0	8		5	7040115
	JT83308	664800	5284650	1	8	7	0	0	0	0	0	0	0	0	0	0	8		8	7040116
	JT83344	664600	5285150	1	8	6	1	0	0	0	0	0	0	1	9	0	8		5	7040126
	JT83421	664550	5284300	1	8	6	2	0	0	0	0	0	0	0	0	1	8		5	7040132
	JT83422	664200	5284600	1	8	6	2	0	0	0	0	0	0	0	0	1	8		5	7040133
	JT83425	663940	5284550	1	7	6	2	0	0	0	0	0	0	0	0	0	8		5	7040136
	JT83430	661635	5283638	1	8	6	6	0	0	0	0	0	0	0	0	1	8		6	7040142
	JT83431	661630	5283620	1	8	6	0	0	0	0	0	0	0	0	0	1	8		5	7040143
	JT83432	661700	5283620	1	8	7	0	0	0	0	0	0	0	0	0	1	8		5	7040144
	JT83433	661750	5283580	1	8	7	1	0	0	0	0	0	0	1	9	1	8		5	7040145
	JT83437	662650	5284100	1	7	6	1	0	0	0	0	0	0	1	9	1	8		5	7040148
	JT83441	663600	5285500	1	7	6	0	0	0	0	0	0	0	0	0	1	8		5	7040149

4B. Concluded.

ROCK TYPE	FIELD NUMBER	UTM EAST	UTM NORTH	SAMPTYPE	COLOUR	GRAINSIZE	TEXTURE	PRIMARY	ALTER	FELDALTER	FABRIC	FLUORITE	MUSCOVITE	PHENOCR%	PHENTYPE	MAFIC%	MAINMETAL	MINMETAL	METAL%	LAB NUMBER
SENT	JT83140A	660490	5284820	1	8	3	0	0	0	0	3	0	0	0	0	0	1	8	5	7040063
	JT83140	660540	5284820	1	8	4	0	0	0	0	3	0	0	0	0	1	1	8	5	7040064
	JT83141	660790	5284450	1	8	6	0	0	0	0	0	0	0	2	9	2	8	1	5	7040065
	JT83264	668700	5287750	1	7	7	0	0	0	0	0	0	0	0	0	2	8		2	7040104
	JT83470	660400	5284100	1	8	2	0	0	0	0	0	0	0	0	0	1	8		5	7040152
	JT83471	660010	5284500	1	8	2	0	0	0	0	0	0	0	0	0	1	8		5	7040153
MISC	JT83264A	668700	5287750	1	5	7	0	0	0	0	0	0	0	0	0	5	8		2	7040105
	JT83477	668500	5286200	1	8	7	0	0	0	0	0	0	0	0	0	1	8		2	7040154

4C. Major-Element Data; see Appendix 4A for rock-type abbreviations.

ROCK TYPE	FIELD NUMBER	SiO_2	TiO_2	Al_2O_3	FeO	Fe_2O_3	MnO	MgO	CaO	Na_2O	K_2O	P_2O_5	LOI	TOTAL	H_2O	S	CO_2
APLT	JT83068	74.6	.27	12.6	.80	.55	.02	.17	.51	4.10	5.22	.02	.60	99.41	.39	0.00	.03
	JT83093	75.4	.27	12.6	.98	.48	.05	.17	.53	3.67	5.22	.02	.67	100.01	.47	.01	.11
	JT83096	75.7	.16	12.0	.60	.90	.02	.06	.38	4.27	4.49	.03	.27	98.88	.28	.03	.07
	JT83151	75.7	.27	12.6	.60	.68	.03	.14	.46	3.77	5.22	.01	.54	100.02	.38	.02	.03
	JT83423	74.9	.25	12.3	.38	.90	.02	.12	.33	3.84	5.19	.02	.61	98.81	.40	.02	.04
	JT83427	74.8	.25	12.4	.65	.66	.02	.16	.47	3.83	5.20	.02	.57	99.03	.47	0.00	.04
	JT83428	75.6	.26	12.5	.71	.72	.03	.17	.44	3.79	5.34	.01	.50	100.02	.47	.02	.03
	JT83429	74.1	.28	12.3	.68	.68	.04	.16	.45	3.87	5.24	.02	.59	98.41	.38	.02	.03
	JT83436	74.9	.26	12.4	.89	.52	.04	.19	.45	3.86	5.33	.02	.55	99.36	.51	0.00	.04
MAX		75.7	.28	12.6	.98	.90	.05	.19	.53	4.27	5.34	.03	.67		.51	.03	.11
MIN		74.1	.16	12.0	.38	.48	.02	.06	.33	3.67	4.49	.01	.27		.28	0.00	.03
MEAN		75.1	.252	12.4	.699	.677	.030	.149	.4467	3.89	5.16	.019	.544		.417	.013	.047
STDEV		.556	.036	.187	.177	.150	.011	.039	.0610	.183	.257	.006	.114		.070	.011	.027
BGRT	JT83069	74.5	.28	12.3	.60	.73	.03	.23	1.59	3.13	4.80	.03	.65	98.87	.48	0.00	.03
	JT83070	73.6	.27	13.0	.80	.68	.02	.27	.47	3.90	5.29	.03	.65	98.98	.45	0.00	.12
	JT83072	70.3	.44	13.3	1.66	1.08	.03	.79	1.01	3.98	4.56	.07	1.05	98.27	.84	0.00	.07
	JT83074	75.0	.21	12.1	.40	.72	.03	.07	1.95	3.34	4.02	.02	.70	98.56	.36	0.00	.12
	JT83079	76.1	.28	12.2	.67	.67	.02	.24	1.05	3.55	4.59	.04	.62	99.98	.45	0.00	.16
	JT83158	73.8	.30	13.1	1.03	.43	.07	.40	.75	3.58	5.10	.04	.83	99.38	.60	.02	.08
	JT83159	73.8	.33	12.9	.88	.66	.05	.43	.69	3.58	5.08	.03	1.01	99.44	1.05	.01	.09
	JT83200	75.2	.26	12.6	.71	.53	.03	.19	.42	3.72	5.34	.03	.68	99.71	.60	.01	.07
	JT83305	74.7	.25	12.3	.70	.65	.03	.16	.13	3.77	5.33	.04	.67	98.73	.54	0.00	.09
	JT83306	75.4	.27	12.2	.55	.82	.04	.22	.20	3.52	5.38	.03	.69	99.27	0.00	0.00	.06
	JT83310	74.1	.27	12.6	.60	.79	.02	.20	.43	3.88	5.18	.02	.65	98.69	.52	0.00	.10
	JT83313	74.6	.26	12.6	.60	.73	.02	.21	.19	3.88	5.15	.02	.67	98.88	.58	0.00	.06
	JT83314	75.8	.25	12.2	.62	.81	.04	.15	.22	3.69	5.42	.01	.58	99.74	.52	0.00	.06
	JT83315	75.0	.27	12.7	.79	.67	.03	.20	.40	3.88	5.22	.02	.67	99.80	.60	0.00	.06
	JT83424	74.4	.33	12.8	.75	.87	.04	.25	.42	3.98	5.30	.03	.70	99.87	.52	.02	.06
	JT83426	73.3	.31	13.0	.85	.87	.04	.43	.76	3.77	5.09	.04	.92	99.33	.77	.01	.03
	JT83435	74.0	.30	13.0	.69	.78	.03	.31	.63	3.83	5.57	.03	.69	99.81			
	JT83479	74.6	.28	12.1	.89	.74	.03	.26	.38	3.57	5.51	.02	.63	98.96	.61	0.00	.03
	JT83484	75.6	.24	12.2	.61	.60	.02	.13	.30	3.60	5.50	.01	.65	99.41	.64	0.00	.05
	JT83486	74.6	.25	12.5	.70	.70	.02	.15	.37	3.77	5.71	.03	.58	99.33	.48	0.00	.05
MAX		76.1	.44	13.3	1.66	1.08	.07	.79	1.95	3.98	5.71	.07	1.05		1.05	.02	.16
MIN		70.3	.21	12.1	.40	.43	.02	.07	.13	3.13	4.02	.01	.58		0.00	0.00	.03
MEAN		74.4	.282	12.6	.755	.727	.032	.264	.6180	3.70	5.16	.030	.715		.558	.004	.073
STDEV		1.22	.047	.381	.255	.136	.012	.156	.4735	.217	.401	.013	.132		.207	.007	.034
DORT	JT83406	49.7	1.25	16.7	6.01	4.13	.18	5.92	8.83	2.36	1.64	.27	2.85	99.79	3.17	0.00	.10
GBBH	JT83071	57.5	1.82	15.2	4.91	3.49	.14	2.75	4.89	4.15	2.83	.34	1.66	99.68	1.61	0.00	.17
	JT83073B	60.9	1.01	14.2	3.48	2.31	.10	2.88	4.38	3.42	3.36	.21	1.90	98.15	1.60	0.00	.33
	JT83199	54.4	2.15	14.2	6.77	3.39	.19	3.93	6.32	3.52	2.21	.35	1.55	98.98	1.67	.06	.08
	JT83261	52.7	2.10	14.0	7.79	2.86	.22	4.63	6.65	3.40	2.07	.36	1.66	98.44	1.83	.10	.05
	JT83262A	58.6	1.30	13.5	5.00	2.85	.16	3.80	5.30	3.74	3.17	.20	1.10	98.67	1.28	0.00	.02
	JT83312	56.3	1.49	15.2	5.42	2.32	.19	4.05	5.05	3.83	2.96	.18	1.90	98.84	2.12	0.00	.10
	JT83491	62.5	.61	17.4	2.48	2.56	.09	1.05	3.48	4.97	2.95	.17	1.25	99.51	1.32	.01	.02
MAX		62.5	2.15	17.4	7.79	3.49	.22	4.63	6.65	4.97	3.36	.36	1.90		2.12	.10	.33
MIN		52.7	.61	13.5	2.48	2.31	.09	1.05	3.48	3.40	2.07	.17	1.10		1.28	0.00	.02
MEAN		57.6	1.50	14.8	5.12	2.83	.156	3.30	5.153	3.86	2.79	.259	1.57		1.63	.024	.110
STDEV		3.46	.571	1.31	1.81	.475	.049	1.19	1.088	.556	.480	.087	.305		.289	.040	.110
GBBR	JT83059	46.3	1.28	17.4	6.98	2.46	.16	8.65	10.43	2.40	.76	.14	2.76	99.72	2.74	.12	.05
	JT83060	53.4	.44	18.0	4.28	1.21	.11	7.56	7.57	2.87	1.88	.03	2.96	100.26	2.82	.01	.12
	JT83073	48.4	1.31	16.4	7.05	1.94	.16	8.45	9.20	2.25	.78	.19	2.67	98.75	2.67	.07	.06
	JT83085	51.1	1.02	17.6	4.28	4.80	.15	4.99	7.29	3.56	2.25	.27	2.51	99.82	2.29	0.00	.03
	JT83095	49.0	1.03	16.7	4.85	5.49	.17	5.76	8.86	2.65	2.03	.29	2.34	99.17	2.65	.03	.09

4C. Continued.

ROCK TYPE	FIELD NUMBER	SiO_2	TiO_2	Al_2O_3	FeO	Fe_2O_3	MnO	MgO	CaO	Na_2O	K_2O	P_2O_5	LOI	TOTAL	H_2O	S	CO_2
	JT83137	45.1	3.83	13.7	8.45	6.88	.34	6.21	9.00	3.40	.52	.56	.81	98.75	1.27	.06	.09
	JT83262	50.7	1.92	14.8	7.53	2.76	.17	5.84	8.45	3.32	1.26	.33	1.41	98.49	1.55	.30	.04
	JT83311	46.5	2.21	15.8	8.16	4.55	.21	7.29	9.22	2.88	.80	.38	1.81	99.81	2.44	.09	.06
	JT83338	47.5	1.23	16.8	7.01	2.19	.17	8.55	10.96	2.38	.34	.11	2.56	99.80	2.97	0.00	.06
	JT83343	47.0	1.35	17.2	7.16	2.51	.17	8.40	9.45	2.75	.68	.20	2.90	99.77	3.12	.07	.07
	JT83487	44.3	3.50	13.8	9.74	5.31	.27	7.03	8.10	3.05	1.15	.66	2.48	99.34	3.06	0.00	.02
	JT83492	44.9	1.84	17.2	8.00	3.58	.18	7.97	9.70	2.67	.40	.34	2.36	99.14	3.11	.05	.17
MAX		53.4	3.83	18.0	9.74	6.88	.34	8.65	10.96	3.56	2.25	.66	2.96		3.12	.30	.17
MIN		44.3	.44	13.7	4.28	1.21	.11	4.99	7.29	2.25	.34	.03	.81		1.27	0.00	.02
MEAN		47.9	1.75	16.3	6.96	3.64	.188	7.23	9.019	2.85	1.07	.292	2.30		2.56	.067	.072
STDEV		2.78	1.01	1.47	1.70	1.74	.061	1.26	1.077	.419	.654	.182	.643		.597	.083	.042
GRDR	JT83404	69.6	.37	14.3	1.95	.94	.09	.74	2.67	4.00	2.56	.06	1.09	98.32	1.08	.01	.06
	JT83407	68.4	.37	14.6	1.60	1.33	.09	.97	2.75	4.20	2.52	.06	1.30	98.14	1.22	0.00	.07
	JT83410	70.2	.35	14.1	1.47	.96	.08	.67	2.36	3.98	2.82	.05	1.44	98.48	1.21	.01	.25
MAX		70.2	.37	14.6	1.95	1.33	.09	.97	2.75	4.20	2.82	.06	1.44		1.22	.01	.25
MIN		68.4	.35	14.1	1.47	.94	.08	.67	2.36	3.98	2.52	.05	1.09		1.08	0.00	.06
MEAN		69.4	.363	14.3	1.67	1.08	.087	.793	2.593	4.06	2.63	.057	1.28		1.17	.007	.127
STDEV		.917	.012	.229	.248	.220	.006	.157	.2060	.122	.163	.006	.176		.078	.006	.107
PGRA	JT83056	76.4	.28	10.6	.74	.42	.08	.33	1.24	2.80	4.17	.04	.78	97.88	.70	.03	.23
	JT83086	75.3	.17	11.1	0.00	2.21	.03	.09	.09	3.46	4.86	.03	1.14	98.48	.40	.68	.03
	JT83087	76.7	.17	10.5	.28	1.83	.02	.01	.03	3.66	4.33	.01	.63	98.17	.25	0.00	.06
	JT83091	77.6	.17	9.9	.43	1.65	.01	.01	.02	3.34	4.27	.01	1.03	98.44	.43	.04	.11
	JT83126	77.4	.14	9.3	.31	2.32	.02	.07	.03	2.67	3.98	.01	.97	97.16	.63	.04	.03
	JT83127	77.5	.18	10.4	0.00	1.97	.03	.05	.01	3.11	4.43	.01	1.54	99.17	.71	1.19	.03
	JT83129	69.3	.21	15.1	0.00	2.75	.04	.06	.01	.12	8.66	.01	2.78	99.04			
	JT83134	77.0	.16	10.7	0.00	2.36	.04	.03	.04	3.53	4.41	.01	1.31	99.59	.45	1.23	.06
MAX		77.6	.28	15.1	.74	2.75	.08	.33	1.24	3.66	8.66	.04	2.78		.71	1.23	.23
MIN		69.3	.14	9.3	0.00	.42	.01	.01	.01	.12	3.98	.01	.63		.25	0.00	0.00
MEAN		75.9	.185	10.9	.220	1.94	.034	.081	.1838	2.84	4.89	.016	1.27		.510	.401	.069
STDEV		2.77	.043	1.77	.273	.703	.021	.104	.4275	1.15	1.54	.012	.673		.173	.549	.073
PGRM	JT83067	74.3	.36	8.8	.41	6.14	.06	.16	.06	1.65	5.15	.02	.93	97.99			
	JT83081	76.2	.12	10.5	.54	1.20	.04	.10	.22	3.52	4.06	.02	.50	96.97	.33	0.00	.13
	JT83100	76.3	.18	10.5	1.51	.76	.08	.12	.13	2.47	5.22	.03	.89	98.14	.68	.33	.06
	JT83124	73.8	.57	8.0	.11	5.80	.19	.08	.13	1.75	4.62	.03	.79	95.87			
	JT83124B	76.6	.18	10.5	.32	2.15	.07	.04	.01	3.90	3.79	.01	.58	98.09	.39	.03	.06
	JT83131	76.3	.21	11.3	.62	1.10	.02	.02	.01	3.42	4.79	.09	.96	98.79			
MAX		76.6	.57	11.3	1.51	6.14	.19	.16	.22	3.90	5.22	.09	.96		.68	.33	.13
MIN		73.8	.12	8.0	.11	.76	.02	.02	.01	1.65	3.79	.01	.50		.33	0.00	0.00
MEAN		75.6	.270	9.89	.585	2.86	.077	.087	.0933	2.79	4.61	.033	.775		.467	.060	.042
STDEV		1.21	.168	1.24	.487	2.46	.060	.052	.0821	.964	.578	.029	.193		.187	.133	.052
PGRT	JT83064	75.8	.17	10.9	.29	2.44	.02	.02	.04	3.92	4.09	.01	.51	98.15	.26	0.00	.02
	JT83065A	75.8	.17	11.3	.40	2.46	.02	.05	.01	3.84	4.48	.01	.77	99.31	.39	0.00	.06
	JT83066	77.0	.12	11.2	.35	1.62	.03	.06	.17	3.72	4.56	.01	.62	99.41	.31	0.00	.12
	JT83083	76.3	.23	10.8	.43	2.36	.04	.11	.03	3.53	4.58	.02	.58	99.01	.33	0.00	.18
	JT83091A	76.3	.18	10.6	.40	2.38	.03	.02	.04	3.46	4.59	.02	.59	98.61	.22	.01	.13
	JT83099	76.6	.16	11.2	.34	1.79	.01	.01	.24	3.64	4.52	.04	.38	98.88	.31	.05	.13
	JT83125	76.5	.15	10.9	.22	2.34	.04	.07	.03	3.68	4.31	.04	.68	98.91	.43	.03	.04
	JT83152	76.6	.18	10.8	.85	1.81	.06	.04	.16	3.58	4.58	.01	.42	99.08	.12	.02	.03
	JT83155	77.0	.25	11.3	.49	1.81	.02	.04	.12	3.65	4.54	.01	.52	99.75	.36	.02	.33
	JT83259	76.7	.18	11.1	.64	1.82	.03	.03	.03	3.97	4.66	.03	.43	99.62	.39	.01	.07
	JT83307	76.8	.18	10.9	.47	1.92	.04	.07	.10	4.02	3.95	.04	.60	99.09	.47	0.00	.09
	JT83308	76.3	.19	11.2	.46	1.45	.03	.02	.02	3.62	4.68	.04	.47	98.48	.39	0.00	.08
	JT83344	75.9	.26	12.4	.66	.77	.04	.15	.27	3.85	5.18	.01	.44	99.93	.42	0.00	.06

4C. Concluded.

ROCK TYPE	FIELD NUMBER	SiO_2	TiO_2	Al_2O_3	FeO	Fe_2O_3	MnO	MgO	CaO	Na_2O	K_2O	P_2O_5	LOI	TOTAL	H_2O	S	CO_2
	JT83421	76.8	.15	10.8	.30	2.34	.01	.02	.10	4.10	3.99	.01	.40	99.02	.30	0.00	.04
	JT83422	77.9	.19	10.8	.42	1.50	.04	.06	.05	3.57	4.71	.01	.43	99.68	.32	.01	.06
	JT83425	77.7	.17	11.0	.18	2.12	.04	.02	.09	3.83	4.49	.01	.46	100.11	.31	.02	.03
	JT83430	76.7	.14	11.1	.30	1.61	.06	.05	.09	3.36	4.85	.01	.49	98.71	.33	.02	.02
	JT83431	77.1	.14	11.0	.73	1.32	.10	.05	.04	3.97	4.87	.02	.44	99.78	.29	.01	.05
	JT83432	76.2	.19	10.6	.34	2.27	.12	.05	.01	3.66	4.83	.01	.44	98.72	.31	0.00	.03
	JT83433	76.5	.18	10.7	.65	1.39	.03	.02	.04	3.59	4.73	.01	.38	98.17			
	JT83437	77.1	.15	10.9	.15	2.18	.11	.07	.16	3.77	4.77	.01	.45	99.82	.34	.01	.03
	JT83441	76.4	.17	11.0	.28	1.63	.04	.02	.08	4.12	4.66	.01	.36	98.77	.29	0.00	.05
MAX		77.9	.26	12.4	.85	2.46	.12	.15	.27	4.12	5.18	.04	.77		.47	.05	.33
MIN		75.8	.12	10.6	.15	.77	.01	.01	.01	3.36	3.95	.01	.36		.12	0.00	0.00
MEAN		76.6	.177	11.0	.425	1.88	.044	.048	.0873	3.75	4.57	.018	.404		.328	.010	.075
STDEV		.537	.034	.372	.183	.447	.030	.033	.0731	.208	.289	.012	.106		.076	.013	.072
SENT	JT83140	68.8	.22	15.5	.87	2.95	.07	.05	.20	6.51	4.46	.01	.66	100.25			
	JT83140A	64.0	.44	16.4	3.45	1.53	.06	.11	.28	6.08	5.38	.07	1.77	99.52	1.06	.99	.09
	JT83141	63.3	.51	16.6	3.74	2.14	.17	.26	.18	5.33	5.44	.11	1.33	99.11	1.34	.04	.27
	JT83264	64.6	.68	15.5	1.71	3.95	.22	.04	.74	5.28	5.65	.06	.87	99.22	.82	0.00	.03
	JT83470	62.4	.17	17.2	2.35	2.15	.13	.10	.78	6.25	5.98	.02	1.06	98.59	.79	.01	.32
	JT83471	67.7	.18	15.7	2.04	1.54	.15	.11	.46	6.63	3.91	.02	.72	99.11	.78	.01	.06
MAX		68.8	.68	17.2	3.74	3.95	.22	.26	.78	6.63	5.98	.11	1.77		1.34	.99	.32
MIN		62.4	.17	15.5	.87	1.53	.06	.04	.18	5.28	3.91	.01	.66		.78	0.00	0.00
MEAN		65.1	.367	16.1	2.36	2.38	.133	.112	.4400	6.01	5.14	.048	1.07		.958	.175	.128
STDEV		2.55	.209	.717	1.08	.930	.061	.079	.2671	.582	.786	.039	.421		.243	.400	.133
MISC	JT83264	58.6	1.15	14.4	5.49	4.93	.65	.16	2.70	4.87	4.85	.21	1.05	99.01	1.32	.01	.02
	JT83477	71.6	.41	12.6	1.13	2.30	.08	.12	.65	4.20	5.36	.03	.33	98.76	.45	.01	.08

4D. Trace-Element Analysis; see Appendix 4A for rock-type abbreviations.

ROCK TYPE	FIELD NUMBER	Li	Be	F	V	Cr	Ni	Cu	Zn	Ga	Rb	Sr	Y	Zr
APLT	JT83068	10	4.8	734	11	0			41	21	170	35	97	259
	JT83093	11	5.6	696	9	0			90	23	176	37	101	262
	JT83096	5	4.7	65	8	3			21	21	157	20	118	325
	JT83151	9	5.4	204	14	0			44	23	156	38	89	264
	JT83423	6	4.6	105	9	0	1	3	55	19	163	30	73	221
	JT83427	7	5.1	282	12	0	1	4	49	21	166	34	93	253
	JT83428	8	5.1	415	12	0	1	4	56	24	179	35	98	257
	JT83429	8	6.5	555	12	0	1	5	90	25	160	35	104	242
	JT83436	9	5.6	492	14	2	2	3	39	24	174	36	97	251
MAX		11	6.5	734	14	3	2	5	90	25	179	38	118	325
MIN		5	4.6	65	8	0	1	3	21	19	156	20	73	221
MEAN		8.1	5.27	394	11	.56	1.2	3.8	54	22	167	33	96.7	259.3
STDEV		1.9	.592	246	2.2	1.1	.45	.84	23	1.9	8.4	5.5	12.1	27.90
BGRT	JT83069	9	28.8	164	24	1			30	22	150	110	185	215
	JT83070	11	4.2	174	18	3			44	17	171	44	69	234
	JT83072	13	6.0	235	36	9			47	23	129	71	73	235
	JT83074	9	2.6	80	23	0			10	16	136	111	67	185
	JT83079	15	3.3	89	18	1			26	17	149	52	55	234
	JT83158	16	4.2	169	20	0			49	18	204	56	62	223
	JT83159	17	3.9	235	14	0			57	16	192	60	67	232
	JT83200	9	5.3	98	13	0			51	21	187	34	88	201
	JT83305	11	4.5	132	13	0			45	24	200	14	99	248
	JT83306	12	3.6	71	12	3			81	18	172	21	73	235
	JT83310	10	4.4	159	15	4			49	21	179	33	82	224
	JT83313	11	5.1	59	16	5			42	20	175	36	86	238
	JT83314	9	4.6	111	10	4			106	21	178	29	80	231
	JT83315	11	4.9	141	14	3			52	20	183	33	80	239
	JT83424	9	4.9	250	17	2	1	3	54	20	174	52	80	274
	JT83426	15	4.7	250	21	3	3	5	66	20	189	61	68	233
	JT83435	12	5.9	260	16	0	2	4	44	19	209	41	86	228
	JT83479	8	3.0	164	12	0	2	4	48	17	156	32	113	259
	JT83484	8	4.5	111	6	0	1	3	51	23	183	25	63	211
	JT83486	8	4.8	348	10	0	1	4	54	17	185	34	83	241
MAX		17	28.8	348	36	9	3	5	106	24	209	111	185	274
MIN		8	2.6	59	6	0	1	3	10	16	129	14	55	185
MEAN		11	5.66	165	16	1.9	1.7	3.8	50	20	175	47	83.0	231.0
STDEV		2.8	5.52	76.8	6.5	2.4	.82	.75	19	2.4	22	26	27.5	19.17
DORT	JT83406	36	1.7		271	74	27	26	96	16	63	427	32	143
GBBH	JT83071	22	4.1	1255	236	9			109	24	104	187	62	259
	JT83073B	21	3.9	708	141	57	21	23	73	16	115	186	64	244
	JT83199	22	3.1		319	44	18	55	146	22	70	246	68	202
	JT83261	29	3.0		320	86	29	63	182	23	74	258	63	206
	JT83262A	12	3.0		183	88	29	25	127	23	70	181	112	668
	JT83312	26	3.9	836	211	66	17	19	123	18	112	164	66	223
	JT83491	14	4.7		58	3	4	4	57	22	100	311	50	425
MAX		29	4.7	1255	320	88	29	63	182	24	115	311	112	668
MIN		12	3.0	708	58	3	4	4	57	16	70	164	50	202
MEAN		21	3.67	933	210	50	20	32	117	21	92	219	69.3	318.1
STDEV		6.1	.655	286	94	34	9.3	23	42	3.0	20	54	19.7	172.2

4D. Continued.

Nb	Ag	Sn	Ba	La	Ce	Pb	Th	U
36	.1	1	274	62	212	12	28	5
35	.1	2	265	75	226	32	26	5
42	.1	2	20	57	223	7	29	6
35	.1	1	253	48	174	11	29	4
33	.1	2	253	37	197	10	21	4
34	.1	2	288	57	210	12	24	5
34	.1	1	268	61	234	13	30	5
34	.1	6	291	90	267	30	27	5
35	.1	1	320	69	256	10	25	5
42	.1	6	320	90	267	32	30	6
33	.1	1	20	37	174	7	21	4
35.3	.10	2.0	248	62	222	15	27	4.8
2.65	0.0	1.6	88.1	15	29	9.1	2.9	.62
27	.1	1	276	24	132	23	26	5
25	.1	1	351	31	143	10	23	3
44	.1	2	323	69	216	15	28	8
26	.1	1	241	40	147	8	21	4
24	.1	1	356	37	142	11	21	4
24	.1	2	416	47	149	19	25	5
26	.1	2	427	40	187	15	26	3
31	1	1	293	59	199	15	27	4
37	.1	3	216	51	269	7	27	3
38	.1	2	238	31	277	8	30	5
32	.1	1	309	51	230	8	27	3
35	.1		334	48	215	7	19	4
34	.1		326	39	220	13	26	4
31	.1	2	322	37	205	13	23	4
30	.1	1	379	35	156	14	24	3
24	.1	1	434	51	186	16	28	4
28	.1	1	331	62	206	15	26	5
31	.1	1	309	65	191	7	23	4
31	.1	1	119	37	183	16	29	5
32	.1	2	146	59	237	14	28	4
44	.1	3	434	69	277	23	30	8
24	.1	1	119	24	132	7	19	3
30.5	.10	1.4	307	46	194	13	25	4.1
5.31	0.0	.62	83.9	13	41	4.4	2.9	1.0
12	.1		465	10	83	2	9	
18	.1	2	266	33	152	5	15	2
24	.1		331	39	126	7	19	
20	.1		0	17	226	10	13	
16	.1		87	18	184	18	2	8
20	.1		289	37	192	2	13	
18	.1		110	25	179	13	8	
22	.1	2	489	38	140	8	11	3
24	.1	2	489	39	226	18	19	8
16	.1	2	0	17	126	2	2	2
19.7	.10	2.0	225	30	171	9.0	12	4.6
2.69	0.0	0.0	168	9.5	34	5.3	5.4	3.2

4D. Continued.

ROCK TYPE	FIELD NUMBER	Li	Be	F	V	Cr	Ni	Cu	Zn	Ga	Rb	Sr	Y	Zr
GBBR	JT83059	58	1.2	174	210	177	103	83	71	15	54	374	24	80
	JT83060	42	1.9	250	83	124	117	44	66	15	92	285	28	77
	JT83073	36	1.8	333	188	154	112	42	81	17	33	284	34	102
	JT83085	31	2.4	341	248	103	27	115	89	19	89	554	22	106
	JT83095	32	2.4	746	273	132	31	80	123	16	111	524	21	105
	JT83137	36	2.1	848	557	78	29	55	118	20	45	309	57	225
	JT83262	25	2.3		272	128	43	42	109	20	40	289	59	288
	JT83311	27	1.6	454	330	124			137	21	34	458	38	127
	JT83338	43	1.1		212	198	115	72	76	19	22	202	28	80
	JT83343	38	1.4		187	94	73	51	76	22	33	329	29	110
	JT83487	38	2.3		476	139	36	50	145	34	47	264	54	215
	JT83492	21	1.5		273	178	107	52	99	20	18	347	31	116
MAX		58	2.4	848	557	198	117	115	145	34	111	554	59	288
MIN		21	1.1	174	83	78	27	42	66	15	18	202	21	77
MEAN		36	1.83	449	276	136	72	62	99	20	51	352	35.4	135.9
STDEV		9.7	.472	254	129	36	39	23	27	5.0	30	108	13.7	68.22
GRDR	JT83404	10	1.9		42	5	1	8	55	17	90	189	28	155
	JT83407	15	1.8		42	2	1	14	52	14	88	172	29	157
	JT83410	13	1.9		29	1	1	4	46	16	81	180	36	151
MAX		15	1.9		42	5	1	14	55	17	90	189	36	157
MIN		10	1.8		29	1	1	4	46	14	81	172	28	151
MEAN		13	1.87		38	2.7	1.0	8.7	51	16	86	180	31.0	154.3
STDEV		2.5	.058		7.5	2.1	0.0	5.0	4.6	1.5	4.7	8.5	4.36	3.06
PGRA	JT83056	17	2.5	126	27	2	4	17	56	16	179	57	45	186
	JT83086	10	9.7	42	8	2			193	26	211	9	181	722
	JT83087	6	8.3		4	0			52	26	195	5	146	944
	JT83091	5	8.3	1	9	3			42	27	214	10	137	1454
	JT83126	10	10.0	23	6	0			53	21	186	6	236	1230
	JT83127	7	9.1	46	5	0			101	26	214	5	168	1088
	JT83129	23	4.3	311	12	0	1		840	36	431	7	139	1190
	JT83134	9	10.5	42	4	1			180	28	204	6	226	849
MAX		23	10.5	311	27	3	4	17	840	36	431	57	236	1454
MIN		5	2.5	1	4	0	1	17	42	16	179	5	45	186
MEAN		11	7.84	84.4	9.4	1.0	2.5	17	190	26	229	13	160	957.9
STDEV		6.1	2.88	107	7.6	1.2	2.1		269	5.7	83	18	59.8	388.1
PGRM	JT83067	10	43.8	54	10	0			149	26	309	0	1619	6800
	JT83081	8	10.9	35	6	0			77	25	148	18	181	580
	JT83100	10	7.7	35	11	1			122	23	263	20	229	1604
	JT83124	8	51.9	141	15	0			162	11	279	4	2968	19208
	JT83124B	5	10.5	33	6	0			147	27	185	10	375	1376
	JT83131	5	13.6	32	8	1			56	19	198	6	799	581
MAX		10	51.9	141	15	1			162	27	309	20	2968	19208
MIN		5	7.7	32	6	0			56	11	148	0	181	580
MEAN		7.7	23.1	55.0	9.3	.33			119	22	230	9.7	1029	5025
STDEV		2.3	19.5	42.9	3.4	.52			43	6.0	62	7.9	1091	7333
PGRT	JT83064	5	9.3	21	8	3	1	5	58	27	201	3	182	797
	JT83065A	10	12.3	11	6	0	1	5	150	26	209	4	211	890

4D. Continued.

Nb	Ag	Sn	Ba	La	Ce	Pb	Th	U
7	.1		70	4	59	2	0	
8	.1		235	15	69	8	0	
9	.1		146	11	66	1	0	
10	.1		555	15	50	1	7	
7	.1		449	21	73	6	3	
14	.1		180	7	125	1	9	
12	.1		120	23	165	1	5	
7	.1	1	0	11	195	6	0	0
6	.1		7	7	91	3	7	
10	.1		106	5	110	1	2	
15	.1		72	14	188	1	0	
10	.1		34	11	120	1	0	
15	.1	1	555	23	195	8	9	0
6	.1	1	0	4	50	1	0	0
9.58	.10	1.0	164	12	109	2.7	2.8	.40
2.87	0.0		173	6.0	51	2.5	3.4	
13	.1		704	19	99	7	14	
12	.1		581	15	74	5	13	
13	.1		657	19	80	10	12	
13	.1		704	19	99	10	14	
12	.1		581	15	74	5	12	
12.7	.10		647	18	84	7.3	13	
.58	0.0		62.1	2.3	13	2.5	1.0	
17	1.8	3	407	35	134	188	22	3
61	.1	8	59	26	150	76	51	7
70	.1	7	31	3	63	12	23	6
104	.1	11	29	2	47	36	32	7
96	.1	8	102	28	167	16	56	8
77	.1	9	77	7	76	67	40	8
89	.8	4	153	7	23	481	37	6
70	.1		32	57	235	20	25	
104	1.8	11	407	57	235	481	56	8
17	.1	3	29	2	23	12	22	3
73.0	.40	7.1	111	21	112	112	36	6.4
26.9	.62	2.8	127	19	72	160	13	1.6
809	.1	40	47	33	762	33	364	64
52	.1	5	96	21	188	10	31	6
97	.1	11	142	18	121	56	44	10
1860	.1	90	220	190	1550	44	725	113
187	.1	14	154	21	336	9	77	11
61	.2	5	113	3	53	27	620	10
1860	.2	90	220	190	1550	56	725	113
52	.1	5	47	3	53	9	31	6
511	.12	28	129	48	502	30	310	36
721	.04	33	58.6	70	573	19	308	44
64	.1	7	48	57	205	14	47	7
74	.1	9	41	58	229	16	31	6

4D. Concluded.

ROCK TYPE	FIELD NUMBER	Li	Be	F	V	Cr	Ni	Cu	Zn	Ga	Rb	Sr	Y	Zr
	JT83066	6	6.7	62	6	8			40	29	200	12	162	580
	JT83083	8	8.8	39	6	0			51	25	167	14	158	761
	JT83091A	4	8.4	32	6	4			89	28	186	10	154	1084
	JT83099	4	3.9	51	6	5			40	27	136	15	69	493
	JT83125	6	8.9	30	7	0			120	28	205	8	164	698
	JT83152	6	13.0	341	6	0			123	28	218	9	306	1354
	JT83155	6	6.3	77	9	0			18	24	147	14	125	628
	JT83259	19	8.4	111	4	0			101	29	219	1	67	356
	JT83307	8	11.3	74	9	1			53	26	140	18	171	726
	JT83308	9	7.4	37	6	2			127	25	192	7	152	672
	JT83344	7	5.8	89	11	4	1	6	111	22	179	24	85	236
	JT83421	4	11.3	58	5	1	1	5	46	26	148	8	217	774
	JT83422	4	7.3	51	5	2	1	4	124	27	183	13	130	579
	JT83425	6	7.6	77	5	0	1	5	31	25	192	10	167	762
	JT83430	7	9.3	83	5	4	1	6	139	24	193	11	155	517
	JT83431	29	6.5	189	4	2	1	7	334	28	205	7	66	504
	JT83432	23	9.5	129	4	2	1	18	329	27	259	12	135	758
	JT83433	5	8.5	42	3	0	1	13	126	27	219	12	135	796
	JT83437	6	9.2	56	4	1	1	63	228	29	240	23	225	634
	JT83441	11	7.4	83	6	5	1	11	86	27	202	7	63	574
MAX		29	13.0	341	11	8	1	63	334	29	259	24	306	1354
MIN		4	3.9	11	3	0	1	4	18	22	136	1	63	236
MEAN		8.8	8.50	79.2	6.0	2.0	1.0	12	115	27	193	11	150	689.7
STDEV		6.5	2.17	70.6	1.9	2.2	0.0	16	86	1.8	31	5.7	59.4	233.8
SENT	JT83140	8	22.8	836	4	2			259	48	133	27	226	1868
	JT83140A	12	3.4	144	9	0			131	32	150	26	92	966
	JT83141	20	4.1	144	8	0			88	30	166	50	67	671
	JT83264	8	1.6	108	17	0	1	4	56	29	76	18	31	50
	JT83470	12	8.4	3382	1	0	1	3	222	35	203	87	135	1116
	JT83471	17	6.2	2560	2	0	1	2	126	38	120	19	188	1307
MAX		20	22.8	3382	17	2	1	4	259	48	203	87	226	1868
MIN		8	1.6	108	1	0	1	2	56	29	76	18	31	50
MEAN		13	7.75	1196	6.8	.33	1.0	3.0	147	35	141	38	123	996.3
STDEV		4.8	7.74	1426	5.9	.82	0.0	1.0	78	7.0	43	27	74.2	612.0
MISC	JT83264A	11	1.7	220	16	0	1	7	97	27	57	20	48	136
	JT83477	5	2.2	189	14	0	1	3	73	26	81	26	88	994

4D. Concluded.

Nb	Ag	Sn	Ba	La	Ce	Pb	Th	U
61	.1	2	52	34	192	5	27	6
70	.1	12	61	9	214	8	17	7
74	.1	6	36	29	195	23	31	7
20	.1	6	79	34	207	12	9	2
59	.1	12	91	0	206	12	33	5
162	.1	3	71	83	35	27	73	16
29	.1	1	248	14	230	4	47	4
45	.1		0	3	93	9	20	4
71	.1	4	97	60	328	11	34	8
61	.1	5	21	7	143	24	26	6
39	.1	3	270	49	251	20	28	4
67	.1	4	77	53	224	8	32	7
57	.3	4	82	17	196	12	27	5
72	.1	5	42	33	248	7	34	7
51	.2	5	54	57	322	25	19	5
46	.1	5	46	15	130	23	24	4
101	.3	7	59	28	223	60	36	7
75	.1	5	48	25	140	22	37	7
71	.3	4	59	55	248	37	34	7
53	.1	1	33	21	143	11	26	5
162	.3	12	270	83	328	60	73	16
20	.1	1	0	0	35	4	9	2
64.6	.13	5.2	73.4	34	200	18	31	6.2
27.9	.07	3.0	64.3	22	67	13	13	2.7
524	.1	16	102	190	554	20	70	12
198	.3	5	772	73	186	60	27	7
132	.1	2	859	21	168	4	6	4
20	.1	6	509	25	94	1	5	1
237	.1	3	35	211	523	9	31	7
352	.1	10	43	224	580	13	44	8
524	.3	16	859	224	580	60	70	12
20	.1	2	35	21	94	1	5	1
244	.13	7.0	387	124	351	18	32	6.5
176	.08	5.2	377	95	224	22	23	3.7
15	.1	3	1515	10	22	1	5	1
19	.1	1	416	115	372	7	16	2

4E. Summary of geochemical data from the Long Harbour Group, Mooring Cove Formation, and Musgravetown Group in the Grand Le Pierre area.

	Long Harbour Group								
	MAFIC ROCKS N = 3		RHYOLITE N = 4		FELDSPAR PORPHYRY N = 1	TUFF N = 13		RHYOLITES (Whalen, 1976) N = 44	
	X	s	X	s		X	s	X	s
SiO_2	45.9	2.54	78.0	0.9	70.1	69.85	2.36	76.0	2.23
Al_2O_3	13.65	1.32	11.12	1.02	14.3	14.48	1.43	11.76	1.39
Fe_2O_3	4.97	1.61	0.84	0.24	2.34	2.31	0.98	2.12	1.05
FeO	7.49	0.96	0.56	0.10	1.16	0.81	0.39	0.58	0.36
MgO	7.52	2.21	0.15	0.09	0.78	0.72	0.42	0.08	0.07
CaO	9.67	1.42	1.29	1.47	1.75	1.71	0.78	0.14	0.21
Na_2O	2.83	0.97	1.56	0.82	5.41	4.10	0.86	3.64	1.13
K_2O	1.16	0.58	4.14	0.97	2.18	3.41	1.18	4.55	0.92
TiO_2	2.19	0.68	0.17	0.02	0.47	0.54	0.17	0.22	0.08
MnO	0.26	0.05	0.04	0.02	0.10	0.98	0.02	0.06	0.04
P_2O_5	0.42	0.10	0.02	0.01	0.13	0.10	0.06		
LOI	1.41	0.29	1.00	0.47	0.95	1.34	0.47	0.59	0.42
TOTAL	99.01	0.67	98.83	0.44	99.67	99.50	0.53	99.74	
Li	45.3	18.2	238.0	19.3	15	24.1	19.2		
Be	3.2	1.2	3.7	1.5	2.0	2.8	0.5		
F	1298	381.8	460.5	262.9	225.0	392.6	210.1		
V	345.0	79.3	8.3	6.0	30.0	34.8	15.1		
Cr	175.0	127.2	2.0	2.4	0	1.6	5.3	7.0	4.0
Ni	48.5	27.6	1.0	0.1	-	2.0	1.4	14.0	5.0
Cu	19.3	15.5	6.0	1.4	5.0	7.0	4.3	7.0	6.0
Zn	115.3	34.5	31.3	15.6	68.0	64.1	21.1	112.0	105.0
Ga	21.0	5.0	19.3	5.0	15.0	17.2	3.9		
Rb	112.0	68.5	170.5	73.2	52.0	121.8	39.9	174.0	48.0
Sr	330.6	80.8	79.0	69.3	210.0	206.6	97.1	24	40.0
Y	45.3	21.5	65.5	22.8	47.0	56.3	28.4	145.0	45.0
Zr	166.0	81.5	335.0	159.6	215.0	314.3	136.7	945.0	334.0
Nb	9.6	1.2	29.0	11.2	12.0	18.3	7.5	50.0	25.0
Mo	-	-	8	0	-				
Ag	0.1	0	0.1	0	0.1	0.1	0		
Ba	67.7	92.4	159.8	163.5	536.0	833.1	345.9	191.0	218.0
La	12.0	12.0	35.5	23.3	38.0	36.2	12.5		
Ce	142.6	8.3	126.8	68.4	87.0	109.5	59.0		
Pb	1.0	0	49.8	65.0	5	24.9	37.8	41.0	29.0
Th	7.3	2.1	23.5	7.3	7	15.4	3.3		
U	-	-	3.5	2.0	-	3.2	0.6		

4E. Concluded.

	Mooring Cove Fm.* rhyodacite (NTS 1M/11)		Mooring Cove Fm.* rhyodacite (NTS 1M/10)		Musgravetown Gp.* mafic rocks	
Wt.%	$\bar{x}$	s	$\bar{x}$	s	$\bar{x}$	s
SiO_2	66.53	0.75	75.58	4.09	44.16	3.22
TiO_2	0.32	0.02	0.31	.11	2.43	.51
Al_2O_3	15.93	0.33	12.25	1.43	15.16	.50
Fe_2O_3	2.64	1.68	2.82	1.05	7.68	3.21
FeO	1.66	1.37	.67	.39	5.58	2.97
MnO	0.13	0.10	1.11	1.93	.24	.04
MgO	0.18	0.02	.45	.46	4.32	1.96
CaO	1.31	0.18	.31	.26	7.27	1.18
Na_2O	5.57	0.29	3.81	2.62	3.96	.43
K_2O	4.43	0.23	3.38	1.37	1.00	.61
P_2O_5	0.06	0.01	.02	.02	.54	.39
LOI	0.79	0.19	.58	.19	6.78	1.16
g/t						
Rb	71	10.69	110	51.50	33	32
Sr	126	18.00	13	25.50	490	65
Y	168	7.10	164	34.43	49	18
Zr	763	8.39	865	166.73	201	72
Nb	81	0.58	36	8.81	17	8
Zn	146	2.08	92	58.15	115	27
Cu	6	7.81	14	17.95	29	23
Ni	1	0.58	4	6.35	40	26
Ba	801	180.53	456	780.82	378	181
V	2	1.16	1	.95	242	89
Cr	1	0	0	0	55	44
Ga	30	3.46	22	5.74	22	5
	n = 3		n = 4		n = 5	

* Data from O'Brien, 1988, personal communication

4F. Rare-earth and other elements analyzed by ICP-MS at Memorial University of Newfoundland.

Sample	La	Ce	Pr	Nd	Sm	Eu	Gd	Tb	Dy	Ho
JT-422	15.83	68.32	5.66	23.18	7.96	0.92	8.90	2.10	15.54	3.42
JT-155	14.70	87.20	6.14	26.67	8.83	1.01	9.90	2.06	14.74	3.14
JT-426	43.05	97.54	10.54	37.65	8.03	0.89	7.28	1.37	9.30	1.99
JT-424	27.21	70.00	8.31	32.82	8.21	1.08	7.91	1.47	9.94	2.10
JT-404	23.33	44.68	5.07	18.47	3.61	0.89	3.41	0.59	3.99	0.82
JT-067	36.90	401.82	18.80	84.83	47.67	5.50	71.20	20.47	162.07	38.86
JT-124	173.56	991.82	80.84	347.88	153.66	16.49	186.39	52.00	391.10	89.45
JT-437	42.23	97.86	14.22	58.06	17.13	1.55	17.83	3.73	25.87	5.55
JT-343	8.70	21.63	3.03	13.80	3.53	1.18	3.60	0.64	4.12	0.83
JT-433	20.13	53.15	7.19	29.63	9.03	0.85	9.08	2.08	15.40	3.43
Duplicates										
JT-155	14.63	85.78	6.01	27.01	8.85	1.05	9.95	1.99	14.41	3.08
JT-404	23.39	44.92	5.09	18.41	3.77	0.76	3.17	0.64	3.82	0.82
JT-422	15.52	68.22	5.59	23.00	7.87	0.87	8.69	2.05	14.91	3.33
JT-426	42.58	96.95	10.58	37.15	8.01	0.93	7.43	1.40	8.81	1.96
JT-424	26.50	69.61	8.22	32.49	7.96	1.00	7.33	1.45	9.61	1.99
SY-2 STD	65.65	150.45	18.68	70.01	14.72	2.32	13.97	2.58	18.65	4.34
Normalizing Value*	0.38	0.96	0.14	0.71	0.23	0.09	0.31	0.06	0.38	0.09

4F. Concluded.

Sample	Er	Tm	Yb	Lu	Hf	Th	Y	Zr	^{160}Gd
JT-422	10.69	1.67	11.10	1.67	10.45	19.78	86.09	327.32	8.58
JT-155	9.91	1.74	13.75	2.06	7.66	33.62	79.01	359.97	9.31
JT-426	6.19	0.92	6.20	0.93	6.93	20.00	52.38	185.77	6.80
JT-424	6.38	0.97	6.31	0.98	6.90	14.88	54.71	208.48	7.65
JT-404	2.58	0.42	2.72	0.44	4.05	9.44	23.14	143.90	3.17
JT-067	128.54	20.72	137.54	18.80	117.69	246.10	992.88	4096.95	68.71
JT-124	303.69	50.59	345.94	45.10	353.85	464.23	1711.52	10675.74	184.33
JT-437	17.26	2.59	16.65	2.40	11.88	26.16	149.38	379.56	17.46
JT-343	2.35	0.34	2.31	0.33	2.18	1.25	21.05	75.48	3.61
JT-433	11.31	1.79	11.95	1.81	13.89	27.39	85.06	442.46	8.88
Duplicates									
JT-155	9.78	1.76	13.47	2.04	7.71	34.07	78.17	354.19	9.00
JT-404	2.52	0.41	2.83	0.44	4.00	9.40	22.86	142.33	3.15
JT-422	10.61	1.66	11.04	1.62	9.97	19.80	83.50	322.25	8.41
JT-426	5.94	0.91	6.09	0.90	6.73	19.56	52.38	172.53	6.80
JT-424	6.11	0.94	6.21	0.95	6.52	14.61	53.83	204.74	7.01
SY-2 STD	13.82	2.32	16.07	2.64	8.19	361.71	113.12	260.87	13.31
Normalizing Value*	0.25	0.04	0.25	0.04	0.18	0.04	2.25	5.54	0.31

* From Evensen *et al.*, 1978.

4G. Mesonorms and agpaitic indices; see Appendix 4A for rock-type abbreviations.

ROCK TYPE	FIELD NUMBER	Qz	Or	Ab	An	Co	Bi	Ri	Ns	Hy	Act	Wo	Mt
APLT	JT83068	28.39	30.53	37.44	.43	0.00	1.33	-.00	0.00	0.00	0.00	.45	.58
	JT83093	31.06	30.18	33.48	2.39	0.00	1.84	0.00	0.00	0.00	0.00	0.00	.51
	JT83096	31.43	26.86	39.16	.32	0.00	.38	.00	0.00	0.00	0.00	.34	.96
	JT83151	30.84	30.83	34.31	2.07	0.00	.69	-.00	0.00	0.00	0.00	0.00	.72
	JT83423	30.58	31.19	35.39	.88	0.00	.45	.00	0.00	0.00	0.00	0.00	.42
	JT83427	30.18	30.86	35.19	1.32	0.00	.92	0.00	0.00	0.00	0.00	.05	.71
	JT83428	30.39	31.33	34.48	1.20	0.00	1.02	.00	0.00	0.00	0.00	.04	.76
	JT83429	29.46	31.27	35.77	.74	0.00	.95	0.00	0.00	0.00	0.00	.20	.73
	JT83436	29.67	31.04	35.33	.64	0.00	1.69	-.00	0.00	0.00	0.00	.26	.55
MAX		31.43	31.33	39.16	2.39	0.00	1.84	.00	0.00	0.00	0.00	.45	.96
MIN		28.39	26.86	33.48	.32	0.00	.38	-.00	0.00	0.00	0.00	0.00	.42
MEAN		30.22	30.45	35.62	1.111	0.00	1.029	-.000	0.00	0.00	0.00	.1477	.661
STDEV		.9306	1.399	1.723	.7164	0.00	.5080	.0000	0.00	0.00	0.00	.1696	.162
BGRT	JT83069	33.54	28.66	29.01	5.51	0.00	.98	0.00	0.00	0.00	0.00	.61	.79
	JT83070	28.13	30.96	35.80	2.27	.05	1.59	.00	0.00	0.00	0.00	0.00	.73
	JT83072	26.51	24.89	36.95	4.80	.13	4.73	-.00	0.00	0.00	0.00	0.00	1.17
	JT83074	35.30	24.45	31.08	6.38	0.00	.27	0.00	0.00	0.00	0.00	1.14	.58
	JT83079	33.96	26.88	32.46	3.73	0.00	1.19	0.00	0.00	0.00	0.00	.16	.71
	JT83158	30.23	29.03	32.87	3.64	.37	2.85	0.00	0.00	0.00	0.00	0.00	.46
	JT83159	30.44	29.28	32.93	3.41	.33	2.33	.00	0.00	0.00	0.00	0.00	.71
	JT83200	30.43	31.31	34.00	1.95	0.00	1.28	.00	0.00	0.00	0.00	0.00	.56
	JT83305	30.63	31.71	34.79	.44	.19	1.06	.00	0.00	.00	0.00	0.00	.70
	JT83306	32.24	32.06	32.40	.87	.25	.83	-.00	0.00	0.00	0.00	0.00	.83
	JT83310	29.41	30.92	35.77	1.57	0.00	.80	.00	0.00	0.00	0.00	0.00	.85
	JT83313	30.32	30.62	35.71	.91	.30	.91	0.00	0.00	0.00	0.00	0.00	.78
	JT83314	31.33	32.16	33.73	.59	0.00	.71	0.00	0.00	0.00	0.00	0.00	.86
	JT83315	29.80	30.50	35.40	1.71	0.00	1.33	0.00	0.00	0.00	0.00	.00	.71
	JT83424	28.40	31.05	36.26	1.43	0.00	1.15	-.00	0.00	0.00	0.00	0.00	.92
	JT83426	28.78	29.46	34.63	3.46	0.00	2.09	.00	0.00	0.00	0.00	0.00	.93
	JT83435	27.61	32.53	34.89	1.72	0.00	1.37	0.00	0.00	0.00	0.00	.11	.83
	JT83479	30.64	32.37	32.92	.60	0.00	1.70	0.00	0.00	0.00	0.00	.11	.79
	JT83484	31.36	32.72	33.04	.77	0.00	.79	-.00	0.00	0.00	0.00	0.00	.64
	JT83486	28.72	33.81	34.52	.19	0.00	.94	0.00	0.00	0.00	0.00	.25	.75
MAX		35.30	33.81	36.95	6.38	.37	4.73	.00	0.00	.00	0.00	1.14	1.17
MIN		26.51	24.45	29.01	.19	0.00	.27	-.00	0.00	0.00	0.00	0.00	.46
MEAN		30.39	30.27	33.96	2.298	.081	1.445	.0000	0.00	.0000	0.00	.1192	.765
STDEV		2.186	2.510	1.920	1.802	.130	.9819	.0000	0.00	.0000	0.00	.2806	.152
DORT	JT83406	12.65	0.00	22.04	31.20	0.00	16.12	0.00	0.00	1.84	12.36	0.00	4.49
GBBH	JT83071	13.91	8.24	38.33	14.91	0.00	14.33	0.00	0.00	0.00	0.00	.55	3.75
	JT83073B	20.15	11.62	32.11	14.09	0.00	14.61	0.00	0.00	0.00	0.00	1.46	2.52
	JT83199	15.06	0.00	32.89	17.09	0.00	21.74	0.00	0.00	0.00	.95	1.93	3.69
	JT83261	14.26	0.00	31.92	17.60	0.00	20.46	0.00	0.00	0.00	8.78	.42	3.13
	JT83262A	16.20	6.68	34.60	10.87	0.00	20.18	-.00	0.00	0.00	0.00	4.13	3.07
	JT83312	13.57	4.13	35.51	15.91	0.00	22.28	0.00	0.00	0.00	0.00	1.39	2.50
	JT83491	14.29	14.08	45.26	16.59	.04	5.75	0.00	0.00	0.00	0.00	0.00	2.71
MAX		20.15	14.08	45.26	17.60	.04	22.28	0.00	0.00	0.00	8.78	4.13	3.75
MIN		13.57	0.00	31.92	10.87	0.00	5.75	-.00	0.00	0.00	0.00	0.00	2.50
MEAN		15.35	6.395	35.80	15.29	.006	17.05	-.000	0.00	0.00	1.391	1.410	3.05
STDEV		2.286	5.429	4.735	2.300	.016	5.943	.0000	0.00	0.00	3.279	1.379	.515

4G. Continued.

Hm	Il	Ru	Ap	Cr	Zr	A.I.
0.00	.38		.04	0.0	.03	.99
0.00	.38	.15	.04	0.0	.03	.93
0.00	.23		.06	.00	.04	.99
0.00	.38	.14	.02	0.0	.03	.94
.36	.36	.03	.04	0.0	.03	.98
0.00	.36		.04	0.0	.03	.96
0.00	.37		.02	0.0	.03	.97
0.00	.40		.04	0.0	.03	.98
0.00	.37		.04	.00	.03	.98
.36	.40	.15	.06	.00	.04	.99
0.00	.23	.03	.02	0.0	.03	.93
.041	.358	.11	.040	.00	.03	.97
.122	.051	.06	.013	.00	.00	.02
0.00	.40		.06	.00	.03	.84
.00	.38	.19	.06	.00	.03	.94
0.00	.63	.32	.15	.00	.03	.86
.13	.30		.04	0.0	.02	.81
.00	.40		.09	.00	.03	.89
0.00	.43	.21	.09	0.0	.03	.88
0.00	.47	.24	.06	0.0	.03	.88
0.00	.37	.17	.06	0.0	.02	.95
0.00	.36	.18	.09	0.0	.03	.97
.03	.39	.19	.06	.00	.03	.96
0.00	.39	.08	.04	.00	.03	.96
0.00	.37	.19	.04	.00	.03	.95
0.00	.35	.07	.02	.00	.03	.98
0.00	.38	.14	.04	.00	.03	.95
0.00	.47	.12	.06	.00	.03	.96
0.00	.44	.17	.09	.00	.03	.91
0.00	.42		.06	0.0	.03	.95
0.00	.40		.04	0.0	.03	.98
-.00	.34	.03	.02	0.0	.03	.98
0.00	.36		.06	0.0	.03	1.00
.13	.63	.32	.15	.00	.03	1.00
-.00	.30	.03	.02	0.0	.02	.81
.008	.403	.16	.063	.00	.03	.93
.030	.068	.07	.028	.00	.00	.05
0.00	1.81		.59	.01	.02	.34
0.00	2.61		.73	.00	.03	.65
0.00	1.47		.46	.01	.03	.65
0.00	3.12		.76	.01	.03	.58
0.00	3.06		.79	.01	.03	.56
0.00	1.87		.43	.01	.08	.71
0.00	2.14		.39	.01	.03	.63
0.00	.86	.43	.36	.00	.05	.65
0.00	3.12	.43	.79	.01	.08	.71
0.00	.86	.43	.36	.00	.03	.56
0.00	2.16	.43	.560	.01	.04	.63
0.00	.83		.190	.01	.02	.05

4G. Continued.

ROCK TYPE	FIELD NUMBER	Qz	Or	Ab	An	Co	Bi	Ri	Ns	Hy	Act	Wo	Mt
GBBR	JT83059	3.24	0.00	22.06	35.28	.00	7.35	0.00	0.00	14.35	18.50	0.00	2.63
	JT83060	10.08	0.00	26.03	30.85	0.00	17.95	0.00	0.00	7.55	8.21	0.00	1.28
	JT83073	5.77	0.00	20.94	33.39	0.00	7.64	0.00	0.00	18.71	12.05	0.00	2.10
	JT83085	8.36	.07	32.78	26.05	0.00	21.70	0.00	0.00	0.00	0.00	2.35	5.15
	JT83095	10.29	0.00	24.72	28.76	0.00	19.93	0.00	0.00	0.00	6.27	2.92	5.96
	JT83137	4.68	-.00	31.91	21.38	0.00	5.14	0.00	0.00	10.04	11.51	0.00	7.52
	JT83262	11.10	0.00	30.87	22.54	0.00	12.33	0.00	0.00	3.19	17.77	0.00	2.99
	JT83311	3.94	0.00	26.61	28.63	0.00	7.78	0.00	0.00	13.66	12.17	0.00	4.89
	JT83338	5.61	0.00	21.86	34.94	0.00	3.29	0.00	0.00	14.11	23.45	0.00	2.34
	JT83343	1.85	0.00	25.30	33.39	.00	6.59	0.00	0.00	18.12	12.94	0.00	2.69
	JT83487	1.91	0.00	28.80	21.49	0.00	11.43	0.00	0.00	15.60	5.29	0.00	5.84
	JT83492	0.00	0.00	23.95	34.92	.00	3.91	0.00	0.00	21.66	6.55	0.00	3.87
MAX		11.10	.07	32.78	35.28	.00	21.70	0.00	0.00	21.66	23.45	2.92	7.52
MIN		0.00	-.00	20.94	21.38	0.00	3.29	0.00	0.00	0.00	0.00	0.00	1.28
MEAN		5.570	.0057	26.32	29.30	.000	10.42	0.00	0.00	11.42	11.22	.4397	3.94
STDEV		3.672	.0196	4.004	5.357	.000	6.319	0.00	0.00	7.302	6.512	1.034	1.91
GRDR	JT83404	29.65	12.19	37.22	13.53	.13	5.57	-.00	0.00	0.00	0.00	0.00	1.02
	JT83407	27.40	12.11	39.11	13.91	0.00	5.33	-.00	0.00	0.00	0.00	0.00	1.44
	JT83410	30.04	14.61	37.08	12.01	.29	4.28	0.00	0.00	0.00	0.00	0.00	1.04
MAX		30.04	14.61	39.11	13.91	.29	5.57	0.00	0.00	0.00	0.00	0.00	1.44
MIN		27.40	12.11	37.08	12.01	0.00	4.28	-.00	0.00	0.00	0.00	0.00	1.02
MEAN		29.03	12.97	37.81	13.15	.141	5.063	-.000	0.00	0.00	0.00	0.00	1.17
STDEV		1.423	1.422	1.135	1.005	.147	.6859	.0000	0.00	0.00	0.00	0.00	.238
PGRA	JT83056	40.86	24.57	26.42	4.25	.00	2.10	0.00	0.00	0.00	0.00	.41	.46
	JT83086	35.21	29.76	32.43	.28	.06	.35	0.00	0.00	0.00	0.00	0.00	.07
	JT83087	37.74	26.64	33.07	.00	0.00	.04	.59	.24	0.00	0.00	0.00	0.00
	JT83091	40.56	26.40	30.18	0.00	0.00	.04	1.16	.14	0.00	0.00	0.00	0.00
	JT83126	46.09	24.98	25.65	.11	.60	.28	0.00	0.00	0.00	0.00	0.00	.51
	JT83127	41.08	27.26	29.21	.00	.50	.19	0.00	0.00	0.00	0.00	0.00	.07
	JT83129	35.09	54.63	1.15	.02	6.46	.24	0.00	0.00	0.00	0.00	0.00	.10
	JT83134	37.90	26.93	32.85	.15	.08	.11	0.00	0.00	0.00	0.00	0.00	.10
MAX		46.09	54.63	33.07	4.25	6.46	2.10	1.16	.24	0.00	0.00	.41	.51
MIN		35.09	24.57	1.15	0.00	0.00	.04	0.00	0.00	0.00	0.00	0.00	0.00
MEAN		39.32	30.15	26.37	.6003	.961	.4181	.2199	.047	0.00	0.00	.0513	.164
STDEV		3.629	10.02	10.57	1.476	2.23	.6895	.4347	.090	0.00	0.00	.1451	.202
PGRM	JT83067	44.28	32.31	15.93	.19	.47	.63	0.00	0.00	.00	0.00	0.00	.37
	JT83081	38.84	25.03	33.31	.76	0.00	.39	0.00	0.00	0.00	0.00	0.00	1.16
	JT83100	40.61	30.69	23.35	.51	.64	2.83	0.00	0.00	0.00	0.00	0.00	.84
	JT83124	44.90	29.53	17.11	.36	0.00	.32	0.00	0.00	0.00	0.00	0.00	.77
	JT83124B	37.89	23.24	36.12	0.00	0.00	.15	.58	0.00	0.00	0.00	0.00	.21
	JT83131	36.58	29.33	31.88	0.00	.50	.08	0.00	0.00	0.00	0.00	0.00	1.09
MAX		44.90	32.31	36.12	.76	.64	2.83	.58	0.00	.00	0.00	0.00	1.16
MIN		36.58	23.24	15.93	0.00	0.00	.08	0.00	0.00	0.00	0.00	0.00	.21
MEAN		40.51	28.36	26.28	.3033	.268	.7335	.0966	0.00	.0000	0.00	0.00	.737
STDEV		3.422	3.481	8.687	.3010	.299	1.045	.2366	0.00	.0000	0.00	0.00	.382
PGRT	JT83064	35.89	25.09	36.48	0.00	0.00	.08	.22	0.00	0.00	0.00	.00	.25
	JT83065A	34.62	27.16	35.53	0.00	.15	.19	0.00	0.00	0.00	0.00	0.00	.64

4G. Continued.

Hm	Il	Ru	Ap	Cr	Zr	A.I.
0.00	1.83		.30	.03	.01	.27
0.00	.62		.06	.02	.01	.38
0.00	1.89		.41	.03	.01	.28
0.00	1.46		.58	.02	.01	.47
0.00	1.49		.63	.02	.01	.39
0.00	5.58		1.22	.01	.03	.45
-.00	2.77		.71	.02	.04	.46
0.00	3.17		.82	.02	.02	.35
0.00	1.75		.24	.03	.01	.26
-.00	1.93		.43	.02	.01	.31
-.00	5.13		1.45	.02	.03	.46
0.00	2.65		.74	.03	.01	.28
0.00	5.58		1.45	.03	.04	.47
-.00	.62		.06	.01	.01	.26
-.00	2.5		.633	.02	.02	.36
.000	1.4		.400	.01	.01	.08
0.00	.53	.27	.13	.00	.02	.66
-.00	.53	.26	.13	.00	.02	.66
0.00	.51	.25	.11	.00	.02	.68
0.00	.53	.27	.13	.00	.02	.68
-.00	.51	.25	.11	.00	.02	.66
-.00	.525	.26	.123	.00	.02	.67
.000	.016	.01	.012	.00	.00	.01
0.00	.41		.09	.00	.02	.86
1.56	.05	.10	.07	.00	.09	.99
1.25	.25	.10	.02	0.0	.12	1.02
1.05	.25	.12	.02	.00	.19	1.02
1.39	.21	.10	.02	0.0	.16	.94
1.39	.05	.11	.02	0.0	.14	.96
1.98	.07	.12	.02	0.0	.16	.64
1.64	.06	.08	.02	.00	.11	.99
1.98	.41	.12	.09	.00	.19	1.02
0.00	.05	.08	.02	0.0	.02	.64
1.28	.168	.11	.036	.00	.12	.93
.588	.132	.01	.026	.00	.05	.13
4.36	.54	.27	.04	0.0	.89	.95
.11	.18	.03	.04	0.0	.07	.98
0.00	.26	.13	.07	.00	.21	.93
3.89	.51	.14	.07	0.0	2.6	.99
1.35	.26	.13	.02	0.0	.18	1.01
.07	.30	.15	.13	.00	.07	.96
4.36	.54	.27	.13	.00	2.6	1.01
0.00	.18	.03	.02	0 0	.07	.93
1.63	.342	.14	.063	.00	.66	.97
2.00	.147	.08	.038	.00	.98	.03
1.57	.25	.09	.02	.00	.10	1.00
1.34	.24	.12	.02	0.0	.11	.99

4G. Concluded.

ROCK TYPE	FIELD NUMBER	Qz	Or	Ab	An	Co	Bi	Ri	Ns	Hy	Act	Wo	Mt
	JT83066	35.82	27.53	34.30	.27	0.00	.23	-.00	0.00	0.00	0.00	.05	.65
	JT83083	36.60	27.74	32.80	.04	.03	.42	0.00	0.00	0.00	0.00	0.00	.63
	JT83091A	37.04	28.15	31.97	0.00	0.00	.08	.51	0.00	.00	0.00	0.00	.34
	JT83099	36.05	27.52	33.71	.76	0.00	.04	0.00	0.00	0.00	0.00	0.00	.49
	JT83125	36.99	26.21	34.22	0.00	.15	.27	0.00	0.00	0.00	0.00	0.00	.30
	JT83152	36.24	27.80	32.88	-.00	0.00	.15	.39	0.00	0.00	0.00	.05	1.56
	JT83155	36.15	27.38	33.56	.60	.19	.15	0.00	0.00	0.00	0.00	0.00	.68
	JT83259	34.24	28.07	33.79	0.00	.00	.11	2.01	.39	0.00	0.00	0.00	0.00
	JT83307	36.45	23.88	37.19	.03	0.00	.27	0.00	0.00	0.00	0.00	0.00	.83
	JT83308	35.77	28.58	33.66	0.00	.20	.08	.00	0.00	0.00	0.00	0.00	.77
	JT83344	31.09	30.52	35.04	1.27	0.00	.81	0.00	0.00	0.00	0.00	0.00	.82
	JT83421	36.20	24.21	36.41	.00	0.00	.08	.70	.30	0.00	0.00	0.00	0.00
	JT83422	36.97	28.36	31.88	0.00	0.00	.23	1.15	.06	0.00	0.00	0.00	0.00
	JT83425	36.30	26.99	34.16	0.00	0.00	.08	.27	.21	.00	0.00	0.00	0.00
	JT83430	36.83	29.55	31.24	.41	.14	.19	0.00	0.00	0.00	0.00	0.00	.56
	JT83431	34.28	29.20	31.87	0.00	0.00	.19	2.78	.78	0.00	0.00	0.00	0.00
	JT83432	36.16	29.41	30.34	0.00	0.00	.19	1.16	.87	0.00	0.00	0.00	0.00
	JT83433	36.11	28.98	31.36	0.00	0.00	.08	2.09	.22	0.00	0.00	0.00	0.00
	JT83437	35.82	28.63	32.00	-.00	0.00	.26	.50	.68	0.00	0.00	.09	0.00
	JT83441	34.82	28.24	33.40	0.00	0.00	.08	.67	1.25	0.00	0.00	.00	0.00
MAX		37.04	30.52	37.19	1.27	.20	.81	2.78	1.25	.00	0.00	.09	1.56
MIN		31.09	23.88	30.34	-.00	0.00	.04	-.00	0.00	0.00	0.00	0.00	0.00
MEAN		35.75	27.69	33.54	.1534	.039	.1920	.5660	.216	.0000	0.00	.0086	.388
STDEV		1.322	1.657	1.821	.3293	.072	.1663	.8018	.358	.0000	0.00	.0234	.414
SENT	JT83140	12.34	26.00	57.47	0.00	0.00	.18	.70	0.00	0.00	0.00	.08	1.29
	JT83140A	7.02	28.66	55.10	1.11	.14	5.47	0.00	0.00	0.00	0.00	0.00	1.61
	JT83141	10.63	28.80	48.67	.37	2.01	6.21	0.00	0.00	0.00	0.00	0.00	2.28
	JT83264	10.49	33.81	48.16	1.80	0.00	.15	0.00	0.00	0.00	0.00	0.00	3.12
	JT83470	1.88	33.54	56.45	1.22	0.00	3.20	0.00	0.00	0.00	0.00	.79	2.26
	JT83471	12.35	21.14	59.58	1.40	0.00	3.17	0.00	0.00	0.00	0.00	.06	1.61
MAX		12.35	33.81	59.58	1.80	2.01	6.21	.70	0.00	0.00	0.00	.79	3.12
MIN		1.88	21.14	48.16	0.00	0.00	.15	0.00	0.00	0.00	0.00	0.00	1.29
MEAN		9.118	28.66	54.24	.9826	.358	3.062	.1172	0.00	0.00	0.00	.1540	2.03
STDEV		4.045	4.776	4.745	.6709	.811	2.548	.2871	0.00	0.00	0.00	.3137	.663
MISC	JT83264	8.06	25.42	45.29	3.08	0.00	6.81	0.00	0.00	0.00	0.00	2.22	5.34
	JT83477	24.41	32.15	37.73	0.00	0.00	.45	1.35	0.00	0.00	0.00	.69	1.20

Qz – Quartz
Or – Orthoclase
Ab – Albite
An – Anorthosite
Co – Corundum
Bi – Biotite
Ri – Riebeckite
Ns – Na-Silicate
Hy – Hypersthene
Act – Actinolite
Wo – Wollastonite
Mt – Magnetite
Hm – Hematite
Il – ilmenite
Ru – Rutile
Ap – Apatitie
Cr – Chromite
Zr – Zircon
A.I. – Agpaitic Index

4G. Concluded.

Hm	Il	Ru	Ap	Cr	Zr	A.I.
.73	.17		.02	.00	.07	.99
1.28	.33	.17	.04	0.0	.10	1.00
1.43	.26	.11	.04	.00	.14	1.01
.96	.23	.07	.09	.00	.06	.98
1.49	.22	.11	.08	0.0	.09	.99
.21	.26		.02	0.0	.17	1.01
.84	.36	.18	.02	0.0	.08	.97
1.03	.26	.13	.06	0.0	.04	1.04
.82	.26	.08	.09	.00	.09	1.00
.53	.27	.14	.07	.00	.08	.99
0.00	.37	.17	.02	.00	.03	.96
1.59	.22	.02	.02	.00	.10	1.03
.92	.27	.09	.02	.00	.07	1.02
1.47	.24	.04	.02	0.0	.09	1.02
.79	.20	.10	.02	.00	.07	.98
.57	.20	.08	.04	.00	.06	1.07
1.48	.27	.14	.02	.00	.10	1.06
.73	.26	.10	.02	0.0	.10	1.04
1.49	.21		.02	.00	.08	1.04
1.08	.24	.05	.02	.00	.07	1.08
1.59	.37	.18	.09	.00	.17	1.08
0.00	.17	.02	.02	0.0	.03	.96
1.01	.254	.10	.037	.00	.09	1.01
.451	.048	.04	.023	.00	.03	.03
1.08	.30		.02	.00	.23	1.01
0.00	.62	.31	.15	0.0	.12	.97
.00	.72	.36	.23	0.0	.08	.88
.72	.96	.15	.13	0.0	.01	.96
0.00	.24		.04	0.0	.14	.98
0.00	.25		.04	0.0	.16	.97
1.08	.96	.36	.23	.00	.23	1.01
0.00	.24	.15	.02	0.0	.01	.88
.300	.516	.27	.102	.00	.12	.96
.480	.298	.11	.082	.00	.07	.04
0.00	1.66		.45	0.0	.02	.93
.66	.58		.06	0.0	.12	1.01

MAPS
NOT
FILMED

CARTES
OMISES